List of Poster Presentation

(Authors W-Z)

Table of Content

ACSIL P-27

LINEAR-HYPERBRANCHED AMPHIPHILIC POLYPHOSPHATE ESTERS– A NOVEL FATLIQUOR ON THE LEATHER

Wang Xuechuan, Xiaoxiao Guo, Haijun Wang

College of Bioresources Chemical and Materials Engineering, Shaanxi University of Science and Technology; XI'AN, SHAANXI, P.R. CHINA 710021(email:15802958501@qq.com)

Leather-making process is a way of preserving skins to stop decomposition and to provide a strong and flexible material. From now, the environmental pollution caused by leather making is the primary concern in the development of leather industry. Fatliquoring is one of the key operations in the manufacturing of leather which can protect the leather against cracking, and the traditional fatliquor is also the cause of environmental pollution. So it is necessary to develop the eco-friendly materials to replace the traditional fatliquor. In recent study, the dendritic molecular has three-dimensional molecular structure, making certain filling possible.

The fatliquor of the linear-hyperbranched polyphosphate ester ($PAMAM_{G1}$-3-P) has been constructed through random multibranching esterification of lauroyl chloride and phosphate ester as a branching agent. Importantly, the polymer shows the small particle size. Here, the $PAMAM_{G1}$-3 and $PAMAM_{G1}$-3-P were applied in the collagen fibers of leather to improve the fibers distance and mechanical property of collagen fibers, and the addition of polymer certainly effect on the thermal properties of leather. From XRD, SEM, and XPS, the analysis elucidates that the $PAMAM_{G1}$-3-P can enhance the distance of collagen fibers with crosslinking the collagen fibers, but does not destroy collagen fibers. Additionally these polymers display significant flexibility, which could replace ordinary fatliquor in future. The result provides a new application of using linear-hyperbranched amphiphilic polyphosphate esters into traditional leather materials to enhance the performances of leather.

Keywords: PAMAM; Phosphorylation; Amphiphilic; Fatliquor; Cross-linking

Introduction

Leather-making process is a way of preserving skins to stopdecomposition and to provide a strong and flexible material [1]. The demand for the production of leather continues to grow because oftheir comfortableness,softness, extensibility and so on [2]. However, in the process of leather, animal hides as the raw materials have poor flexibility, and the skin undergoes several structural and molecular changes such as the degrease of collagen fibers and the loss of elasticity. Hence, the leathershould be treated through a series of physical and chemical treatments to obtain outstanding performances. Fatliquoring is one of the key operations in the manufacturingof leather which can protect the leather against cracking [3]. There are many methods to enhance the flexibility and softness of leather, such as adding to the natural oils. The oils can penetrate into the leather and play lubricating roles, so that themolecular chain segments can be easily moved. But the problem is that the natural oils arein short supply. On the other hand, the odor and hand feeling of leathers treated with natural oils are not ideal. Therefore the latest research focuses on the development of synthetic fatliquor to improve the properties of leather.

Dendritic polymers and hyperbranched polymers have attracted significant interestdue to their promising properties of combined functionalized macromolecules and nanoparticles.In the last few years, considerable attention was taken to the synthesis of branched polymers and setting up a relationship between their structures and properties [4-10]. Furthermore, the polyphosphate ester exhibits good flexibility based on the pentavalent phosphorus [11,12]. Interestingly, the structure of hyperbranched polyphosphate esters are similar to phospholipids in structure, and phospholipids can form adsorption films or chemical adsorption films on the fibers, and those films can not only lubricate fibers but also protect the surface of fibers.Thus, we decided to design and synthesize some amphiphilic hyperbranched polyphosphate esters, which combine the advantages of hyperbranched polymers and phospholipids.

In this work, the amphiphilic polymer with a polar phosphates headgroup and hydrophobic aliphatic tails has been synthesized, via esterification of dendritic polyamide with lauroyl chloride and subsequent capping reaction of phosphorus pentoxide. Here, the synthetic polymers were applied to the fatliquoring processof leather extracted from chrome tanned leather and no environmental pollution. The incorporation of hyperbranched polymer into the leather would improve the properties such as thickness, mechanical properties, and fibers separations of the treated leather were evaluated. In this work, we employed the linear-hyperbranched amphiphilic polyphosphate ester as the efficient additive for leather. The interactions of synthetic polymers and collagen fibers of leather are explored and the structure relations of collagen fibersare also investigated.

Material and methods

Materials: The polyamidoamine dendrimers ($PAMAM_{G1}$) was purchased from Weihai CY Dendrimer Technology Company. N,N-Dimethylformamide (DMF) was dried over calcium hydride

and then purified by vacuum distillation. Lauroyl chloride was purchased from Aladdin Chemical Reagent Corporation and distilled. Triethylamine (TEA) was refluxed with phthalic anhydride, potassium hydroxide, calcium hydride in turn and distilled just before use. Tetrahydrofuran (THF) was dried by refluxing with the fresh sodium-benzophenone complex under N_2 and distilled just before use. Methanol and dichloromethane were purchased from Sigma-Aldrich. Phosphorus pentoxide (P_2O_5) was dried over anhydrous $MgSO_4$. Other reagents were purified by common purification procedures. The goat wet blue was supplied by Liquan Shunji leather Co., Ltd.

Characterizations: Nuclear magnetic resonance (NMR) analyses were recorded on the ADVANCE Ⅲ 400MHz spectrometers with deuterium oxide (D_2O) as solvents. Fourier transform infrared spectrometer (FTIR) spectra were recorded on a VECTOR-22 instrument by KBr sample holder method. Dynamic light scattering (DLS) measurements were performed in aqueous solution using a Zetasizer NANO-ZS90 apparatus equipped with a 4.0 mW laser at λ=633nm. All the samples of 0.2mg/mL were measured at 20^{o}C and at a scattering angle of 90°.

Synthesis of linear-polyamidoamine dendrimers ($PAMAM_{G1}$-3) : The $PAMAM_{G1}$-3 was obtained by the esterification of $PAMAM_{G1}$ with lauroyl chloride, and $C_{12}H_{23}$ alkyl tails were attached by the reaction of terminal hydroxyl groups in DMF in the presence of TEA as an acceptor of HCl. As the reaction proceeded, TEA hydrochloride precipitates, the reaction medium, and its quantity corresponds to the consumed lauroyl chloride. Meanwhile, the esterification fraction was controlled to be 0.3750 with $PAMAM_{G1}$. The corresponding specimen is named as $PAMAM_{G1}$-3. $PAMAM_{G1}$ (10.0 mmol) and TEA (30.0 mmol) dissolved in 40 mL DMF were added into a dried three-neck flask with a magnetic stirrer, a dry nitrogen inlet and a drying tube. The freshly distilled lauroyl chloride (30.0 mmol) was then added dropwise into the $PAMAM_{G1}$ solution, and the solution was stirred for 12 h at room temperature. The precipitate of triethylamine hydrochloride was filtered off. After filtration, the solvents were distilled off, and the residue was dissolved in 20 mL dichloromethane and washed with water for three times. After the oil-phase was dried with anhydrous magnesium sulfate salt, some pale yellow solid was obtained.

Synthesis of linear-polyamidoamine polyphosphate ester dendrimers ($PAMAM_{G1}$-3-P) : $PAMAM_{G1}$-3-P was prepared by thephosphorylation of $PAMAM_{G1}$-3 using P_2O_5 as a reactant. The synthetic route of $PAMAM_{G1}$-3-P is shown in Figure 1. $PAMAM_{G1}$-3(10.0 mmol) was dissolved in 40 mL THF and then the P_2O_5 (80.0 mmol) was added slowly to $PAMAM_{G1}$-3. The mixture was stirred for 6 h at 60^{o}C. After the esterification reaction, the deionized water (10 mL) was added into the same flask for 3.5 h at 65^{o}C to improve the content of phosphomonoester. The crude product was dissolved in 20 mL alcohol and then filtrated. The filtrate was evaporated under vacuum to obtain some transparent and colorless oil. The monoester, disester and phosphoric acid were determined by potentiometric titration, and the content of monoester is 52.68%, disester is 39.37% and phosphoric acid is 7.95%.

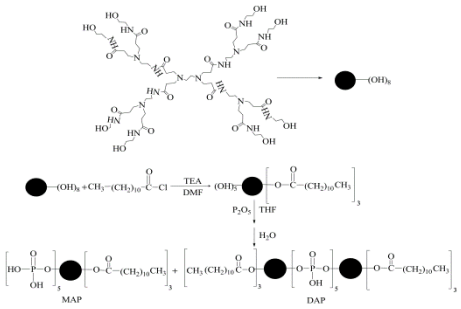

Figure 1. Detailed Scheme for synthesis of $PAMAM_{G1}$-3-P.

Preparation of Leather. The raw leather was taken from the spinal part of goat wet blue. The synthesized $PAMAM_{G1}$-3 (8 g) and $PAMAM_{G1}$-3-P (8 g) were respectively added to 100 mL deionized water under stirring with a magnetic bar at 50°C. The mixtures were applied to the fatliquoring process for the goat wet blue as shown in Table 1.

Table 1. Fatliquoring process of goat leather

Operation	Dosage/%	Drug names	Time/min	Temperature/°C	pH
Washing	200	water	20	40	
	100	water			
Neutralizing	0.5	$NaHCO_3$	30	40	5.5~5.8
	1	$NaHCO_3$	2×20+30		
Washing	200	water	10	40	
	100	water			
Fatliquoring	8	$PAMAM_{G1}$-3/$PAMAM_{G1}$-3-P	60	55	
	1	formic acid	30		3.5~4.0
Washing	200	water	10	40	

The morphologies of collagen fibers before and after fatliquoring treatment were observed by an environmental scanning electron microscope (E-SEM) FEI Q45(FEI Co.) operated at 5 KV. XPS measurements were performed on an X-ray photoelectron spectrometer (XPS, Kratols Axis Supra) with a monochromatic focused Al Kα X-ray source (1486.6 eV) to determine C, N, O, Cr, and other elements on the slice surface. The detection was performed at 90° with respect to the sample surfaces. The pressure in the sample chamber was maintained at 10^{-9} mbar. The peak fitting was performed with the software package of Casaxps, and surface elemental stoichiometry was determined from peak-area ratio. The binding energy (BE) of C1s (284.6 eV) was selected for energy

calibration. X-ray diffraction data (XRD) were obtained using a 2.2 kW rotating anode X-ray diffractometer (D8 Advance, Bruker, Germany) with a fixed Cu Kα radiation of 0.154 nm. The real lattice space *d*, that represents characteristic structure dimension of collagen fiber, can be calculated by $d=n\lambda/(2\sin\vartheta)$, where λ is the X-ray wavelength, ϑ is half of diffraction angle, and *n* is1.

The physical-mechanical property of collagen fibers was examined by using the standard IULTCS methods. The mechanical properties of no-fatliquoring leather, $PAMAM_{G1}$-3 fatliquoring leather and $PAMAM_{G1}$-3-P fatliquoring leather were analyzed using an electronic universal testing machine (UTM2102, Shenzhen Suns Technology Stock Co., Ltd.). The mechanical properties of collagen fibers were compared after conditioning the leather for 48 h at 20 ± 2°C with a relative humidity of 65 ± 2%. The strain rate was 50 mm/min and each test was carried out on five samples (1 cm×10 cm) to obtain a mean value. We marked the thickness before fatliquoring as d_1 (mm) and the thickness in the same place after fatliquoring as d_2 (mm). T_p (thickening rate) can be calculated according to the formula:

$$T_p=(d_2-d_1)/d_1$$

Results and Discussion

Characterization of linear-polyamidoamine polyphosphate ester dendrimers ($PAMAM_{G1}$-3-P): The resulting $PAMAM_{G1}$-3 and $PAMAM_{G1}$-3-P were characterized by ^{1}H NMR, ^{13}C NMR, and FTIR. Comparing with the FTIR spectra of $PAMAM_{G1}$, $PAMAM_{G1}$-3 and $PAMAM_{G1}$-3-P in Figure 2, it was found that the absorbance of hydroxyl groups at 3286 cm^{-1} reduced dramatically after the esterification reaction. Simultaneously, the new absorbance appeared at 1738 cm^{-1} is the characteristic absorptions of the O=C-O stretching, indicating the formation of ester bond. In addition, comparing with the spectra of $PAMAM_{G1}$-3 and $PAMAM_{G1}$-3-P in Figure 2, it was noted that the absorbance of hydroxyl groups at 3412 cm^{-1} reduced dramatically after the esterification reaction. Meanwhile, the new absorbance appeared at 1268, 1178 and 986 cm^{-1} which is attributed to the asymmetrical, symmetrical stretching of P=O and P-O-C, respectively.

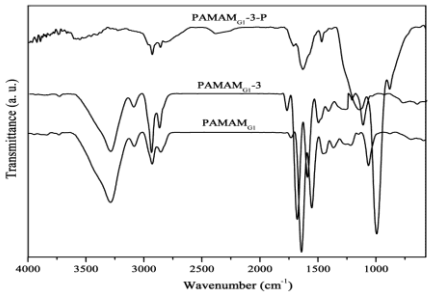

Figure 2. FTIR spectra of $PAMAM_{G1}$, $PAMAM_{G1}$-3 and $PAMAM_{G1}$-3-P.

The ^{1}H NMR and ^{13}C NMR spectra of the resulting PAMAM$_{G1}$ and PAMAM$_{G1}$-3-P were exhibited in Figure 3. In Figure 3a, some new signals appeared at 0.64, 0.92 and 1.02~1.15 ppm in the ^{1}H NMR spectra of PAMAM$_{G1}$-3-P comparing with that of PAMAM$_{G1}$, which could be assigned to the protons of methyl PAMAM-OOC$(CH_2)_{10}$**CH_3**, the methylene (PAMAM-OOC(**CH_2**$)_{10}CH_3$, and the PAMAM-OOC**CH_2**$(CH_2)_9CH_3$ respectively in alkyl tails. Meanwhile, the new signal was observed at 3.89 ppm in the spectrum of PAMAM$_{G1}$-3-P, which connected to the tertiary amine (-NH-CH_2-**CH_2**-O-) of the phosphorus in terminal protons of PAMAM$_{G1}$-3-P.

In addition, the chemical structures of polymers were identified by the ^{13}C NMR spectra (Figure 3b). The signal at 164.6 ppm appeared in the ^{13}C NMR spectrum of PAMAM$_{G1}$-3-P, which demonstrated that the lauroyl chloride has been grafted at PAMAM$_{G1}$. Meanwhile, the new signals appeared at 20.40~33.70 ppm in the ^{13}C NMR spectra of PAMAM$_{G1}$-3-P. After the terminal hydroxyl groups of PAMAM$_{G1}$-3 are capped by the phosphate, the signal at 60.00 ppm of PAMAM$_{G1}$ moved to 64.71 ppm and 69.28 ppm of PAMAM$_{G1}$-3-P. Because the electronegativity of oxygen and phosphorus are stronger than hydrogen, the chemical shift of methylene shifts to low field. What`s more, the signal of PAMAM $_{G1}$ (-NH-**CH_2**-CH_2-O-) at 40.17 ppm shifted to 35.53 ppm in the ^{13}C NMR spectrum of PAMAM$_{G1}$-3-P. The results verified that the phosphate successfully grafting of alkyls on PAMAM$_{G1}$-3.

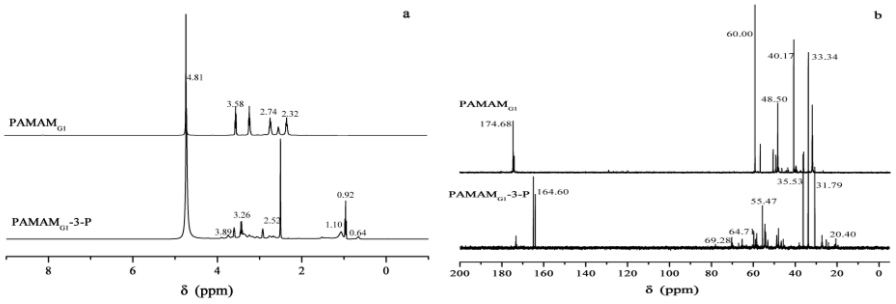

Figure 3.^{1}H NMR and ^{13}C NMR spectra of PAMAM$_{G1}$ and PAMAM$_{G1}$-3-P.

a: ^{1}H NMR spectra, b: ^{13}C NMR spectra.

DLS measurements are important methods to confirm whether polymers could enter the leather. The diameters of PAMAM$_{G1}$-3 and PAMAM$_{G1}$-3-P are 161.6 and 176.0 nm respectively. Apparently, the PAMAM$_{G1}$-3 and PAMAM$_{G1}$-3-P as the fatliquor could permeate to the leather.

Application in leather: The collagen fibers have a macroscopically disordered network structure in nature. Figure 4 shows the morphologies of the collagen fibers after leather drying with the no-fatliquoring, PAMAM$_{G1}$-3 and PAMAM$_{G1}$-3-P respectively under the same process conditions. The results reveal that the PAMAM$_{G1}$-3-P could affect the properties of collagen fibers, but the collagen texture does not change. Macroscopically, it is obvious that the collagen fibers distance increased and the network structures were disordered after fatliquoring. When the PAMAM$_{G1}$-3 and PAMAM$_{G1}$-

3-P filled in collagen fibers, two different forces became strengthened. One of the forces is perpendicular to the capillary pressure difference, and the other is parallel to the capillary flow adhesion force. The adhesion force of capillary flow tends to decrease the order of the aggregation of the collagen fibers. The result shows that the flow of capillary flow in the capillary is the precondition of determining the interaction between $PAMAM_{G1}$-3, $PAMAM_{G1}$-3-P and collagen fibers. As is shown in Figure 4, it seems that the $PAMAM_{G1}$-3, $PAMAM_{G1}$-3-P leads to the disorder of collagen fibers aggregation.

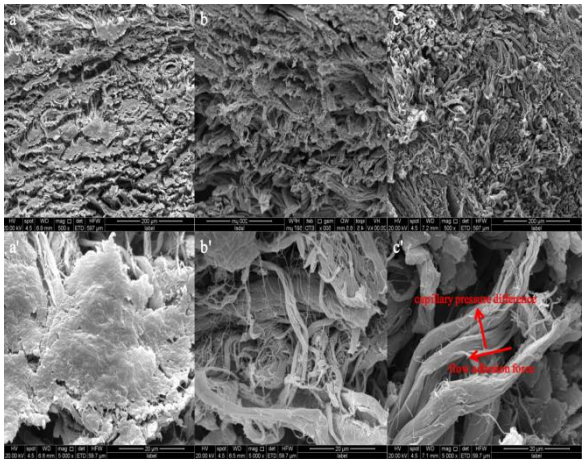

Figure 3. E-SEM microphotographs of collagen fibers treated with different chemicals. (a) without treated, (b) treated with $PAMAM_{G1}$-3, (c) treated with $PAMAM_{G1}$-3-P. (a`), (b`), and (c`) are the images for a, b, and c with a 5,000 higher magnification.

XPS spectra of the collagen fibers show the signals for the elements of C, N, O, Cr^{3+} and so on. Figure 4 show that the XPS spectra of the collagen fibers only contain signals for the elements of C, N, O, and P. After the introduction of $PAMAM_{G1}$-3-P, the bands at 135 and 136 eV can be observed, which are attributed to asymmetric dual peaks of P $2p_{3/2}$ and $2p_{1/2}$ orbit, respectively. Electrons from the O (KLL) Auger energy level are also evidenced in each spectrum, but the amplitude of the corresponding peaks is low. The detailed atomic fractions for C, N, O, Cr and P in various samples are given in Table 2. The results reveal that the $PAMAM_{G1}$ and $PAMAM_{G1}$-3-P have entered the fibers and the formation of the clusters is responsible for the cross-linking between fibrils. This is maybe the reason that $PAMAM_{G1}$-3 and $PAMAM_{G1}$-3-P with multiterminal base can be crosslinked with collagen fibers side chain.

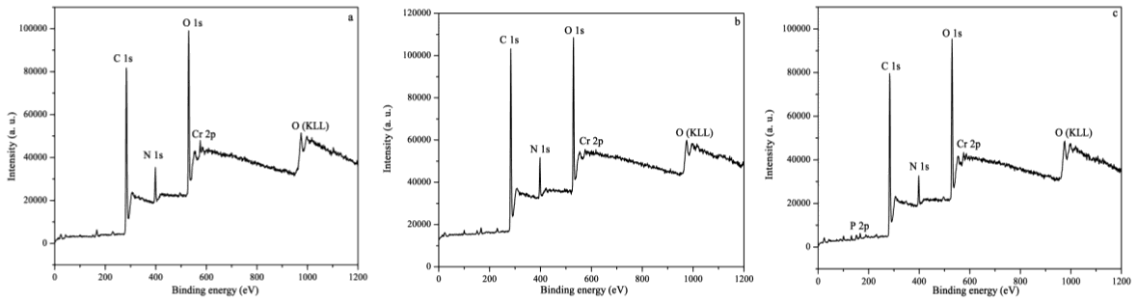

Figure 4. XPS survey spectra: (a) collagen fibers without treated, (b) the collagen fibers treated with $PAMAM_{G1}$-3, (c) the collagen fibers treated with $PAMAM_{G1}$-3-P.

Table 2. Elemental Composition (atm %) obtained by XPS from collagen fibers treated with $PAMAM_{G1}$-3 and $PAMAM_{G1}$-3-P

Sample	C (1s) %	N (1s) %	O (1s) %	Cr (2p) %	P (2p) %
Blank	71.35	6.97	21.24	0.44	0
$PAMAM_{G1}$-3	72.81	7.77	19.16	0.25	0
$PAMAM_{G1}$-3-P	69.01	6.45	22.69	0.41	1.44

The figure of XRD shows the linear intensity profiles of the collagen fibers versus diffraction angle. The collagen fibers are a kind of natural polymer material with multiple layer structure, which shows the periodic change of the structure. Figure 5 shows the XRD grain splits of collagen fibers treated with $PAMAM_{G1}$-3 and $PAMAM_{G1}$-3-P. From the diffraction peak, the lateral spacing between collagen molecules are obtained by Bragg's equation (Table 4).The structural information is given in Table 3.The peak 1 in real lattice space represents the characteristic intermolecular lateral distance within collagen fibers [13]. The peak 2 stands for diffuse reflection caused by much internal structure of collagen fibers.The position of Bragg reflection approximately at peak 3 relates to the axial rise distance between the amino acid residues along collagen triple helices or helical rise per residue [14]. The peak 4 and peak 5 represents the N telopeptide and the C telopeptide. We can see the peak 4 and peak 5 diffraction peaks partially overlap each other because of close position and similar intensity from Figure 5. When the $PAMAM_{G1}$-3 and $PAMAM_{G1}$-3-P were added to leather, diffraction peak 1 became obvious suggesting that the collagen molecules after the addition of polymers still maintained in a regular and orderly manner. Meanwhile, comparing with the blank sample, the lateral spacing of the fibers increased after the addition of polymer. This indicates that $PAMAM_{G1}$-3 and $PAMAM_{G1}$-3-P entered the space between collagen molecules within microfibrils. Besides, the peak 2 corresponding to the amorphous region becomes stronger after $PAMAM_{G1}$-3 and $PAMAM_{G1}$-3-P is introduced. This is because that the internal irregular part of the collagen fibers generated more diffraction peaks after the addition of the polymer. Apart from peak 1 and 2, the distance of

peak 3 became smaller after the addition of the $PAMAM_{G1}$-3 and $PAMAM_{G1}$-3-P, and the reason may be the hydroxyl remnant of polymer crosslink with side-chain carboxyls of aspartic and glutamic acids at a single helix chain, leading to structural distortion of collagen molecules. The analysis elucidates that the polymer can alter the diffraction signal from the collagen helix but does not destroy collagen fibers.

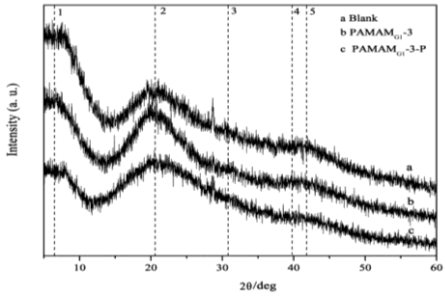

Figure 5. X-ray diffraction diagram of collagen fibers intensity:(a) collagen fibers without treated, (b) the collagen fibers treated with $PAMAM_{G1}$-3, (c) the collagen fibers treated with $PAMAM_{G1}$-3-P.

Table 3. Binding energies and atomic fractions from the XPS C 1s core level spectra for C element in the collagen fibers treated with $PAMAM_{G1}$-3 and $PAMAM_{G1}$-3-P

Sample	C-H		C-C		C-O/C-N		C=O	
	Binding energy (eV)	Atomic fractions (%)	Binding energy (eV)	Atomic fractions (%)	Binding energy (eV)	Atomic fractions (%)	Binding energy (eV)	Atomic fractions (%)
Blank	282.93	19.06	284.60	48.65	286.25	26.67	288.53	5.61
$PAMAM_{G1}$-3	283.18	23.74	284.60	38.97	286.01	34.33	288.39	2.97
$PAMAM_{G1}$-3-P	282.98	19.22	284.60	43.64	286.03	33.57	288.52	3.57

Appropriate mechanical responses are required for any material to be considered for a range of applications, specifically where mechanical stability is an essential prerequisite [15,16]. Collagen fibrils have little strength in either flexion or torsion, but they exhibit high tensile strength and tear strength. Those properties are largely attributable to the presence of the cross-links between polymers and collagen fibers. The physical and mechanical properties of the collagen fibers are presented in Figure 6, including tensile and tear properties. The physical and mechanical properties were analyzed by the main Chinese standard requirements and ISO standard for garment leather (QB 1872-1993, ISO/FDIS 14931: 2003). From the two kinds of different directions of horizontal and vertical, the stress of the leather is different. With stretching, the leather become progressively tauter, and the slope of the stress strain curve increase. In Figure 6a and 6b, when the leather are too

highly aligned like untreated leather, the strain becomes strong but the stress becomes poor. Meanwhile, the strains of leather which were treated with $PAMAM_{G1}$-3-P reduce, and the stress becomes better than untreated leather. The results demonstrate that the aggregation phenomenon of collagen fibers decrease and the leather has the slightly better performance of tensile strength. It is because that the $PAMAM_{G1}$-3-P can promote more movement between collagen fibers, and augment the distance of collagen fibers. Tear strength means the maximum load the sample carries when a gap appears, i.e. a deformation of axial tension. The tear strength of the three samples were higher than the occupation standard of garment leather (≥20 N/mm), indicating the $PAMAM_{G1}$-3-P do not destroy the structure of leather [17].

The physical and mechanical properties of leather fatliquored by $PAMAM_{G1}$-3-Pare improved compared with those of leather treated with $PAMAM_{G1}$-3 and untreated leather. This is due to that the permeation of $PAMAM_{G1}$-3-P into the leather is anticipated to assist in strong crosslinking with the collagen fibers matrix paving way for the formation of a network structure. The mechanical properties of the leather are closely related to the distribution of $PAMAM_{G1}$-3-P in leather.

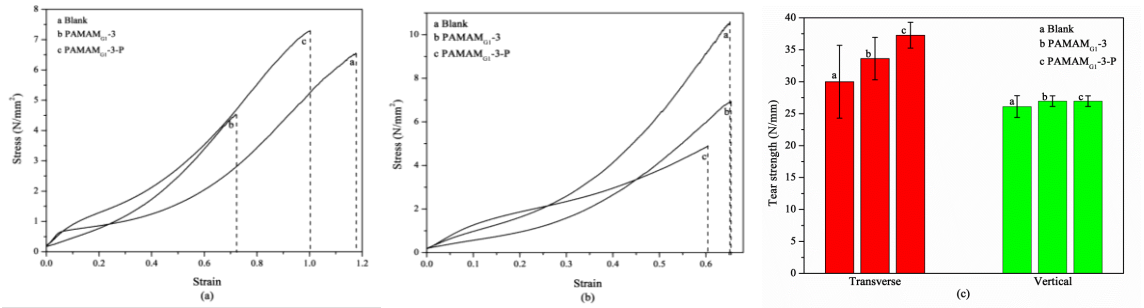

Figure 7. Physical and mechanical properties of leather from three samples: (a) stress (transverse) versus strain curves of three samples of without treated (a Blank), treated with $PAMAM_{G1}$-3 (b $PAMAM_{G1}$-3), and treated with $PAMAM_{G1}$-3-P (c $PAMAM_{G1}$-3-P); (b) stress (vertical) versus strain curves of three samples; (c) tear strength of the transverse/vertical direction.

Except for physical and mechanical properties, thickening rate is an index to characterize the fullness of leather treated with $PAMAM_{G1}$-3 and $PAMAM_{G1}$-3-P. The results of thickening rate of leather are shown in Figure 8. Compared with the thickening rate of leather treated with $PAMAM_{G1}$-3 and $PAMAM_{G1}$-3-P, the thickening rate of leather treated with $PAMAM_{G1}$-3-P increased obviously. $PAMAM_{G1}$-3 and $PAMAM_{G1}$-3-P are used as reinforcement filler in the leather and could penetrate into and fill between collagen fibers. The result shows that the fatliquoring agent with adding polymers can improve the filling property of leather.

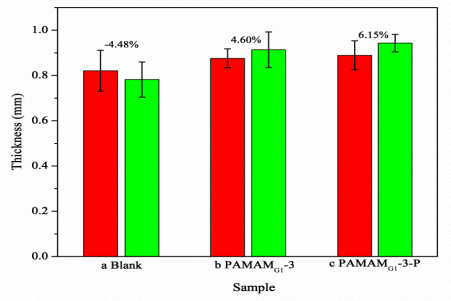

Figure 11. Thickening rate of leather before and after fatliquoring: (a) the leather without treated, (b) the leather treated with PAMAM$_{G1}$-3, (c) the leather treated with PAMAM$_{G1}$-3-P.

Conclusion

In summary, we synthesized linear-hyperbranched phosphate ester(PAMAM$_{G1}$-3-P) which has small particle sizes. PAMAM$_{G1}$-3-P can crosslink with the collagen fibers without destroying their triple helix conformation and makes the collagen fibers separate from each other. So the leather gets softer and thicker after the introduction of hyperbranched phosphate esters. In addition, PAMAM$_{G1}$-3-P can greatly improve the tensile and tear strength of leather. Therefore, the amphiphilic hyperbranched phosphate esters are suitable for ecological leather, and have favorable implications in leather.

Acknowledgements

The financial support by National Natural Science Foundations of China (No. 21276151), Key Scientific Research Group of Shaanxi province (No. 2013KCT-08), and Scientific Research Group of Shaanxi University of Science and Technology (No. TD12-04).

References

1. Wu B, Mu C, Zhang G, Lin W, Effects of Cr^{3+} on the structure of collagen fiber. *Langmuir* 2009, **25**, 11905-11910.

2. Sizeland K H, Edmonds R L, Basil-Jones M M, Kirby N, Hawley A, Mudie S, Haverkamp R G, Changes to Collagen Structure during Leather Processing. *J. Agric. Food Chem.* 2015, **63**, 2499-2505.

3. Thanikaivelan P, Rao J R, Nair B U, Ramasami T, *Crit. Rev. Environ. Sci. Technol.* 2005, **35**, 37-39.

4. Vuković J, Steinmeier D, Lechner M D, Jovanović S, Božić B, Thermal degradation of aliphatic hyperbranched polyesters and their derivatives. *Polym. Degrad. Stab.* 2006, **91**, 1903-1908.

5. Kurniasih I N, Keilitz J, Haag R, Dendritic nanocarriers based on hyperbranched polymers. *Chem. Soc. Rev.* 2015, **44**, 4145-4164.

6. Zigmond J S, Pavía-Sanders A, Russell J D, Wooley K L, Dynamic Anti-Icing Coatings: Complex, Amphiphilic Hyperbranched Fluoropolymer Poly (ethylene glycol) Cross-Linked Networks with an Integrated Liquid Crystalline Comonomer. *Chem. Mater.* 2016, **28,** 5471-5479.

7. Zheng Y, Li S, Weng Z, Gao C, Hyperbranched polymers: advances from synthesis to applications. *Chem. Soc. Rev.* 2015, **44,** 4091-4130.

8. Graff R W, Wang X, Gao H, Exploring Self-Condensing Vinyl Polymerization of Inimers in Microemulsion To Regulate the Structures of Hyperbranched Polymers. *Macromolecules* 2015, **48**, 2118-2126.

9. Cheng W, Kumar J N, Zhang Y, Liu Y, pH-and redox-responsive self-assembly of amphiphilic hyperbranched poly (amido amine) s for controlled doxorubicin delivery. *Biomater. Sci-UK.* 2015, **3,** 597-607.

10. Qiang T T, Gao X, Ren J, Wang X C, A chrome-free and chrome-less tanning system based on the hyperbranched polymer. *ACS. Sustain. Chem & Eng.* 2015, **4,** 701-707.

11. Chen D, Wang J, Synthesis and characterization of block copolymer of polyphosphoester and poly (ε-caprolactone). *Macromolecules* 2006, **39,** 473-475.

12. Xiao C, Wang Y, Du J, Chen X, Wang J, Kinetics and mechanism of 2-ethoxy-2-oxo-1,3,2-dioxaphospholane polymerization initiated by stannous octoate. *Macromolecules* 2006, **39,** 6825-6831.

13. Sionkowska A, Wisniewski M, Skopinska J, Kennedy C J, Wess T J, Molecular interactions in collagen and chitosan blends. *Biomaterials* 2004, **25**, 795-801.

14. Beck K, Brodsky B J, Supercoiled protein motifs: the collagen triple-helix and the α-helical coiled coil, Str*uct. Biol.* 1998, **122,** 17-29.

15. Beck K, Brodsky B J, Supercoiled protein motifs: the collagen triple-helix and the α-helical coiled coil, *Struct. Biol.* 1998, **122**, 17-29.

16. Meiyazhagan A, Cristian Chipara A, Tharangattu Narayanan N, Ayyappan A, Radhakrishnan S, Palanisamy T, Vajtai R, Sendurai M A,Ajayan P M, Three-Dimensional Porous Sponges from Collagen Bio-Wastes.*ACS.Appl.Materi. Interf.* 2016, **8,** 14836-14844.

17. Basil-Jones M M, Edmonds R L, Cooper S M, Kirby N, Hawley A, Haverkamp R G, Collagen fibril orientation and tear strength across ovine skins.*J. Agric. Food. Chem.* 2013, **61**, 12327-12332.

PREPARATION AND PROPERTIES OF COLLAGEN-BASED FOAMING AGENT

WANG Xue-chuan, WANG Lin, XUWei

(College of Bioresources Chemical and Materials Engineering, Shanxi University of Science and Technology,Xi'an 710021 China, e-mail: wangxc@sust.edu.cn)

Leather tanning is the process of the animal skins being processed into leather, but most of the collagen-based materials become a solid waste or solid contaminants due to the process of splitting, cutting, grinding and trimming operations. Our country produces about 140 million tons of leather solid wastes per year, of which about 80% is composed of collagen protein or rich in protein resources, therefore, those leather solid wastes can be recycled to some other useful substances. As a raw material of protein-based foaming agent, it has the significant value of theoretical research and practical use. On basis of the public literatures, gelatin possess foamability and foam stability but it's foam height is not high enough that leading to the poor surface activity.Thus, collagen-based foaming agent was synthesized by the amidation reaction between collagen powder and lauroyl chloride to improve surface activity of the protein-based foaming agent. Structure and properties of the collagen-based foaming agent were studied by gel permeation chromatography, infrared spectroscopy, X-ray diffraction, thermal analysis and surface tension instruments, etc. It can be seen from GPC result that the relative molecular mass of collagen-based foaming agent was increased after modification compared to that of lauroyl chloride, indicating that lauroyl chloride was grafted onto the collagen molecules. Through the comparison of the IR absorption peaks, It was further demonstrated that lauric acid segments were grafted onto collagen polypeptide through reaction of acyl chloride and amino groups, FT-IR analysis also confirmed that the synthesis reaction accorded well with Schotten - Baumann mechanism. GPC and IR results confirmed that collagen-based foaming agent had the due structure. XRD results illustrated that the incorporation of lauroyl can increase the tacticity and crystallinity of the collagen molecular chain segments. Collagen foaming agent can be dissolved in water and ethanol, is slightly soluble in methanol, acetone and not in common organic solvents. And its CMC and surface tension are 1.5g/L and 39.5 mN/m.

Key words: Collagen; lauroyl chloride; foaming agent; Structure and Performance

1.Introduction

The foaming gent, also known as blowing agent, refers to promote bubbles by physical or chemical method to form closed holes or pore structure of the material. Compared with the surfactant foaming agent, the protein foaming agent has better foaming and foam stabilizing performance, raw material easy to obtain, environment friendly, although the price is higher, but still was recognized by the market. Therefore, the development of the foaming agent is experiencing from the transition of the surfactants to the biological protein[1].

Leather tanning is the process of the animal skins being processed into leather, but most of the collagen-based materials become a solid waste or solid contaminants due to the process of splitting, cutting, grinding and trimming operations [2]. Our country produces about 140 million tons of leather solid wastes per year[3], of which about 80% is composed of collagen protein or rich in protein resources[4,5], therefore, those leather solid wastes can be recycled to some other useful substances. As a raw material of protein-based foaming agent, it has the significant value of theoretical research and practical use. On basis of the public literatures, such as Yao Yunzhen[6] study found gelatin possess foamability and foam stability but it's foam height is not high enough that leading to the poor surface activity. This article, lauroyl chloride as hydrophobic groups was used to graft the collagen, to enhance its surface activity and improve the foam height, to prepare a collagen foaming agent. And the properties of the prepared collagen foaming agent were studied.

2. Material and Discussion

2.1Experimental material

Industrial collagen powder(Hebei Zhongpi Dongming Environmental Science and Technology Co., Ltd),Lauroyl chloride(Aladdin, AR),Sodium hydroxide(Tianjin Darson Chemical Products Sales Co., Ltd. AR),Formaldehyde(Tianjin Hedong Hongyan Chemical Reagent Factory. AR),Phenolphthalein(Tianjin Tianli Chemical Reagent Co., Ltd. AR),Thymol blue(Tianjin Bodi Chemical Co., Ltd. AR)

2.2 Experimental methods and procedures

2.2.1 Preparation of collagen foaming agent

A certain amount of collagen powder and 100mL water were added into a 250mL three-necked flask and mixed well, Heated to a certain temperature under mechanical agitation, mixing 30 min until it completely dissolved, the pH was adjusted to about 8.5 with 20% NaOH, then a certain amount of lauroyl chloride was added to reaction for a certain time to stop heating, cooling, discharging.

2.2.2 The preparation principle of collagen foaming agent

The collagen foaming agent was prepared by the Schotten-Baumann reaction mechanism.

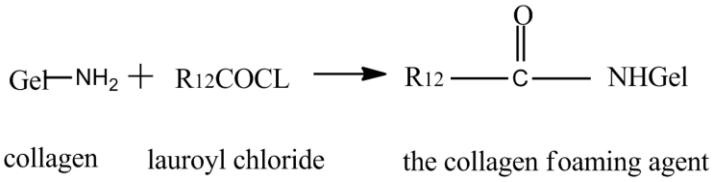

2.3 Analytical characterization

2.3.1 Gel permeation chromatography (GPC) [7]

Collagen powder was mixed with a certain concentration of solution, collagen foaming agents are also the same, polyethylene glycol was used as the standard, the relative molecular mass was measured.

2.3.2 Infrared spectroscopy (FTIR)

The collagen powder and the collagen foaming agent were dried in an oven, the KBr pellet method was used, and compared.

2.3.3 X-ray diffraction analysis

The crystallinity of the collagen and collagen foaming agent powder was measured by a 2200PC X-ray diffractometer, use copper target, the tube voltage was 40 kV and the tube current was 40 mA, the scanning angle range of the sample is 4 ~ 60°.

2.3.4 Thermal performance analysis (DSC)

The thermal stability of collagen and collagen foaming agent was characterized by STA409PC comprehensive thermoanalysis, temperature range is 25 ~ 800℃, the heating rate of 10℃/min.

2.4 Performance measurement

2.4.1 Determination of solubility[8]

Weigh 2 mL collagen protein foaming agent to put in a test tube, under 25℃ water bath, then add 10mL of water and a variety of organic solvents, and the dissolution was observed.

2.4.2 Determination of surface tension

Surface tension is an important property of liquid, surface activity is the ability to reduce the surface tension of a liquid, Is an important study indicators of surfactant. There are many ways to determine surface tension, in this paper, the collagen foaming agent was prepared into a series of

different concentrations of aqueous solution（CW，g/L）, the surface tension was measured with QBYZ-1 automatic surface tension meter（γ，mN/m）, and γ-CW mapping, thus, the surface tension of the collagen foaming agent was calculated

3 Results and Discussion

3.1 Analytical characterization

3.1.1 GPC analysis of industrial collagen and collagen foaming agent

.

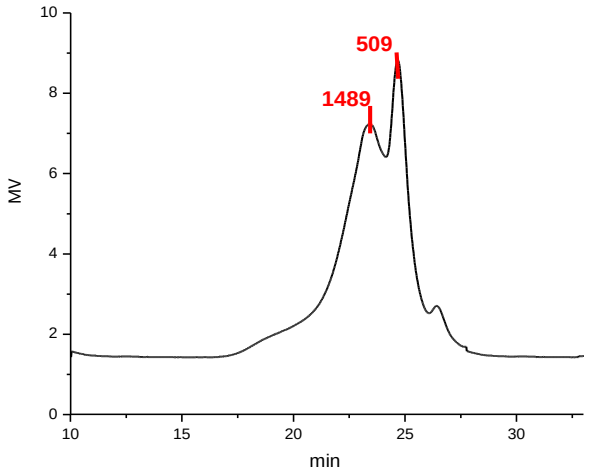

Figure 1 GPC drawing of collagen

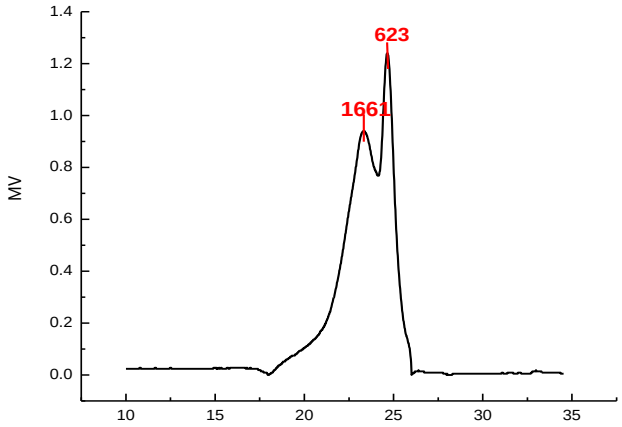

Figure 2 GPC drawing of collagen-based foaming agent

Figure 1 is the relative molecular mass distribution of collagen, figure 2 is the GPC measurement result of collagen protein foaming agent.The relative molecular mass of collagen is composed of two parts, statistical average relative molecular mass of 1489 and 509,as can be seen from these data,collagen is a mixture of peptides and amino acids. And the relative molecular mass of the collagen protein foaming agent is mainly composed of two parts.the average relative molecular masses were 1671 and 623,compared with before the modification,the relative molecular mass increased significantly.As can be seen in Figures 1 and 2,the relative molecular mass of lauroyl chloride was 218 ,the chlorine atoms are lost during the reaction(relative molecular mass is 35). It can be seen from GPC result that the relative molecular mass of collagen-based foaming agent was increased after modification compared to that of lauroyl chloride, indicating that lauroyl chloride was grafted onto the collagen molecules.

3.1.2 Infrared analysis of collagen foaming agent

Figure 3 is collagen and collagen protein foaming agent of infrared spectra,the methylene-stretching vibration peak (2926cm^{-1}) of the collagen foaming agent (b) was significantly enhanced as compared with the collagen solution (a),this is because the lauroyl chloride is grafted to collagen peptides[9,10];The N-H stretching vibration band (3350, 3180 cm^{-1}) of the primary amide was significantly enhanced compared with the collagen solution,this may be caused by the newly formed amide groups;R-NH_2 absorption peak 830cm^{-1} collagen solution was significantly reduced, it was further demonstrated that lauric acid segments were grafted onto collagen polypeptide through reaction of acyl chloride and amino groups, FT-IR analysis also confirmed that the synthesis reaction accorded well with Schotten - Baumann mechanism.

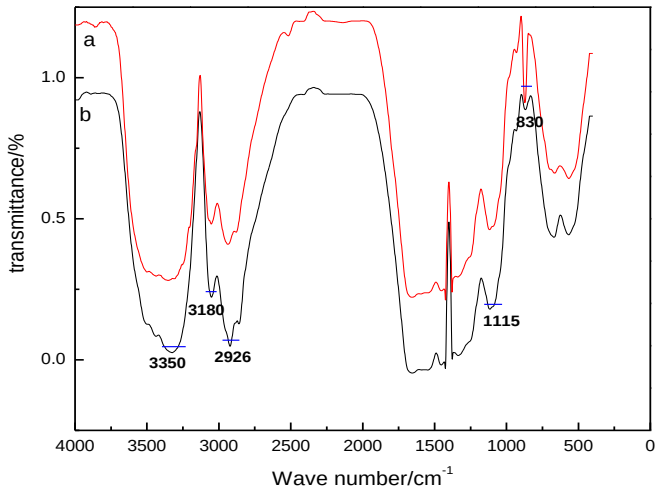

Figure 3 Infrared spectra of collagen (a) and collagen foaming agent (b)

3.1.3 X-ray diffraction analysis

As can be seen from the figure, the crystallinity of unmodified collagen was 8.00%, the crystallinity of collagen foaming agent is 13.45%,it was found that the crystallinity after modification was increased obviously, shows that collagen molecular chain segments of order increase.The possible reason is that unmodified collagen grains are too small,the crystal has a dislocation defect,since the introduction of the hydrophobic group causes the collagen foaming agent segments to be staggered with each other,collagen molecules from the chaotic become regular,crystallization trend increased[11]. It was further demonstrated that lauric acid segments were grafted onto collagen polypeptide through reaction of acyl chloride and amino groups.

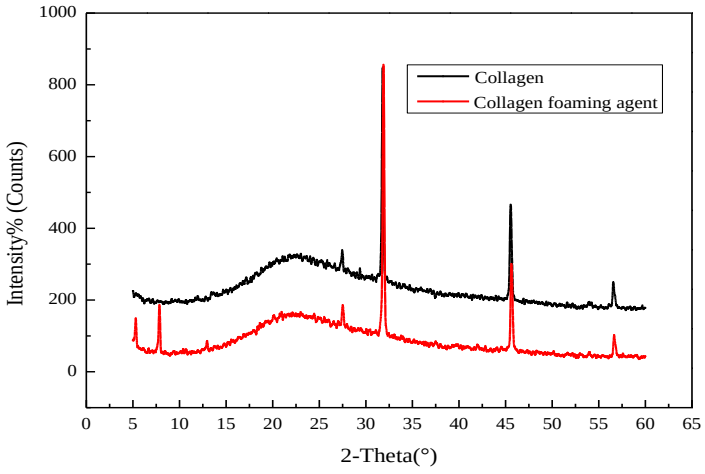

Figure 4 X-ray diffraction pattern of collagen and collagen foaming agent

3.1.4 Thermal Performance Analysis (DSC)

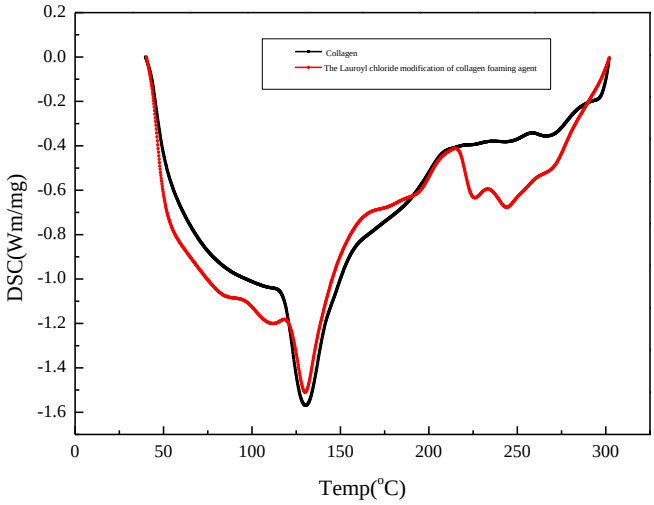

Figure 5 DSC diagram of collagen and collagen foaming agent

Collagen and collagen foaming agent DSC figure such as 5,can be seen from the figure,the DSC curve of collagen and collagen foaming agent has obvious exothermic peak at 130℃,Because the crystalline form of collagen changes[12];The glass transition temperature of the collagen was 173 °C,the glass transition temperature of the collagen foaming agent was 178 °C,it can be seen that both glass transition temperatures are similar,this is because the formation of the glassy state is due to the asymmetric molecular structure of the polymer,it may be that there is not enough energy to rearrange crystals.While the polymer is difficult to form 100% of the crystallization, there are always some amorphous,but the glass transition of amorphous polymer is not obvious.Collagen foaming agent at 225 ℃ and 245 ℃ has weak exothermic peak,it may be under the protection of nitrogen,residual lauroyl chloride macromolecules do not form oxides,can only be gradually carbonized, release heat.

3.2 Performance Measurement of collagen and collagen blowing agent

3.2.1 Determination of solubility

Solubility is one of the most basic physical properties of chemicals,in the case of surface-active substances having "hydrophilic-lipophilic" property,solubility directly affects its performance and range of applications. Thus, firstly, the dissolution of unmodified collagen and collagen foaming agent in water and common organic solvents was investigated qualitatively.Unmodified Collagen and collagen foaming agent in water and several common organic solvents in the dissolved situation

shown in Table 1.Can be seen from the table: Under 25 ℃, unmodified collagen and collagen foaming agent can be well dissolved in water and ethanol,micro dissolved in methanol, acetone,without being dissolved in a common organic solvent, such as methylene chloride, petroleum ether and toluene, paraffin wax, n-butyl alcohol, etc.,indicating that modification has little effect on its solubility.

Table 1 Solubility of Collagen and Collagen Foaming Agents in Different Solvents

Solvent	Collagen dissolved	Collagen foaming agent dissolved
water	Soluble	Soluble
Methanol	Slightly soluble	Slightly soluble
Anhydrous ethanol	Soluble	Soluble
acetone	Slightly soluble	Slightly soluble
methylene chloride	Insoluble	Insoluble
Petroleum ether	Insoluble	Insoluble
Toluene	Insoluble	Insoluble
paraffin wax	Insoluble	Insoluble
Butanol	Insoluble	Insoluble

3.2.2 Determination of surface tension

The surface tension of the unmodified collagen and the collagen foaming agent is shown in Fig6、7. Comparison of the figure can be drawn: the surface tension of the unmodified collagen is about 60 mN/m, the surface tension of the collagen foaming agent was 39.5 mN/m, the modified collagen foaming agent has a lower surface tension value and a higher surface activity.

Collagen foaming agent is composed of hydrophilic group hydrolyzed collagen polypeptide and lipophilic lauric acid, in the aqueous solution, the collagen foaming agent showed a good surface activity, the surface tension decreases sharply with the increase of the concentration in the dilute concentration range, when reached a certain concentration of its surface tension is almost no longer change. When the concentration of collagen foaming agent in the aqueous solution reached a certain level, collagen foaming agent molecules in the solution surface was saturated, the solution began to form micelles. As can be seen from the figure, its CMC and surface tension are 1.5g/L and 39.5 mN/m

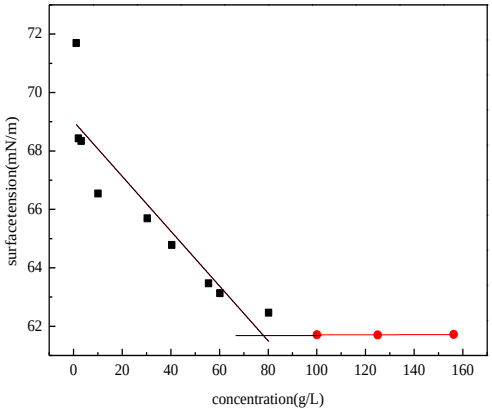

Figure 6 Surface tension of unmodified collagen

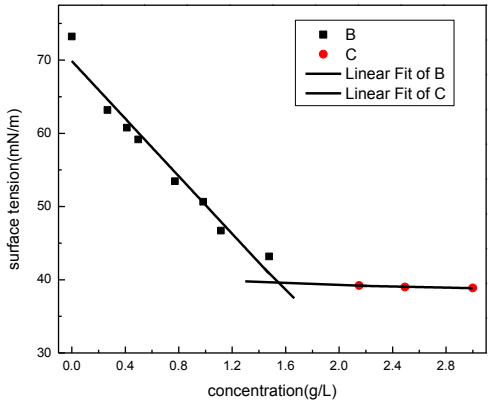

Figure 7 Surface tension of collagen foaming agent

4. Conclusion

(1) The FT-IR and GPC spectra of lauroyl chloride modified collagenconfirms the success of the crosslinking reaction,FTIR can be seen in lauroyl chloride acid chloride bond cross-linked to the collagen amino bond,the increase of molecular weight after modification in GPC can also be seen that the acid chloride bond reacts with the amino bond.

(2)The solubility and surface activity of the collagen foaming agent were studied, the results show: collagen foaming agent can be dissolved in water and ethanol, slightly soluble in methanol, acetone, and insoluble in common organic solvents; Under 25 ℃, its CMC and surface tension are 1.5g/L and 39.5 mN/m.

5. Acknowledgements

First of all, I would like to sincerely thank Professor Wang Xuechuan for guiding and cultivating me; secondly, I would like to thank Associate Professor Xu Wei for his guidance and help; and I would like to thank Professor Ren Longfang and Associate Professor Qiang Tao for their suggestions and help. I would like to express my gratitude to the School of Resource and Environment of Shaanxi University of Science and Technology for my training and to the platform offered by the Green Chemicals Institute for Leather &Synthetic Leather .

6.References

[1] Savoly A, Elk D. Foaming agent composition and process.CA:2081299[P]. 2003-07-29.

[2] Wang bi. Study on Collagen Properties of Tannery Wastes and Blending Biofilm Materials with Polysaccharides [D]. Sichuan: Doctoral Dissertation of Sichuan University, 2003.

[3] Ren jun li,Qiuhuayu,Fulihong. Collagen and Its Application in Papermaking Industry [J] .Chinese Journal of Paper Technology, 2003,18 (2): 106.

[4] Wang kun yu,Zhang ming rang,Chen yuan wei, et al. Study on extracting edible collagen and collagen polypeptide from chrome shavings [J].Sichuan food fermentation, 2000, (3): 35-45.

[5] Dong gui ping, Lan yun jun,Bao li hong. The leather of the green process of a chrome shoe waste recycling [J] Western Leather, 2006, (4): 12-16.

[6] Yao yun zhen,Qiu ting ting. Gelatin solution on the foaming performance [J] .Gelatin Science and Technology, 2014,36(4):187-193.

[7] Jiang ting da. Collagen and collagen [M]. Beijing: Chemical Industry Press, 2006,5.

[8] Zhang min. Preparation and Properties of Monosaccharide Surfactants [J]; Journal of Qingdao University of Science and Technology,2012.

[9] Yakimets I，Wellner N，Smith A C，et al.Mechanical properties with respect to water content of gelatin films in glassy state[J].Polymer,2005,46（26）：12577-12585.

[10] Lin L H，Chen K M.Preparation and surface activity of gelation derivative surfactants[J].Colloids and Surfaces A:Physicochemical and Engineering Aspecs,2006,272（1-2）：8-14.

[11] Wang qun. Study on the Synthesis and Application of Modified Collagen Surface Sizing Agent [J]; Journal of Shaanxi University of Science and Technology,2015.

[12] Hao xiao li. Preparation of paper-based sizing agent based on waste skin collagen and its properties [D]. Shaanxi :Doctoral Dissertation of Shaanxi University of Science and Technology, 2014.

SFS P-48

CONVERSION OF LEATHER WASTES TO AN ECO-FRIENDLY SUPERABSORBENT POLYMER

Wang Ru *, Shouhong Yi,Zaiyin Hu,Yaling Wang, Yuling Tang

College of chemical Engineering,Sichuan University, Chengdu, 610065, China

National Engineering Laboratory for Clean Technology of Leather Manufacture, Chendu, 610065, China.

**Email:wangru@scu.edu.cn*

This paper provides an environmentallyfriendlyand economical method to manage the problem of solid leather waste (leather scraps, LW) generated by leather industry, through converting leather waste resources into a value-added product mainly used for agriculture. A leather waste -based superabsorbent polymer was synthesized by grafting copolymerization of neutralized acrylic acid (AA) and ammonized maleic anhydride (MA) onto the hydrolyzed waste collagen obtained from leather waste (PLW-g-(AA-co-MA)). To achieve an improved absorbency performance, major factorssuch as the ammonization degree of MA, amount of crosslinker and initiator were explored, through which a leather waste -based product with a maximum absorbency of1618 g/g in distilled water (177g/g in 0.9 wt % sodium chloride solution) was received. Simultaneously, the biodegradability of this polymer has also been investigated *via* enrichment culture technique and 16S rRNA gene sequence analysis. We isolated a bacterium from soil identified as a strain of Ensifer sp.Y1 that can use PLW-g-(AA-co-MA) as carbon source to grow and the samples, before and after the biodegradation, were characterized by SEM and TG. Both the excellent water absorbency and biodegradability of PLW-g-(AA-co-MA) showed that the introduction of the wastes into superabsorbent is a green method of utilizing leather wastes, which could not only reduce the production cost, improve the biodegradability of product but also make the technique environmental friendly, thus making it more possible for superabsorbent polymer to be used in agriculture fields.

Keywords: Superabsorbent polymer; Leather waste; Biodegradability;Enrichment culture technique

Introduction

Leather industry, one of the polluting industries because of generation of huge amount of liquid and solid leather wastes. Out of 1000 kg of raw hide, nearly 850 kg is generated as soild leather wastes which are raw trimmings, fleshings, chrome shavings, buffing dusts and keratin wastes and leather scraps (Kanagaraj et al. 2006). The traditional ways to manage solid leather wastes are disposing of them on land sites and chemical thermal process, which causes an overload on the

environment and pause a burden on the economy of tanning industry (Jian and Wuyong 2008; Hamer 2003). However, the solid leather wastes contain about 95% of collagen, which is an important biological source of proteins and amino acids that contain varieties of functional groups such as -OH, -COOH and -NH_2. The traditional processes fail to make the best use of the proteins and amino acids of the solid leather wastes. Recently, Many reports have exhibited the utilization of the waste collagen from leather waste to prepare polymers, such as packing materials (Langmaier, Kolomaznik and Mokrejs et al.2008), biodegradable soil mulching in agriculture (Hoffmann 2003),biodegradable epoxide films (Langmaier et al.2006) and bio-superabsorbent polymer (Hu Z and Shouhong 2015),which not only provides an environmentally sound method to deal with leather waste pollution but also lows the production cost of producing polymers .

Superabsorbent polymers (SAPs), owing to its excellent water-absorption and -retention capabilities, have been widely used in hygienic products, horticulture and agriculture (Zohuriaan-Mehr and Kabiri 2008; Masuda 1994). However, most available SAPs are mainly petroleum-based synthetic polymers with high production cost and poor biodegradability, which leads to depletion of petro-chemical and severe pollution to the environment (Thakur et al.2014; Zhang Y N 2015). Thus, the current research interest has focused on the demand for biopolymer materials that are eco-friendly or biodegradable in nature. The renewable natural or waste resources, such as starch (Li A 2007), cellulose (Bao Y 2011), wheat straw (Liang R 2009), collagen (Pourjavadi et al. 2006; Sadeghi 2010) and waste mulberry branches (Zhang Y 2014) have been introduced into the construction of superabsorbent materials.

Based on the above consideration, we have synthesized a waste collagen-based superabsorbent biopolymer using leather waste (leather scraps) as model material, and AA and MA as graft monomers.Additionally, the biodegradability of this biopolymer was also evaluated through microorganisms enrichment culture technique.

Experiment

Chemicals andMedia

N,N'-methylene bisacrylamide(MBA), ammonium persulfate (APS), sodium bisulfite, acrylic acid(AA)and maleic anhydride (MA) all were purchased from Kelong Cor.(Chengdu, China). Leather waste (leather scraps, LW) was obtained from National Engineering Laboratory for Clean Technology of Leather Manufacture,Chendu,China.All agents were used of analytical grade and all solutions were prepared with distilled water.

Luria-Bertani (LB) and mineral salt medium (MSM) were prepared as the referred (Zhang J et al. 2011); for solid medium, 15.0 g/L agar was added and all involved mediums were sterilized at 121 ^{o}C for 20 min by autoclaving.

Preparation of collagen hydrolyzate

11.0 g crushed LW sample with a width of 2.0 mm was added to 100 mL potassium hydroxide solution with an approximate concentration of 1mol/L, which was kept in a 60 ^{o}C water bath, under a

mechanical stirrer, to react for 1 h. Then this mixture was transferred to volumetric flask to lead a standard volume of collagen hydrolyzate.

Preparation of the collagen-based SAP

A series of samples were prepared according to the following procedure: acrylic acid was neutralized in an ice-water bath by a 20 wt% alkaline solution consisted of potassium hydroxide and ammonia (the weight ratio of potassium hydroxide to ammonia is 1.2), after which the neutralized acrylic acid was added to the beaker filled with ammonized maleic anhydride. Then, the obtained mixture was sequentially added with collagen hydrolyzate (15 wt% of the total mass), N, N- methylene-bis-acrylamide, ammonium persulfate and sodium bisulfite (the weight ratio of ammonium persulfate to sodium bisulfite is 2), which was placed in a 60 ^{o}C water bath to react for 10 min under a mechanical stirrer and then was changed to be kept stand in 80 ^{o}C water bath for 4 h. Finally, the collagen-based SAP was obtained through drying, crushing.

Swelling measurements using tea bag method

A weighed collagen-based SAP sample (0.1 ± 0.001 g) was immersed in distilled water (0.9 wt % sodium chloride solution). After being kept standing for 24 h at room temperature, the swollen samples were handled with an 80 mesh filter cloth to remove the unabsorbed water. The water (saline solutions) absorbency (Q_{H2O} or Q_{salt}) of SAP samples was determined by weighing the swelled samples and was calculated using the following equation: $Q_{H2O} = (m_2-m_1)/m_1$

Where, m_1 and m_2 are the weight of the dry sample and the water (saline solutions)-swollen sample, respectively.Q_{H2O} or Q_{salt} was calculated as grams of water per gram of sample.

Biodegradation

To isolate collagen-based SAP-degrading bacteria, a conventional enrichment culture was carried out (Surhio,Talpur and Nizamani 2014). Initially, 2.0 g of soil collected from a field in Sichuan Province, China was added to a 250 mL Erlenmeyer flask containing 100 mL of MSM solution amended with collagen-based SAP (100 mg /L). The suspension was incubated for 7 d at 30 ^{o}C in an orbital incubator shaker operated at 120 rpm. Subsequently, 5 mL of the enrichment culture was serially transferred four times to fresh medium, each time containing a higher concentration of collagen-based SAP (100~600 mg/l) and incubated under the same conditions. Then, the final enrichment was streaked onto the collagen-based SAP agar plates and LB agar plates to get a purified isolate by repeated streaking. The isolate was identified by biochemical characteristics as well as 16S rRNA gene sequence analysis according to the previous reference (Ya-li et al.2014). Optimal growth conditions of the strain were explored by UV-visible spectrophotometer. The growth of isolate using collagen-based SAP as sole carbon in MSM was tested by the spread plate method on LB Nutrient agar plates and the collagen-based SAP, before and after the biodegradation of 15d in MSM by the isolate, was characterized by SEM and TG.

Characterization

The micrographs of samples were taken using SEM instrument (FEI Quanta 250, USA) after coating the sample with gold film. TG was recorded on a HTG-2 ther-mogravimetric analyzer, in the

temperature range of 25–800 °C at a heating rate of 10 °C /min using dry nitrogen purge at a flow rate of 30 mL /min.

Results and discussions

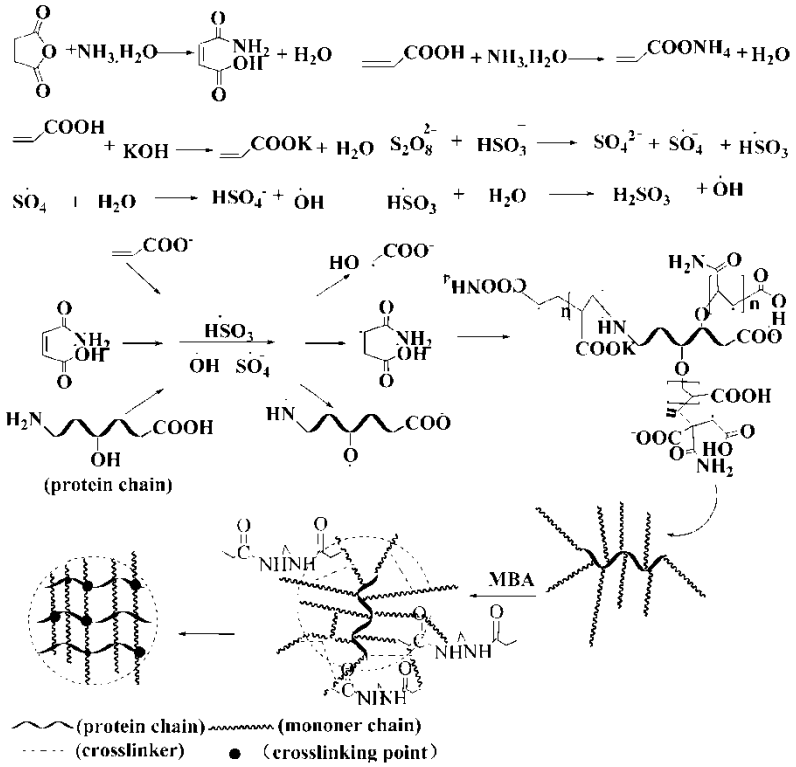

Fig. 1 Proposed mechanism of PLW-g-(AA-co-MA)

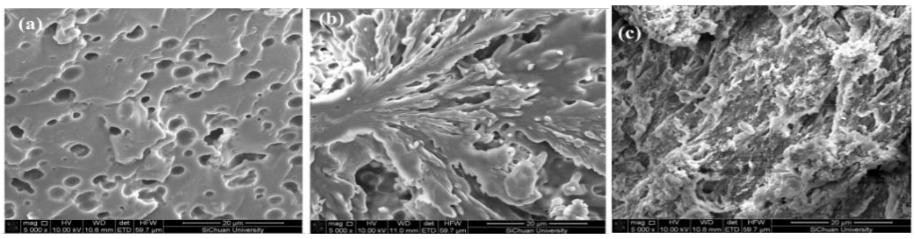

Fig. 2 SEM images of PLW-g-(AA-co-MA): (a) before biodegradation, (b) control (control is the same experimental process to (c) except that control was non-inoculation), (c) after biodegradation

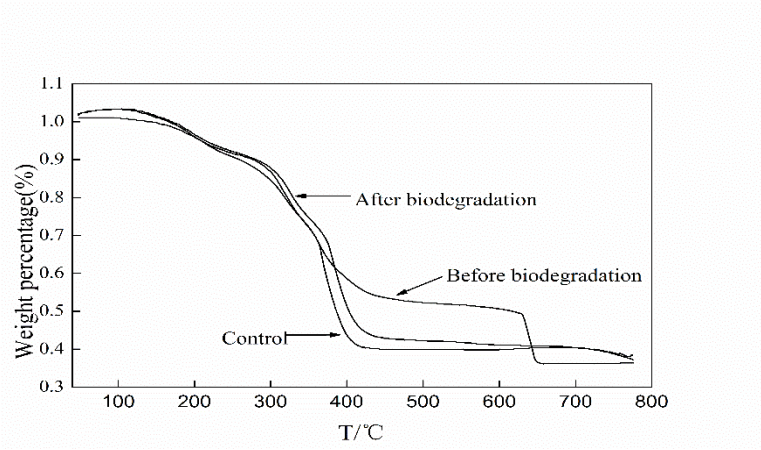

Fig. 3 TG profiles of PLW-g-(AA-co-MA): (a) before biodegradation, (b) control (control is the same experimental process to (c) except that control was non-inoculation), (c) after biodegradation

Optimization of the Grafting Variables

Effect of Initiator Content on Water Absorbency

As can be seen in Figure 4, the maximum absorbency in distilled water and 0.9 wt % NaCl solutionwere 1618 g/g and 136g/g, respectively, at 0.2 wt% of APS initiator. The water absorption initially increased and then decreased as the increasing amount of initiator, which was caused by the change of number of active free radicals in the reaction system. Excess initiator was prone to lead the primary radicals to terminating the chain propagation reaction, cause degradation of free radical of collagen backbones and produce possible phenomenon referred to as “self cross-linking”, resulting in low water absorbency.(Pourjavadi and Kurdtabar 2007)

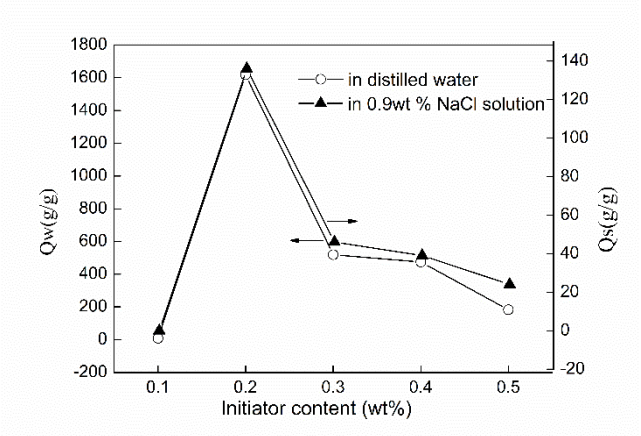

Fig. 4 Influence of mass content of initiator on the absorbency of PLW-g-(AA-co-MA)

Effect of Cross linker Content on Water Absorbency

As exhibited in Fig. 5, the water absorbency presented an increase value with the increasing content of MBA while the excess MBA caused a decrease to absorbency, which could be supported by the fact as follows. No network structure was formed at a low concentration of crosslinker and water could be only absorbed by the hydrophilic groups on the surface of the hydrogels, thus the absorbency remained low. Nevertheless, very high concentration of crosslinker would result in

excessively high crosslinking density and smaller voids in the network (Cheng Zet al. 2013),which leads to a cross-linked rigid structure that cannot be expanded to hold a large quantity of water.

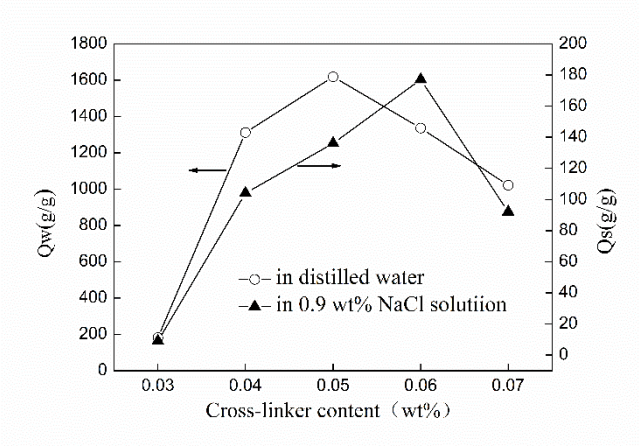

Fig. 5 Influence of mass content of cross-linker on absorbency of PLW-g-(AA-co-MA).

Effect of Weight Ratio of AA to MA on Water Absorbency

In Fig. 6,we observe that the absorbency is substantially increased with increasing of AA/MA ratio followed by a decrease. The change can be owed to both the decreased repulsive forces between neighboring chains and the osmotic swelling pressure produced by the moderate content of ionization of carboxylic groups, because of a less amount of carboxylate groups along with the more amide groups caused by partially ammonized MA, which allows the polymer coils to expand more easily. When the AA content further increased,AA molecules were self-polymerized and highly crosslinked and the excess of ionic units leadto an increase in the solubility of the copolymer at a fixed crosslinker concentration(Mohan,Murthy,Sudhakar 2006),hence the swelling ratio decreased.

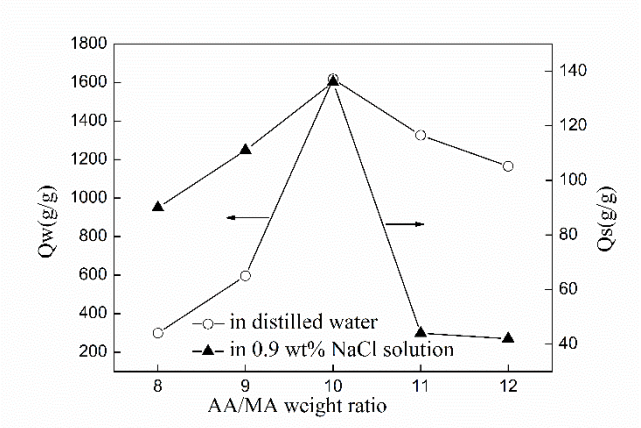

Fig. 6 Influence of AA/MA weight ratio on absorbency of PLW-g-(AA-co-MA).

Effect of Neutralization Degree of AA on Water Absorbency

Fig. 7 shows that when neutralization degree of AA was 77%, the absorbency reached themaximal value. At a low degree of neutralization, the grafting reaction was too fast to control, which decreased the absorbency. With increasing degree of neutralization, the concentration of –COO ¯ increased,which resulted in an enhancement of electrostatic repulsion among the COO ´ groups that can expand the network of the hydrogels and an improvement of osmotic pressure, favoring higher

absorbency (Cheng W et al.2015). However, when the degree of neutralization was over 77%, the activity of AA monomers decreased, thus the reaction rate decreased and solubility increased, decreasing the absorbency.

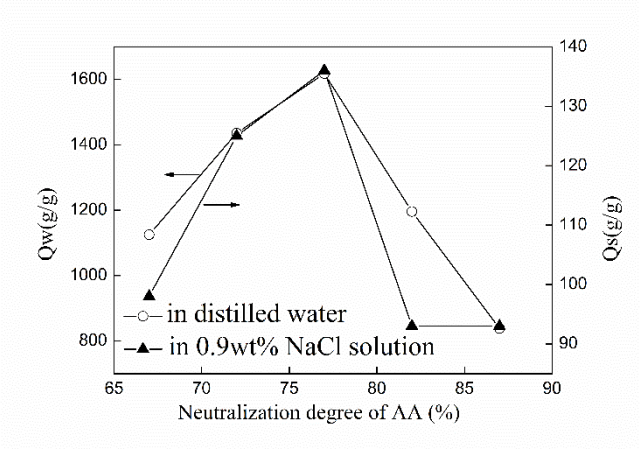

Fig. 7 Influence of neutralization degree of AA on water absorbencyof PLW-g-(AA-co-MA).

Effect of Ammonization Degree of MA on Water Absorbency

Fig. 8 shows that when ammonization degree reached 50%, water absorbency rate reached the maximumvalue. This phenomenon can be explained using the bellow fact.At a low ammonization degree, a considerable part of the MA fail to generate -COO^- and - $CONH_2$, leading a low absorbing capacity. When the ammonization degree is too high, high content of ammonium salt decreased the reaction rate, making the polymer to be more water solubility,and the water absorbency rate decreased.

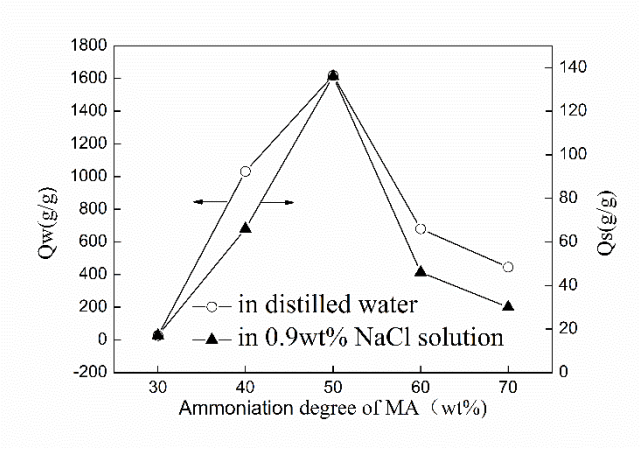

Fig. 8 Influence of ammonization degree of MA on water absorbency of PLW-g-(AA-co-MA).

Biodegradation

Identification and Optimal Growth Conditions of the strain

The strain,characterized as gram-negative,was small dot,milky white and smooth on LB plate. In addition, the16S rRNA partial gene sequence of this bacterium were aligned and compared with the 16S rRNA bacterial gene sequences in GenBank and the results indicated that it bore the closest relationship to *Ensifer* sp with 98% of sequence similarity(GenBank accession no.KX011911)(As shown in Fig. 9). The temperature and pH of *Ensifer* sp.Y1, incubated in LB medium, were studied by

measuring optical density at 600 nm (OD_{600}) using UV-visible spectrophotometer. As shown in Fig.10 (a), the highest growth rate was achieved at 25 ^{o}C and from Fig.10 (b), we can see that the highest growth was achieved at pH 7.0.

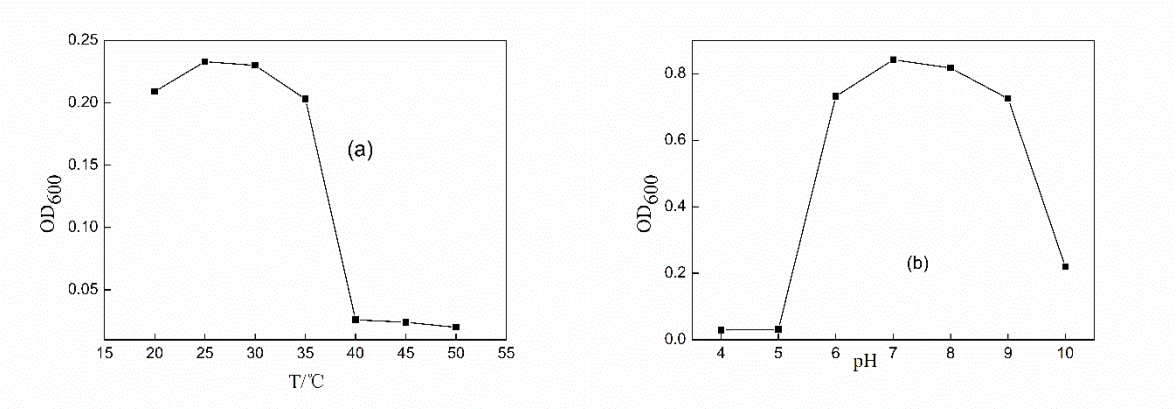

Fig. 10 (a) Effect of temperature and (b) pH on growth of *Ensifer* sp.Y1.

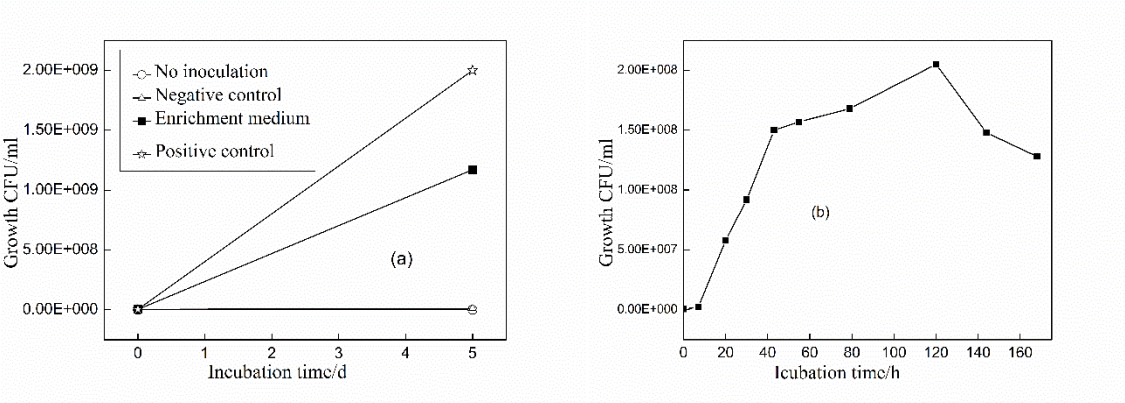

Fig.11 (a) Growth of Ensifer sp.Y1 in different carbon sources; (b) Growth curve of Ensifer sp.Y1 in PLW-g-(AA-co-MA) medium.

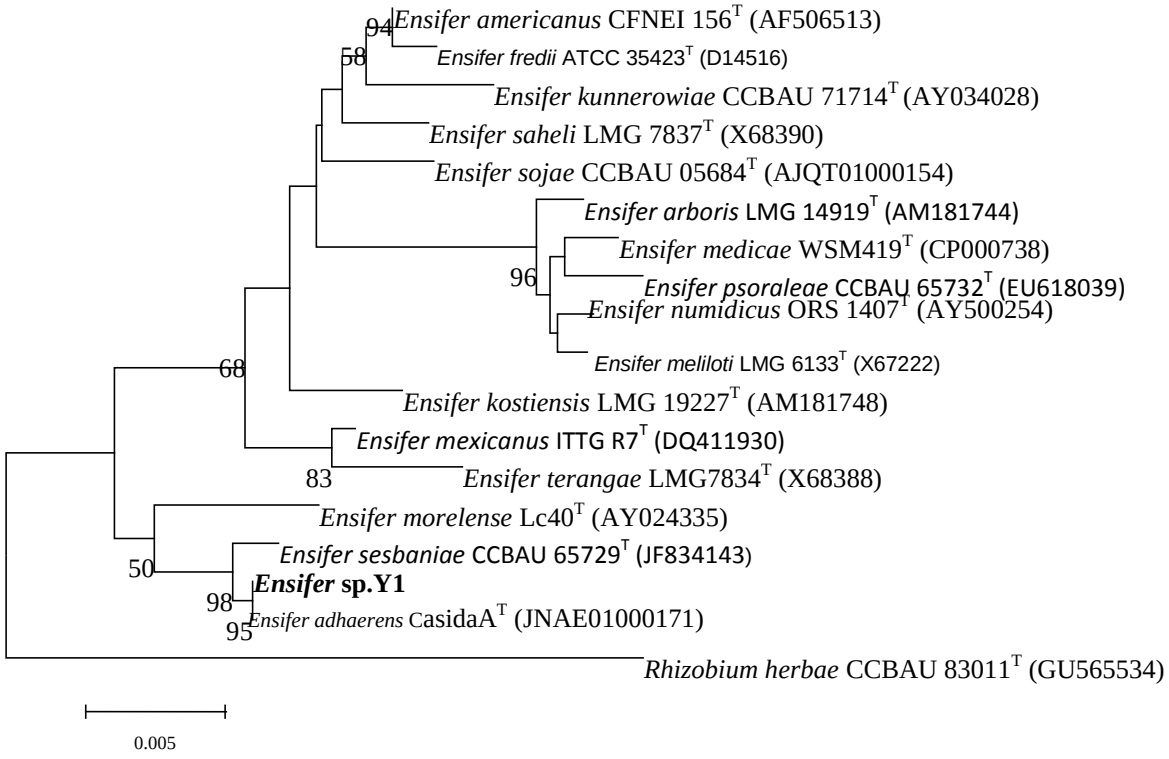

Fig. 9 Neighbor-joining phylogenetic tree, based on 16S rRNA gene sequences, showing the relationship between strain *Ensifer* sp.Y1 and related taxa. Bootstrap values (%) are based on 1000 replicates and are shown for branches. Bar, 0.005 substitutions per nucleotide position.

Utilization of PLW-g-(AA-co-MA) by Ensifer sp.Y1 to Grow

To explore the utilization of PLW-g-(AA-co-MA) by Ensifer sp.Y1 to grow, this strain was inoculated in MSM with a pH of 7.0 containing different carbon source (non-carbon source, PLW-g-(AA-co-MA) and peptone, respectively) and was incubated at 25 ^{o}Cin an orbital incubator shaker operated at 120 rpm. Since the gel imparted an initial turbidity to this medium, turbidometric measurements were rendered difficult (Gosavi, Deopurkar and Ghole 1999), so growth of this strain was monitored by the spread plate method on LB Nutrient agar plates (Olsen and Bakken 1987). Fig.11 (a) showed that PLW-g-(AA-co-MA) can support the growth of Ensifer sp.Y1 while there is a little growth in none carbon source and no growth in no inoculation. From Fig.11 (b), we can observe that 120 h were optimal for Ensifer sp.Y1 growth in Collagen-based SAP medium. SEM images (Fig. 2) showed that the morphology of collagen-based SAP after the biodegradation (c) was destructed seriously compared with the morphology before biodegradation (a) and control (b). TG was performed to investigate how biodegradation affected thermal stability of samples (Fig. 3). The non-biodegraded sample underwent two major changes in thermal stability during TG, but the sample that degraded in bacteria culture and control showed only one thermal-degradation stage, which was due to the reduction of molecular weightand loss of the protein component. The control showed that the process of sterilization by autoclaving, being immersed in MSM solution and re-drying had effect on

the structure of samples, which followed to the fact that increasing recycle times of SAPs caused a decrease to absorbency. However, the sample degraded in bacteria culture had a higher thermal stability temperature than samples of before biodegradation and control because of the higher biodegradation of small molecular weight chains and amorphous regions, leaving the higher concentration of difficult decomposition components (Yang S and Madbouly 2015; Kim 2006).

Conclusion

In the present study, an eco-friendly and biodegradable superabsorbent polymer (PLW-g-(AA-co-MA)) was constructed by free-radical graft copolymerization of AA, MA and LW. The optimal synthesis conditions and biodegradability of this polymer were investigated. Optimum reaction conditions to obtain the maximum absorbency of1618 g/g in distilled water (177 g/g in 0.9 wt% NaCl solution) were found to be: Cross-linking agent 0.05 wt% of monomer mass, AA neutralization degree77%, AA:AM =10, initiator 0.2 wt% of monomer mass and ammonization degree of MA 50%. Additionally, the biodegradability was studied through microorganisms enrichment culture technique utilizing PLW-g-(AA-co-MA) as the sole source of carbon. The optimal growth conditions of this strain isolated from soil, identified as Ensifer sp. Y1, were pH 7.0 and temperature 25 ^{o}C. The test of utilization of PLW-g-(AA-co-MA) by Ensifer sp.Y1 to grow and the SEM images of PLW-g-(AA-co-MA) degraded by this bacteria exhibited that Ensifer sp.Y1 has an excellent ability to degrade PLW-g-(AA-co-MA). Both the excellent water absorbency and biodegradability of PLW-g-(AA-co-MA) showed that the introduction of the wastes into superabsorbent is a green and sound method of utilizing leather wastes.

Acknowledgements

The work was financially supported by the National Natural Science Foundation of China (21176162)

References

Bao Y, Ma J, Li N. Synthesis and swelling behaviors of sodium carboxymethyl cellulose-g-poly (AA-co-AM-co-AMPS)/MMT superabsorbent hydrogel[J]. Carbohydrate Polymers, 2011

Cheng W M, Hu X M, Wang D M, et al. Preparation and Characteristics of Corn Straw-Co-AMPS-Co-AA Superabsorbent Hydrogel[J]. Polymers, 2015, **7(11)**: 2431-2445.

Cheng Z, Li J, Yan J, et al. Synthesis and properties of a novel superabsorbent polymer composite from microwave irradiated waste material cultured Auricularia auricula and poly (acrylic acid-co-acrylamide)[J]. Journal of Applied Polymer Science, 2013, **130(5)**: 3674-3681.

Gosavi U R, Deopurkar R L, Ghole V S. Microbial degradation of superabsorbent HSPAN gel by an indigenously isolated bacterial culture[J]. Macromolecules, 1999, **32(13)**: 4264-4271.

Hamer G. Solid waste treatment and disposal: effects on public health and environmental safety[J]. Biotechnology Advances, 2003, **22(1)**: 71-79.

Hoffmann J, Řezníčková I, Kozáková J, et al. Assessing biodegradability of plastics based on poly (vinyl alcohol) and protein wastes[J]. Polymer degradation and stability, 2003, **79(3)**: 511-519.

Hu Z, Shouhong Y, Tang Y. Synthesis and urea-loading og a novel biosuperabsorbant polymer based on leather waste[J]. Journal of the Society of Leather Technologists and Chemists, 2015, **99(2)**: 51-57.

Jian S, Wenyi T, Wuyong C. Ultrasound-accelerated enzymatic hydrolysis of solid leather waste[J]. Journal of Cleaner Production, 2008, **16(5)**: 591-597.

Kanagaraj J, Velappan K C, Chandra Babu N K, et al. Solid wastes generation in the leather industry and its utilization for cleaner environment-A review[J]. Journal of scientific and industrial research, 2006, **65(7)**: 541-548.

Kim H S, Kim H J, Lee J W, et al. Biodegradability of bio-flour filled biodegradable poly (butylene succinate) bio-composites in natural and compost soil[J]. Polymer Degradation and Stability, 2006, **91(5)**: 1117-1127.

Langmaier F, Mokrejs P, Kolomaznik K, et al. Biodegradable packing materials from hydrolysates of collagen waste proteins[J]. Waste Management, 2008, **28(3)**: 549-556.

Langmaier F, Mokrejs P, Kolomazník K, et al. Cross-linking epoxide resins with hydrolysates of chrome-tanned leather waste[J]. Journal of thermal analysis and calorimetry, 2006, **88(3)**: 857-862.

Li A, Zhang J, Wang A. Utilization of starch and clay for the preparation of superabsorbent composite[J]. Bioresource Technology, 2007, **98(2)**: 327-332.

Liang R, Yuan H, Xi G, et al. Synthesis of wheat straw-g-poly (acrylic acid) superabsorbent composites and release of urea from it[J]. Carbohydrate Polymers, 2009, **77(2)**: 181-187.

Masuda F. Onlap and downlap patterns in Plio-Pleistocene forearc and backarc basin-fill successions, Japan[J]. Sedimentary Geology, 1994, **93(3)**: 237-246.

Olsen R A, Bakken L R. Viability of soil bacteria: optimization of plate-counting technique and comparison between total counts and plate counts within different size groups[J]. Microbial Ecology, 1987, **13(1)**: 59-74.

Pourjavadi A, Kurdtabar M. Collagen-based highly porous hydrogel without any porogen: Synthesis and characteristics[J]. European Polymer Journal, 2007, **43(3)**: 877-889.

Pourjavadi A, Kurdtabar M, Mahdavinia G R, et al. Synthesis and super-swelling behavior of a novel protein-based superabsorbent hydrogel[J]. Polymer bulletin, 2006, **57(6)**: 813-824.

Sadeghi M, Hosseinzadeh H. Synthesis and super-swelling behavior of a novel low salt-sensitive protein-based superabsorbent hydrogel: collagen-g-poly (AMPS)[J]. Turkish Journal of Chemistry, 2010, **34(5)**: 739-752.

Surhio M A, Talpur F N, Nizamani S M, et al. Complete degradation of dimethyl phthalate by biochemical cooperation of the Bacillus thuringiensis strain isolated from cotton field soil[J]. RSC Advances, 2014, **4(99)**: 55960-55966.

Thakur V K, Thakur M K, Raghavan P, et al. Progress in green polymer composites from lignin for multifunctional applications: a review[J]. ACS Sustainable Chemistry & Engineering, 2014, **2(5)**: 1072-1092.

Ya-li F, Wei-da W, Xin-hua T, et al. Isolation and characterization of an electrochemically active and cyanide-degrading bacterium isolated from a microbial fuel cell[J]. RSC Advances, 2014, **4(69)**: 36458-36463.

Yang S, Madbouly S A, Schrader J A, et al. Characterization and biodegradation behavior of bio-based poly (lactic acid) and soy protein blends for sustainable horticultural applications[J]. Green Chemistry, 2015, **17(1)**: 380-393.

Zhang J, Zheng J W, Liang B, et al. Biodegradation of chloroacetamide herbicides by Paracoccus sp. FLY-8 in vitro[J]. Journal of agricultural and food chemistry, 2011, **59(9)**: 4614-4621.

Zhang Y, Liang X, Yang X, et al. An eco-friendly slow-release urea fertilizer based on waste mulberry branches for potential agriculture and horticulture applications[J]. ACS Sustainable Chemistry & Engineering, 2014, **2(7)**: 1871-1878.

Zhang Y N, Cui J Y, Xu S A. Effects of chain structures of corn starches on starch-based superabsorbent polymers[J]. Starch-Stärke, 2015, **67(11-12)**: 949-957.

Zohuriaan-Mehr M J, Kabiri K. Superabsorbent polymer materials: a review[J]. Iranian Polymer Journal, 2008, **17(6)**: 451.

IVL P-40

FIRE RETARADANT LEATHER FOR FIRE SAFETY APPLICATION

Wegene Demisie Jima[#], Mahamani Arumugam and Thanikaivelan Palanisamy

Leather Garment & Goods Manufacturing Technology Directorate, Leather Industry Development Institute, P.O.Box 24692 Code 1000, Addis Ababa, Ethiopia

Co-ordinator, Research and Development Cell, Department of Mechanical Engineering, Sri Venkateswara College of Engineering and Technology, Chittoor-517127,(A.P) , India

Advanced Materials Laboratory, Central Leather Research Institute (Council of Scientific and Industrial Research), Adyar, Chennai 600 020, India. Email: thanik8@yahoo.com

Leather is used for various purposes including upholstery, clothing, footwear and gloves. Leathers meant for lifestyle applications are close to the human being and the safety of human life can depend on such components in case of the items exposed to fire sources. Here, we report a simple method to produce fire resistive leather using organic nanoclay and ammonium dihydrogen phosphate (ADHP) as flame retardant additives in leather finishing process. Treated leathers were characterized by vertical flame test, tear and tensile strength and thermogravimetric analysis (TGA). We demonstrate that the fire resistance properties of leather improved through treatment with nanoclay and ADHP. Leather treated with 10 wt. % nanoclay left more than 20% residue than control leather at 700^{o}C, which indicates the lower decomposition of treated leather as seen by TGA. Additionally, a slight improvement in tear strength was noticed while tensile strength and percentage elongation not altered. Further, we demonstrate that the ignition time for treated leather has increased by more than 5 sec and it did not show any flame time after fire source was removed. In general, leather treated with lower content of organic clay (less than 10 wt. %) in combination with ADHP shows better flame retardance as well as physical properties and can be used for higher fire safety application especially for upholstery products.

Key Words: Nanoclay, Ammonium dihydrogen phosphate (ADHP), Flame retardance, Upholstery, Thermogravimetric analysis (TGA), vertical flame

1. Introduction

Leather is used for various purposes including upholstery in airplanes, ships and furniture in public buildings, clothing, footwear and gloves (Gautieri et al. 2011). Car, airplane and home furniture manufacturers demand high performance leather for upholstery production. Leather used for such use have to be checked for different tests such as flame retardancy than those used for shoes, garment and gloves, especially when used for airplane and car upholstery. The manufacturer of furniture's for home, automobile and airplane additionally consider the method of protecting furniture's from burning in times of accident/ expose to fire source. These need and other factors motivate researchers to develop the materials that have longer ignition time for component design and used for numerous purposes including upholstery. Upholstery was the component of any car/plane/home furniture close to the human being and the safety of human life can be depends on such components in case of the items exposed to fire sources (Kozłowski et al. 1999).

Although leathers have much better flame retardant property than fabric and plastic materials, its use in high fire safety application requires improvement in fire resistance. Safety requirement for commercial aircraft, automotive and building currently accessed by the reaction of material to fire, fire retardant ability and environmental impact of fire additives (Przybyłek 2003).

Flame retardants are additives added to materials such as plastics, textiles, leathers and others through surface finishes and coatings to prevent the spread of fire by inhibit and/or delay the production of flames. A different chemicals were used as flame retardants and those chemicals can also combined for better effectiveness. Flame retardant chemicals inhabits the flame production by one of the following ways:-promotion of excess char formation, generating non-flammable gases and forming a glaze barrier at the surface (Troitzsch 1990).

Among fire resistance additives utilized up to date boron comprising and halogenated fire additives are widely used as fire additive due to generating large volumes of non-flammable gases and creating a glass coating during thermal decomposition. Even though halogenated fire additives are successful in fire retardant have been reported to form toxin that affects environment and humans (Li et al., 2010; Oulton, 1995 and Martin et al., 2006). It also reported that boron containing fire retardants loses its properties by washing. Phosphorus based treatment with stand repeated wash cycle, reduce volatile fuel and increase carbonaceous char (Wakelyn et al. 2007). Due to these phosphorus based flame retardants is the most success full and commercially used flame retardant (Jash and Wilkie 2005). Recently, nano clay montmorillonite and bentonite added to materials in low content (2-5 wt. %) can reduce flammability and heat resistance (Li et al. 2010;Horrocks et al. 2007 andBourbigot et al. 2002).

Nowadays there are an attempt for development of leather products with flame retardant properties, which fit to the standards and demands of the automobile and the aircraft industries. The

flame retardant properties imparted to the products through different leather process steps by applying coating agents containing flame retardant additives. Some additive affect the environment, increase the cost of leather products even though impart sufficient flame retardant properties to leather (Olivares et al. 2014). Preparation of clay polymer nanocomposites (CPNC) is one of the strategies developed in the last decades for imparting flame retardant properties to polymer materials. CPNC have verified as the materials that reduce the flammability of the base polymeric materials in lower concentration and used as substitute for halogenated based flame retardant additives (Olivares et al. 2014; Gilman 1999 and Kiliaris and Papaspyrides 2010).

The aim of this work was to improve fire retardant property of leather using montomorillonite nano clay and ammonium dihydrogen phosphate by surface coating. The influence of fire retardant materials concentration and method of coating were also studied. Tensile and tear strength test, vertical flammability test and thermogravimetric analysis (TGA) are used for studying the flammability and fire retardant properties of the sample product.

2. Materials and methodology

2.1. Materials: Nano clay, MMT surface-treated contains 35-45 wt. % dimethyl dialkyl (C14-C18) amine as the organic modified and ammonium dihydrogen phosphate andwere procured from Sigma Aldrich and used as fire retardant additives. This clay had lateral dimension of 200-300 nm and thickness of 1nm. After surface treatment the particle had size less than 10 micro meter. Black pigment (PP18032) and resin binder (23700) supplied by STAHL chemical laboratories were used as received. Protein binder (Lustral-UT) and wax were purchased from ALPA International private limited. Polyurethane, penetrator, dye solution were procured from Tfl Quinn India Private Limited. Sodium chloride procured from Himedia Laboratories Pvt.Ltd used to reduce viscosity. Leather was purchased from tannery in Chennai and used as base material.

2.2 Procedure for solution preparation and leather treatment: Suspension of nanoclay were prepared by mixing 3, 7, 5 and10 wt. % of leather or 3wt.% of nanoclay/ 2, 5wt.% of ADPH in distilled water and stirring for 1 hour at 700 rpm . Sodium chloride 3% wt. of nano clay were added to reduce the viscosity. Leather was treated with this solution during finishing process. For finishing operation, the above solution were mixed with leather finishing solution prepared. After solution preparation the solution was sprayed on white crust leather through 4-6 cross coating. Drying was takes place between each coat for better absorption. After drying for three hours lacquer/ water at 1:1 ration sprayed on surface of leather through single cross coat to give shiny look. The coated leather where plain plate at 100^{o}C/80pa to insure crosslink of finishing chemicals with leather and further shiny surface. Finally, treated leather was dried at 35 ^{o}C atmosphere before characterization.

2.3 Characterization

Flame retardant property: The fire hazard of a material is determined by a combination of factors including the sample ignition, the heat released during combustion, the total heat released, the

diffusion rate of flame, the production of smoke and its toxicity. Rate of heat release has been described as best fire hazard defining properties so far. Two conditions are necessary for the fire to spread from a material to another and/or to its environment. Firstly, the energy released by first material must be sufficient to ignite the second. Secondly, the heat release must be sufficiently fast not to be cooled by the ambient colder air. By using the cone calorimeter, the various parameters stated above can be measured with the same instrument, while simulating the real conditions of a fire (Zhu et al. 2002).The reaction to fire of treated and untreated crust leathers were evaluated using a vertical flammability test based on procedure defined in ASTM D 6413. The vertical flammability test was used to determine the time to ignition and after flame time.

Thermal stability: The thermal stability of leather can be affected by the presence of flame additives. For this reason, thermogravimetric analysis (TGA) was carried out in a TA-Instruments Q50 analyzer by placing samples in alumina pans and heating rate (ramp 20 °C/min to 700.00 °C) under 60 ml/min nitrogen and air atmosphere gas flow.

Physical Testing: Tensile strength used to determine the load required to break a leather test specimen having a 10 mm width. The load to rupture divided by the original un-stretched cross-sectional area gives the tensile strength according to tensile strength of leather/ ISO 3376:2002/IUP 6/ SATRA TM 43. The specimen shall be cut from the test unit of leather by means of a die and conditioned (conditioned at 20 oC and 65 relative humidity) in accordance ISO 3376:2002/IUP 6. The direction of the long dimension in relation to the backbone shall be noted. Tearing strength of leather measured according to SATRA TM 162 tear strength of leather /ISO 3377:2002/IUP 8 double edge tear/IUP 40 single edge tear standard test method. This test method is intended for determining tear strength of leather by measuring the force required to tear a specimen cut perpendicular to the surface and conditioned at 20 ^{o}C and 65 relative humidity. The specimen were a rectangular piece of leather, 1 × 4 in. (25.4 × 101.6 mm) by the full thickness of the unit. It shall have a 3⁄16 in. (4.76 mm) hole located on the long axis 1 in. (25.4 mm) from one end and shall be split along its axis from the hole to the other end to form two tongues. The direction of the specimen relative to the backbone shall be noted.

3. Result and Discussion

3.1 Flame Property of Treated Leather: Ignition time of treated and control leather shown in Table 1. Three ignition time recorded for each sample and average value calculated. The sample exposed to candle fire source in vertical position and the time to capture the leather were recorded by digital clock. As seen in Table 1 ignition time for treated sample were more than untreated one. The control leather start capturing fire after 8 seconds while leather treated with 10 wt. % of leather capture leather after 13 seconds in Table 1.

There is no much change as concentrations of nanoclay varies. The burning behavior for all concentrations are the same. However, the leather treated with 3wt. % of nano clay and 2wt. % of ammonium dihydrogen phosphate burns slowly and smoking. After removing fire source time observed on the treated sample for few seconds compared to long time for control leather. After

ignition time also reduced as concentration of nanoclay increased but with fewer magnitude between subsequent concentration. Additionally, both treated and control leather burned without melting. However, time to burn and change to char were higher for treated leathers. In contrast, leather treated with combination of nanoclay and ADHP shows better flame retardancy and after ignition the fire removed from sample earlier than other samples. However, leather treated with two combination were burns with smoke and a little melt. Additionally, since ADHP was water soluble the treated leather loose its properties after frequent wash. This draw back can be solved by encapsulation of ADHP before leather treatments.

Table 1 Ignition time of control and treated leather with different nanoclay concentration

Trial	Control	3wt.%NC	5wt.% NC	7wt.% NC	10wt.% NC	3wt.% NC/ADHP
Ignition time 1	7:85	9:02	10:12	9:45	10:65	10:17
Ignition time 1	8:09	7:93	9: 73	11:25	17:77	14:59
Ignition time 1	10:12	11:07	10:43	12:13	13:84	17:84
average	8:68±1:0	9:34±1:3	10:9±0:28	10:94±1:11	14:08±2:91	14.2±3:14

3.2 Thermogravimetric analysis (TGA): When leather heated, its contribution to fire described by formation of volatile fuel gas by breaking down of triple helix molecular chain which leads to reduction of mass and elimination of monomers. This reduction of mass as function of temperature were measured by TGA. TGA result of control leather and treated leather were shown in Figure 1. Additionally, the residue amounts for the control leather and each coated leather are summarized in Table 2. Leather degraded through three main steps with temperature of maximum degradation approximately 86.98 ^{o}C (Table 2) which results residue of 94.57%. This loss of mass corresponds to the collagen which is the main component of leather (Budrugeac et al. 2003; Kaminska and Sionkowska 1996). The residue at $T_{max\,1}$ further degrades by oxidation by forming other carbonaceous species to give other mass loss at $T_{max2.}$ Further the residue at T_{max2} oxidized and loss mass and providing maximum mass loss which was 23.36% at 700 ^{o}C (Table 3).

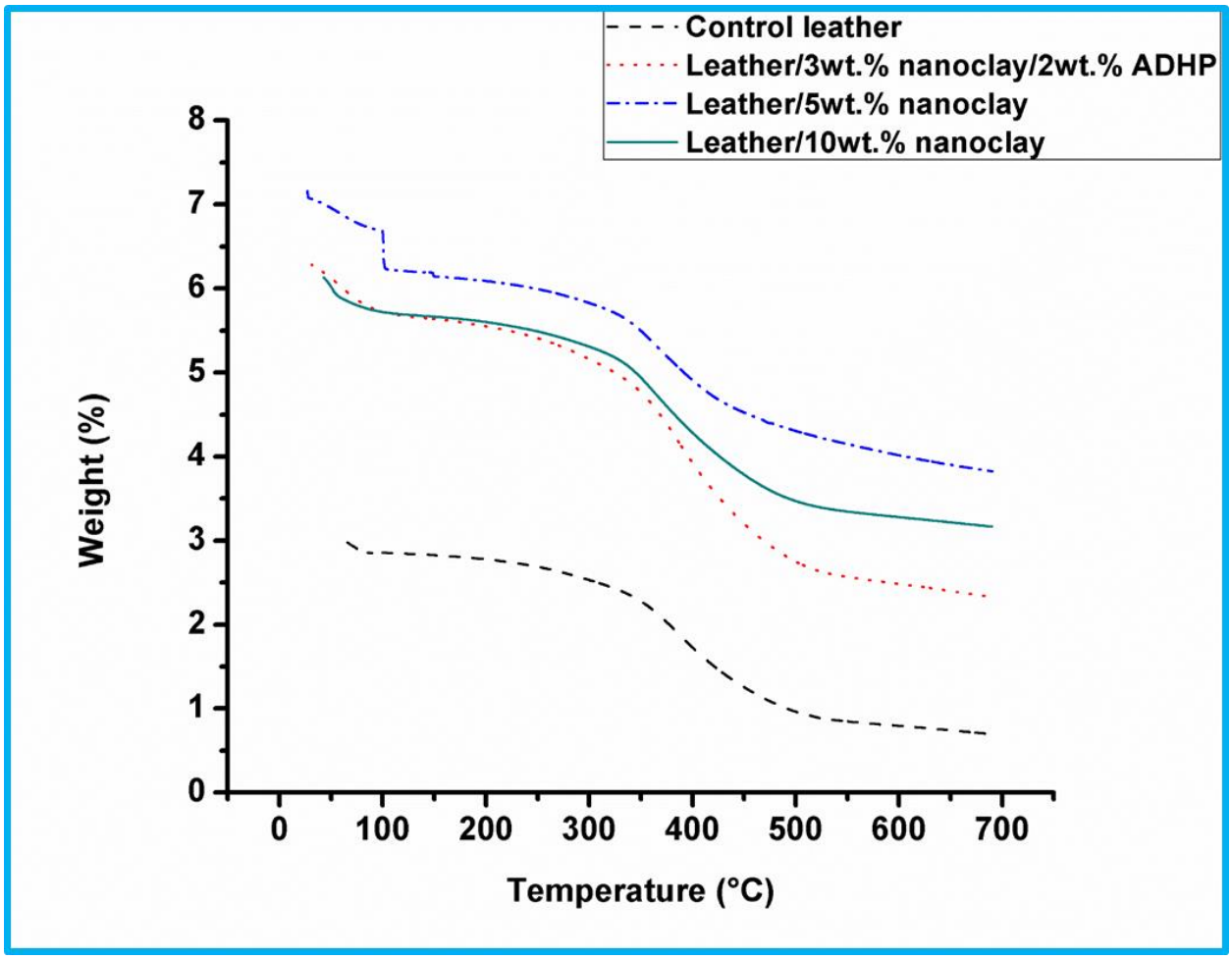

Figure 1 TGA of control leather, leather treated with 3 wt. % nanoclay/2wt.% ADHP, leather treated by 5wt. % and 10wt.% nanoclay at heating rate of 20 ^{o}C/min

Thermal stability of leather affected by nanoclay particles. The presence of nano clay protect leather against thermal degradation which evidenced by shift of TGA curves towards higher temperature Tmax 1 (Table 2). The residue at T max 1 were higher for leather treated with nanoclay as well as nanoclay/ ADPH combination which indicates the thermal degradation of treated leather where lower than control leather. Surprisingly Tmax 1 for treated leather were lower than control leather. This may be due to some of tread leather with nanoparticles start oxidation at Tmax 2 in contrast to control leather in which all sample weight loss start at Tmax 1. By doing so higher residue concentration at 700 ^{o}C for treated leather were recorded. There is small variation in residue and temperature shift for different nanoclay and ADPH concentration treated leather. This may be due to natural properties of leather in which properties are different at different part of leather. Leather treated with both nanoclay and ADPH/ nanoclay combination shows higher residue at three leather degradation steps. Hence treated leather have better fire resistance than control leather.

Table 2 TGA data for control and treated leather at maximum degradation temperature and resulting residues

Sample	$T_{max\ 1}$	$T_{max\ 2}$	$T_{max\ 3}$	Residue at Tmax 1(%)	Residue at Tmax 2(%)	Residue at Tmax 3(%)	Residue at 700 (%)
Control leather	86.98	240.66	522.83	94.57	90.84	29.86	23.36
Leather/3wt.%NC/2wt.% ADPH	50.87	204.40	510.89	97.38	88.18	42.77	36.99
Leather/5wt.% NC	94.94	337.74	500.28	93.46	82.78	56.57	51.63
Leather/10wt.% NC	109.54	329.12	469.76	86.87	79.35	61.79	53.39

3.3 Physical properties of leather: The physical properties are changed by the method in which the chemical process is performed. Tensile strength, tear strength and percentage elongation for example, can be influenced by the tannin, re-tanning and finishing operations. Even though finishing operation didn't have significant impact on the physical properties of leather. The finishing mixture and method of treatment can improve or reduce the physical properties of leather. Hence, we tested tensile strength, tear strength and percentage of elongation of treated leather. The addition of nanoclay and ammonium hydrogen phosphate has no major impact on the physical properties of leather. There is a little difference in look between coated and uncoated fabric especially for higher nanoclay concentration. The color of leather treated with higher nanoclay concentration was light and not shiny. Softness assessment of the leather (by touch of hand) is also reduced for higher nanoclay concentration.

Table 3 Tearing strength and Tensile strength properties of coated and uncoated leathers

sample	Tear strength (N/mm)	Tensile strength (N/mm^2)	Elongation at break (%)
Control	43.88±2.9	22.40±2.6	68.01±8.96
3 wt.% NC	44.04±3.5	21.3±1.2	63.92±4.0
5 wt.% NC	42.17±5.01	24.5±2.1	56.42±7.45
7wt.% NC	47.23±0.85	24.2±2.7	67.42±6.0
10wt.% NC	53.43±4.5	25.09±2.0	68.59±11.0
3wt. NC/2wt.% ADHP	32.17±4.3	19.5±0.7	67.26±4.45
3wt.%NC/5wt.%ADHP	31.5±1.8	18.82±1.70	69.67±7.50

However for lower nanoclay content (below 7wt. % of leather) coated and uncoated samples feel the same. This implies to maintain softness and color tone of treated leather the addition of fire

retardant leather has to be kept below 7wt.% of leather. The tearing strength of coated and uncoated leather shown in Table 3 exhibited slight improvement in tearing strength for nanoclay while reduction in nanoclay/ADHP combination. The data shows improvement of tear strength as the clay content increases while addition of ADHP reduces the tearing properties of leather. The redaction in tear strength of 5wt. % of nanoclay content may be due to leather defects which inherited due to natural or leather tanning conditions. Tensile strength data also shows unclear decrease or increase in the strength properties of leather. The change in data mostly due to natural properties of leather in which properties change from leather to leather and different part of the same leather. There is no big change in elongation at break also as seen form Table 3. Hence, we concluded there is no change in tensile strength and elongation due to addition of fire retardant nanoclay while nanoclay/ADHP increases the elongation of treated leather.

4. Conclusion

A simple method to produce flame retardant leather were demonstrated using organic nanoclay and ammonium dihydrogen phosphate (ADHP) as flame retardant additives. The two additives used separately and in combination to achieve optimum fire resistance properties. Fire resistance properties of leather improved through treatment of leather by flame retardant nanoclay and ADHP. TGA confirms treated leather left higher residue at 700 ^{o}C after heating the sample at 20 ^{o}C/min. Leather treated with 10wt.% nanoclay left residue more than 20% residue than control leather. TGA also confirms treated leather left higher residue than control leather for all three leather degradation steps.

Physical test shows slight improvement in tear strength while tensile strength and percentage elongation did not altered. The tear strength of leather treated with 10 wt. % of organic nano clay exceed the control leather tear strength value by 10N/mm.

The control leather start capturing fire after 8 seconds while leather treated with 10 wt. % of NC and leather treated with NC/ADHP capture leather after 13 seconds. The burning behavior for all concentrations are nearly the same. After removing fire source time observed on the treated sample for few seconds compared to long time for control leather. After ignition time also reduced as concentration of nanoclay increased but with fewer magnitude between subsequent concentration. In general, leather treated with lower content of organic clay in combination with ADHP shows better flame retardant and can be used for higher fire safety application especially for upholstery products.

Acknowledgement

Authors thank Leather Industry Development Institute, Ethiopia and Central Leather Research Institute, India for providing financial support under Twinning Project-II.

5. Reference

1. Gautieri A, Vesentini S, Redaelli A, Buehler, M.J, Hierarchical Structure and Nanomechanics of Collagen Microfibrils from the Atomistic Scale Up. *Nano Letter* 2011, **11**, 757-766.

2. Kozłowski R, Mieleniak B, Muzyczek M, Fire Resistant Composites for Upholstery. *Polymer Degradation and Stability* 1999, **64**, 511-515.
3. Przybyłek M, Forming of Fire-resisting Properties of Leathers. *Materials Science* 2003, **9**, 281-283.
4. Troitzsch J; *International Plastics Flammability; Handbook*. 2nd ed., Hanser Publishing, New York, 1990.
5. Li YC, Schulz J, Mannen S, Delhom C, Condon B, Chang S C, Zammarano M, Grunlan J C, Flame Retardant Behavior of Polyelectrolyte, Clay Thin Film Assemblies on Cotton Fabric. *ACS Nano* 2010, **4**, 3325–3337.
6. Oulton D P; *Fire-Retardant Textiles in Chemistry of the Textiles Industry*; Carr C M, Ed., Springer, Berlin, 1995.
7. Martin C, Ronda J C, Cadiz V, Boron-Containing Novolac Resins as Flame Retardant Materials. *Polymer Degradation and Stability* 2006, **91**,747–754.
8. Wakelyn P J, Bertoniere N R, French A D, Thibodeaux D; *Cotton Fiber Chemistry and Technology*; CRC Press (Taylor and Francis Group), Boca-Raton, 2007.
9. Jash P, Wilkie C A, Effects of surfactants on the thermal and fire properties of poly (methyl methacrylate)/clay nanocomposites. *Polymer Degradation and Stability* 2005, **88**, 401-406.
10. Horrocks A R, Kandola B K, Smart G, Zhang S, Hull T R, Polypropylene Fibers Containing Dispersed Clays Having Improved Fire Performance. I. Effect of Nanoclays on Processing Parameters and Fiber Properties. *Journal of Applied Polymer Science* 2007, **106**, 1707–1717.
11. Bourbigot S, Devaux E, Flambard X, Flammability of Polyamide-6/Clay Hybrid Nanocomposite Textiles. *Polymer Degradation and Stability* 2002, **75**, 397–402.
12. Olivares G S, Solis A S, Calderas F, Medina L, Torres O, Manero, Blasio A D, Alongi J, Sodium montmorillonite effect on the morphology, thermal, flame retardant and mechanical properties of semi-finished leather. *Applied Clay Science* 2014, **102**, 254–260.
13. Gilman J W, Flammability and thermal stability studies of polymer layered-silicate (clay) nanocomposites. *Applied Clay Science* 1999, **15**, 31–49.
14. Kiliaris P, Papaspyrides C D, Polymer/layered silicate (clay) nanocomposites: An overview of flame retardancy. *Progress in Polymer Science* 2010, **35**, 902–958.
15. Zhu J, Start P, Mauritz K A, Wilkie C A, Thermal stability and flame retardancy of poly (methyl methacrylate)-clay nanocomposites. *Polymer Degradation and Stability* 2002, **77**, 253–258.
16. Budrugeac P, Miu L, Bocu V, Popescu C, () 'Thermal degradation of collagen-based materials that are supports of cultural and historical objects',*Journal of Thermal Analysis and Calorimetry* 2003, **72**, 1057-1064.
17. Kaminska A, Sionkowska A, Effect of UV radiation on the infrared spectra of collagen. *Polymer Degradation and Stability*1996,**51**, 19–26.
18. United Nations Industrial Development Organization (UNIDO); *Acceptable Quality Standards in the Leather and Footwear Industry;* Vienna. 1994

SYNTHESIS OF END-CAPPED FLUOROALKYL HYPERBRANCHED POLYMER LATEX AND ITS HYDROPHOBIC PROPERTIES IN LEATHER

Wei Xu, Sha Wang, Lifen Hao, Xuechuan Wang

College of Bioresources Chemical and Materials Engineering, Shaanxi University of Science and Technology, Xi'an Shaanxi, 710021, China;

College of Chemistry and Chemical Engineering, Shaanxi University of Science and Technology, Xi'an Shaanxi, 710021, China

Abstract

Fluoroalkyl-terminated hyperbranched polymers have attracted much attention due to their novel structures, unique properties, and potential application prospects. Especially, this structure will facilitate the fluorine enrichment on the material surface, thus, it is anticipated that higher application cost of the fluorine-contained polymers could be solved in the near future. In this work, polyurethane prepolymer (PU) with NCO terminal groups was manufactured by the stepwise polymerization of isophorone diisocyanate (IPDI), polyethylene glycol (PEG800) and dimethylolpropionic acid (DMPA). Then, fluorine-containing polyurethane prepolymer (FPU) with fluoroalkyl and NCO terminal groups was synthesized by reaction of perfluorohexyl ethyl alcohol and PU. Next, novel fluoroalkyl terminated hyperbranched polyurethane (FHBPU) was fabricated via the grafting reaction of FPU and hydroxy termianted hyperbranched polymer (HPAE). Finally, FHBPU latex was obtained by neutralization, adding water, and high-speed stirring operations and applied in the wet-blue goat waterproofing treatment. Infrared spectrum (IR), proton nuclear magnetic resonance (^{1}H NMR), Transmission Electron Microscope (TEM), nano particle size, and static contact angle analyzer were utilized to characterize structure of the resultants, particle morphology and average size, as well as hydrophobicity such as water contact angle on grain side of the treated crust leather. Results showed that final product had due structure. FHBPU latex particles presented irregular sphere with a polydispersity index of 0.261 and an average diameter of 238.8 nm. The treated crust leather by 1.6% FHBPU active ingredients based on the weight of wet-blue goat had favorable hydrophobicity and water contact angle on its grain side attained 142.9°.

Keywords:Hyperbranched polymer; Leather waterproofing; Polyurethane; Latex particle morphology

Corresponding author: Xuechuan Wang, Email: wangxc@sust.edu.cn

Postal address: College of Bioresources Chemical and Materials Engineering, Shaanxi University of Science and Technology, WeiYang District, Xi'an, Shaanxi, the People's Republic of China

1. Introduction

Being provided with excellent thermal and chemical stabilities, low surface-free energy, water and oil-repellency, etc, fluorine-containing polymers are often utilized as the hydrophobic materials in anti-fouling coatings (He et al. 2010; Xie et al. 2008; Yang et al. 2010). Furthermore, there is much promising prospect in leather water-proofing as the water repellent agent. However, the application cost of fluorine-containing polymers has to be maintained at the high-level due to the expensive provice of the fluorine-containing monomers. Therefore, it is an extremely challenging topic to minimize the fluorine monomer dosage in polymer formulation and simultaneously keep its application performance.

In recent years, hyperbranched polymers have attracted much attention by researchers related to novel structures, unique properties, and potential application prospects. Compared with ordinary polymers, hyperbranched polymers have a large number of active groups (Zhang et al. 2013; Zhang et al. 2014; Haraguchi et al. 2013). Thus, fluoroalkyl groups can be imported into the hyperbranched polymer molecules as therminals to prepare fluoroalkyl-terminated hyperbranched polymers via chemical modification. It is anticipated that the above-mentioned high application cost of fluorine-contained polymers could be solved in the near future. Since this structure will facililate the fluorine enrichment on the material surface and the fluorine dosage could be decreased to a less extent in the polymer formula.

In the present study, hydroxyl-terminated hyperbranched polymer was previously synthsized by the polycondensation of N,N-diethylol-3-amine-methylpropionate as an AB_2-type monomer with trimethylol propane (TMP) as the core moiety, proceeding in one-step procedure in the melt with p-toluenesulfonic acid (p-TSA)as catalyst. Polyurethane prepolymer (PU) with NCO terminal groups was manufactured by the stepwise polymerization of isophorone diisocyanate (IPDI), polyethylene glycol (PEG800) and dimethylolpropionic acid (DMPA). Then, fluorine-containing polyurethane prepolymer (FPU) with fluoroalkyl and NCO terminal groups was synthesized by reaction of perfluorohexyl ethyl alcohol and PU. Next, novel fluoroalkyl terminated hyperbranched polyurethane (FHBPU) was fabricated via the grafting reaction of FPU and hydroxy termianted hyperbranched polymer (HPAE). Finally, FHBPU latex was obtained by neutralization, adding water, and high-speed stirring operations and utilized in the wet-blue goat waterproofing treatment. We characterized structure of the

resultants, particle morphology and average size, ζ potential as well as hydrophobicity such as water contact angle on grain side of the treated crust leather.

2. Materials and methods

2.1. Reagents

Hyperbranched poly(amine-ester) polyol (HPAE) was prepared in our lab according to the reference Wang et al. (2010) and its structure diagram is shown in Figure 1. Isophorone diisocyanate (IPDI), polyethylene glycol (PEG800) and dimethylolpropionic acid (DMPA), of analytically pure grade, were purchased from Jining Baiyi Chemical Com. Ltd, China. Perfluorohexyl ethyl alcohol (S104) was industrial product and obtained from Harbin XEOGIA Fluorine-Silicon Chemical Co. Ltd., China. Acetone, dimethyl formamide (DMF), dibutyltin dilaurate (DBTDL) and triethylamine were purchased from Tianjing Fucheng Chemical Reagent Factory, analytically pure and used as received. Goat wet blue was previously processed in our lab using conventional technology and used as the experimental skin for hydrophobicity analysis.

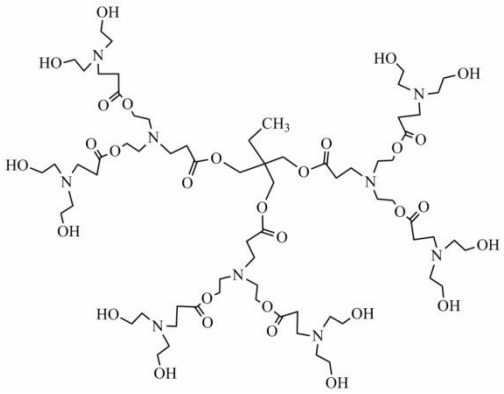

Figure 1. The structural representation of HPAE

2.2 Synthetic procedure for end-capped fluoroalkyl hyperbranched polymer latex (FHBPU)

In a four-necked flask equipped with a mechanical stirrer, a reflux condenser and a thermometer, PEG800 and DMPA were added according to the stoichiometric ratio, dissolved by appropriate acetone, and then bubbled by N_2 for 10 minutes. Suitable amount of IPDI was slowly dropt into the system and a few drops of catalyst DBTDL was also added. The system was gently stirred at 50 °C to react about 4 hrs. Then, the stoichiometric S104 was also slowly dropt and two drops of DBTDL was joined to maintain the reaction for additional 3 hrs. Next, the flask was injected with the stoichiometric HPAE dissolved by acetone and kept for 3 hrs at 50 °C. A flavescent and viscous fluid was acquired. After that, the solvent acetone was removed by vacuum distillation and pH of the system was neutralized to 7 using the triethylamine. Finally, the suitable amount of distilled waters were added into the system and stirred high-speed to acquire the FHBPU latex with approximately 20% solid content. And the whole reaction procedure could be seen from Figure 2.

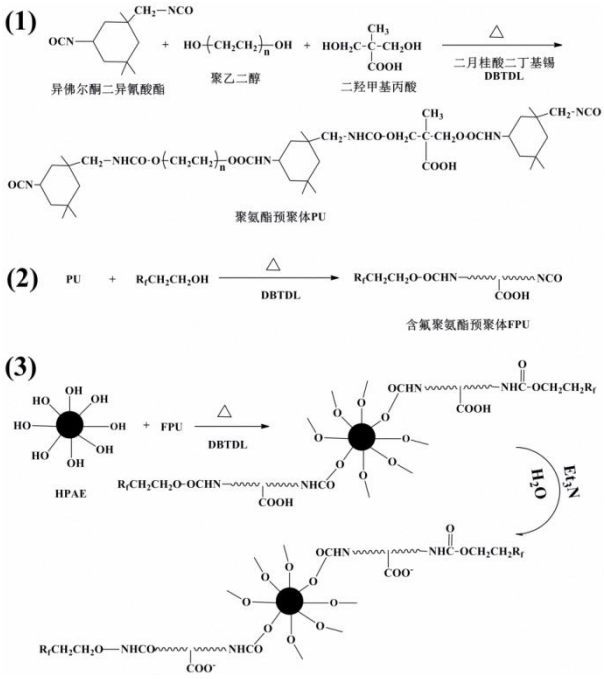

Figure 2. The synthetic route of FHBPU

2.3 Application of FHBPU latex in leather water proofing process

Goat wet-blue was squeezed and shaved to the thickness of 1.0-1.1 mm and leather samples with 20cm×15cm were gained along with the backone line of the wet-blue, weighed. Then, the post tanning processes were implemented according to the reference (Shan 2005), such as retanning, dyeing and fatliquoring, after that, the liquors were discharged and the leather water-proofing process was conducted as the following process:

Process	+	%	Product/Remark	°C	dil.	Time(min)
Water-proofing	+	100	Water	30		
	+	0.4-2	FHBPU			120
	+	2.5	Formic acid		1:10	40
Drain						
Washing × 3	+	100	Water	30		10
Fixation	+	200	Hot water	40		
	+	3	BCS agent			90
Drain						

Washing × 3	+	100	Water	30	10
Horsing, drying,detection for hydrophobicity					

2.4. Characterization

The intermediates and final products were characterized by FTIR using Bruker VECTOR-22 FT-IR Spectrometer. ^{1}H NMR analysis was performed with INOVA-400 spectrometer utilizing $CDCl_3$ as solvent and tatramethylsilane (TMS) as an internal standard.

Transmission electron microscopy (TEM) micrograph of FHBPU latex particles was taken with Hitachi H-800 transmission electron microscope with an acceleration voltage of 15 kV. The samples were stained with 2% phosphotungstic acid (PTA) solution. The particle size and its distribution of the synthesized latex were measured by Nano-ZS particle sizer (Malvern Instruments Company, UK). Sample was diluted with deionized water into an appropriate concentration as indicated by the instrument.

The static water contact angles (WCA) on the treated leather surfaces were measured using an optical contact angle goniometer (JC2000C1, China) and the average of five readings was used as the final contact angle of each sample, and this value of WCA was denoted as the hydrophobicity of the treated leather.

3. Results and Discussion

3.1 Structure characterization of the intermediates and resultants

To confirm the structure of the as-prepared product, FTIR and ^{1}H NMR technologies were exploited to characterize the resultants. First, FTIR spectra of the intermediate PU [Fig. 3(a)], FPU [Fig. 3(b)] and the ultimate product FHBPU [Fig. 3(c)] were examined and are compared in Figure 3. Obviously, typical absorption bands separately at 2960 cm^{-1}, 2862 cm^{-1} and 1460 cm^{-1} in all three diagrams are derived from the methyls and methylenes. The signal at 1718 cm^{-1} should be resulted from the stretching vibration of carbonyl (C=O) and absorption bands at 1246 cm^{-1} and 1042 cm^{-1} are asymmetric and symmetric stretching vibration absorption peaks. Furthermore, the signals at 3320 cm^{-1}, 3310 cm^{-1} and 1540 cm^{-1} are the stretching and bending vibration absorption peaks of amido bond (N-H) in polyurethane backbone (-NHCOO-). The absorption peak at 770 cm^{-1} is originated from the ∇ absorption band of amide group (Wang et al. 2013). The characteristic absorption peak at 2268 cm^{-1} in Figs. 3(a) and (b) should be derived from the isocyanate group (-NCO), but it disappears in Fig. 3(c) from the FHBPU, which denotes that the reaction has been entirely completed between –NCO group from FPU and –OH group from HPAE. However, new signal at 702 cm^{-1} from the FPU and

FHBPU maps should come from the bending vibration absorption peak of C-F bond (Xu et al. 2014), which indicates that the perfluoroalkyl group has been successfully built into the FPU and FHBPU molecules.

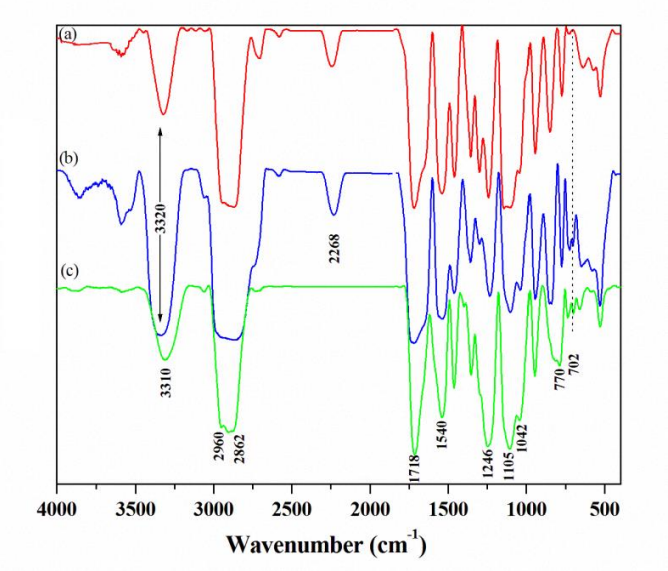

Figure 3. FTIR spectra of (a) PU, (b) FPU and (c) FHBPU

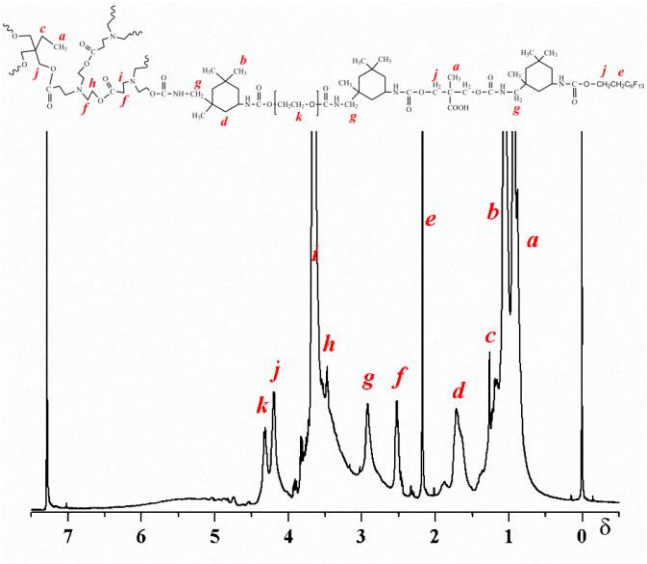

Figure 4 ^{1}H NMR spectrum of the FHBPU

Figure 4 is the ^{1}H NMR spectrum of FHBPU. These spectra demonstrate that the relevant chemical shift signals of the protons from the hydroxyls-terminated polymer core, the IPDI and PEG segments in polyurethane, and the perfluoroalkyl group clearly occur at δ 0.99 (*a*H), 1.22 (*c*H), 2.50 (*f*H), 3.60 (*h*H), 4.20 (*j*H), 1.11 (*b*H), 1.71 (*d*H), 2.91 (*g*H), 4.31 (*k*H), and 2.16 (*e*H), respectively.

Therefore, the combination of IR and ^{1}H NMR indicates that the molecule has the anticipated structure.

3.2 Morphology and its average size of FHBPU latex particle

Morphology, average size and its distribution of one latex colloidal particles will play a crucial role in its performance properties and application fields. Therefore, particles morphology and the average size of the FHBPU emulsions were researched in our studies and the results are displayed in Figs. 5(a) and (b).

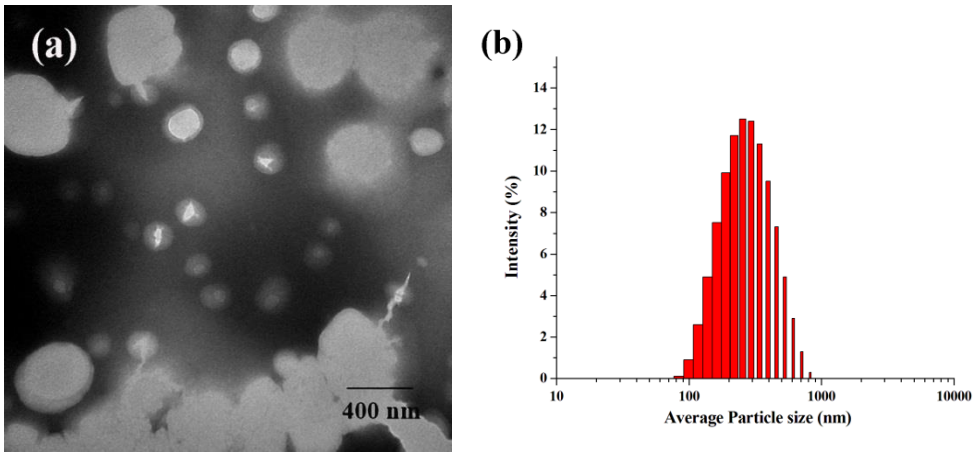

Figure 5 TEM image (a) and size distribution (b) of the FHBPU latex particles

As seen from Fig. 5(a), the FHBPU latex particles present an irregularly spherical pattern with the average diameters of 200 nm and the bigger latex particles bond each other. In addition, we can easily get a conclusion that the particles distributed from 80 to 850 nm, the average particles size and its distribution index were 238.8 nm and 0.261, respectively, from the Fig. 5(b), which demonstrate that the particle size distribution is broader. Of couse, the above two results are in good agreement. So, during the wet processing of leather, the smaller latex particles can rapidly penetrate into the collagen fibers and react with the active sites from the collagen fibers, which impels the collagen fibers dispersed well and further benefits penetration and reaction of the bigger latex ones.

3.3 Hydrophobicity of the treated crust leather by FHBPU latex

Frankly speaking, the hydrophobicity of one solid substrate could be characterized by the WCA on its surface (Song et al. 2005). Thus, to clarify effects of the FHBPU dose on hydrophobicity of the treated crust leather, we determined the WCAs on the treated crust leathers by different amounts of FHBPU latex, and the results are shown in Fig. 6.

As shown in Fig. 6, WCA on the untreated crust leather is 92.5° and it displays the weak hydrophobicity. We ascribed this result to usage of the relevant retanning and fatliquoring agents with hydrophobicity. On the contrary, WCAs on the treated crust leather are obviously increased by the 0.4-2.0% FHBPU active ingredients based on the wet-blue leather. It is 123.6° while the 0.4% FHBPU was used. WCA is not increased until the 1.6% FHBPU was utilized and it attains 142.9° now. This fact could be explained by the followings: on one hand, the distribution of FHBPU active

ingredients will tend to be in equilibrium amongst the leather fibrils and on the leather fibers surface with increase of the FHBPU dose. On the other hand, this highest WCA of 142.9° stems from combined action of the plentiful perfluoroalkyl terminals with low surface free energy and the scraggy grain structure.

In a word, the treated crust leather by a suitable amount of FHBPU latex possesses the favorable water repellency.

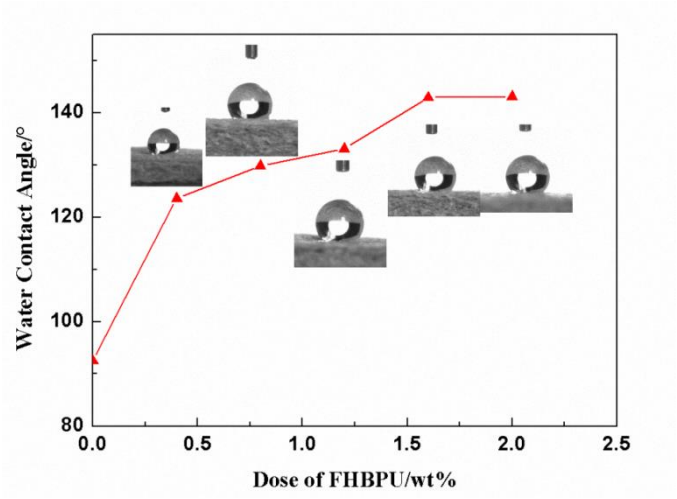

Figure 6 Hydrophobicity of the treated crust leather by different quantity of FHBPU latex

4. Conclusions

(1) Polyurethane prepolymer (PU) with NCO terminal groups has been manufactured by the stepwise polymerization of isophorone diisocyanate (IPDI), polyethylene glycol (PEG800) and dimethylolpropionic acid (DMPA). Then, fluorine-containing polyurethane prepolymer (FPU) with fluoroalkyl and NCO terminal groups has been synthesized by reaction of perfluorohexyl ethyl alcohol and PU. Next, novel fluoroalkyl terminated hyperbranched polyurethane (FHBPU) has been fabricated via the grafting reaction of FPU and hydroxy termianted hyperbranched polymer (HPAE). Finally, FHBPU latex has been obtained by neutralization, adding water, and high-speed stirring operations. IR and ^{1}H NMR results confirm the resultants have the due structure.

(2) FHBPU latex particles present irregular sphere with a polydispersity index of 0.261 and an average diameter of 238.8 nm.

(3) The treated crust leather has favorable hydrophobicity by 1.6% FHBPU active ingredients and WCA on its grain side attained 142.9°.

5. Acknowledgements

We are grateful for the Project from Postdoctoral Science Foundation (2014M562516XB and 2015T80764) of China, Scientific Research Program of Shaanxi Provincial Education Department (15JK1103), the Project from Innovative Research Team of Shaanxi University of Science & Technology (No.TD12-04), and the Doctorial Research Foundation of Shaanxi University of Science and Technology (BJ14-03) for financial supports of our research.

6. References

[1]He L, Liang J Y, Zhao X, et al, Preparation and comparative evaluation of well-defined fluorinated acrylic copolymer latex and solution for ancient stone protection, *Prog. Org. Coat.* 2010, **69**, 352-358.

[2]Xie K L, Hou A Q, Shi Y Q, Synthesis of fluorine-containing acrylate copolymer and application as resins on dyed polyester microfiber fabric, *J. Appl. Polym. Sci.* 2008, **108**, 1778-1782.

[3]Yang Q H, Zhang T Y, Li Z J, Characterization and application of low surface energy fluorinated polymer in leather finishing, *J. Soc. Leath. Tech. Ch.* 2010, **94**, 106-110.

[4]Zhang Y, Yan Y C, Wang Y, et al, The synthesis and solution properties of hyperbranched polyglycerols modified with hexafluorobutyl acrylate, *Colloids and Surfaces A: Physicochem. Eng. Aspects*, 2013, **436**, 563-569.

[5]Zhang F, Deng H T, Zhao X J, et al, Fluorinated hyperbranched polyurethane electrospun nanofibrous membrane: Fluorine-enriching surface and superhydrophobic state with high adhesion to water, *Journal of Colloid and Interface Science*, 2014, **421**, 49-55.

[6]Haraguchi M, Hirai T, Ozawa M, et al, Hydrophobic acrylic hard coating by surface segregation of hyper-branched polymers, *Applied Surface Science*, 2013, **266**, 235-238.

[7]Wang X C, Yuan X Z, Qiang T T, et al, Hyperbranched polymer polyols: their application, modification and use in leather industry, *J. Soc. Leather Technol. Chem.*, 2009, **93**, 61-66.

[8]Shan Z H, *Leather technology (Volume Two)*, Beijing Science Press Published, 2005, 337-342. (In Chinese)

[9]Wang X C, Fu Y Q, Guo P Y, et al, Synthesis, Characterization, and Properties of PCDL Aliphatic Hyperbranched Polyurethane Coatings, *Journal of Applied Polymer Science*, 2013, **130**, 2671-2679.

[10]Xu W, An Q F, Hao L F, et al, Synthesis of self-crosslinking fluorinated polyacrylate soap-free latex and its waterproofing application on cotton fabrics, *Fibers and Polymers*, 2014, **15**, 457-464.

[11]Song X Y, Zhai J, Wang Y L, et al, Fabrication of superhydrophobic surfaces by self-assembly and their water-adhesion properties, *J. Phys. Chem. B* 2005, **109**, 4048-4052.

SFS P-50

PREPARATION OF FAT LIQUOR CUM RETANNING AGENT FROM FLESHING WASTE: WEALTH FROM WASTE APPROACH

Wintana Kassahun, R. Aravindhan, Geetha Basker

Leather Technology Department, Leather Industry Development Institute, Addis Ababa, Ethiopia, email: elidi.@gmail.com

Leather Process Division, CSIR-Central Leather Research Institute, Chennai, India

Fleshing wastes are generated from tanneries during leather processing when flesh of the soaked or limed skin/hide is removed. These wastes contain significant quantity of protein and fat content and are currently being wasted into dumping sites or in open areas, consequently creating the fleshing waste disposal as a major environmental problem of the tanning industries throughout the world. The objective of this work is to develop fatliquor cum retanning agent for use in leather industry from the fleshing waste. The fat extracted from the fleshing was characterized for iodine, saponification and acid value. The fleshing hydrolysate was characterized for degree of hydrolysis, solid content, molecular weight, and particle size and zeta potential measurement.

The leathers were not found to be greasy, indicating that the product penetrated into the leather matrix. The particle size of the prepared product was also determined and was found in the range of the commercially available retanning agents. Physical characterization of the leathers retanned with this new product were carried out and compared with that of control leather processed with commercial fatliquors and retanning agents. Organoleptic properties were evaluated by experts and found to be on par with that of the control leathers. This study proves that the protein and fat from fleshing wastes can be utilized to make a beneficial product. This process also answers the disposal problem associated with the solid waste (fleshing) generated from tanning industries.

Keywords: fleshing waste; fatliquor; retanning; hydrolysis

1. Introduction

Theleatherindustry generallyuseshidesandskinsasrawmaterials,whichare the by-productsof meatandmeatproductsprocessing industry.Inthisrespect,theleatherindustrycouldhaveeasily beendistinguishedasanenvironmentallyfriendlyindustry,sinceitprocesseswasteproducts frommeatproduction(Langmaier F., Kolozmik K. 1999).However,theleatherindustry hascommonly beenregardedasa polluting industry due to the bad smell, organic and inorganic wastes and high

water consumptioncausedduringtraditionalmanufacturingprocesses(TaylorM.M.,CabezaL.F, 1998).Leatherisanimalskinthat hasbeenchemically modifiedtoproduceastrong,flexiblematerialthatresistsdecay.Almostall theworldoutputofleatherisproducedfromcattlehidesandcalfskins,goatskinsandkidskins, andsheepskinsand lambskins.Theleathercangenerallybeprocessedinfour steps i.e. beamhouse, tanning, post-tanning and finishing operation.

1.1 EthiopianLeatherIndustry

Ethiopiaiswellgiftedwithlivestockresourcesbeingamong thetentopintheworld.Theleather industryisoneofthecountry'smostvibrantandimportantindustriesforEthiopianeconomyasit generatesthelargestexportrevenueinindustrialsector.ModerntanninginEthiopiahasstarted 70yearsago(Ethiopian Privatization Agency, 2002).Annualproductionisonly 2millionpiecesofhidesand13.6millionpiecesof skinswhichamounts toonly 21% ofthecountry'slivestockpopulation(Tamper University of technology).Thefactthat productionofhidesandskinsheavilyreliesonthedemandformeatmakestherateofexpansion ofthe leather sector dependent on the rate ofgrowth of meat industry.

Currentlythereare30tanneriesinoperationandmostofthemarelocatedinvicinity ofAddis Ababa.Annually,allleather industriesputtogether use2.3millionpiecesofhidesand44.3 millionpiecesofskinsasaninputforprocessingatfullcapacity operations(LIDI, 2010).Aboutone-thirdofthese tanneriesarefoundinAddisAbaba anditissurrounding(ethiopianleather.org/sector.asp)

1.2 General andSpecificObjectives

Theprimaryobjectiveofthisresearchstudy isthedevelopmentofafatliquor cum retanning agentforuseinleatherindustry fromthewastesgenerated by theindustryitself,soasto find an effectiveutilization for thelargequantities of solid wastes generated.

2. Material and Methods

Thischapterpresentsthe raw material,chemicaland reagentrequired for theseresearch and the experimental procedures followed, the instruments used for extraction, instrumentusedforhydrolysis,characterizedandanalysis,andillustrationdepicting the experimental setup.

2.1 Experimental Setup

2.1.1 General Process Descriptions:

Calculatedquantitiesoffleshing fromeachrawmaterial(cowhides,sheepandgoat) are taken.Thefleshingwastesamplewasbroughtfrom LIDI Modeltannery andM/sBatu TanneryPLC.Thefleshingmaterialwaswashed, de-limedandwascutintosmallpieces.

Thealkaline hydrolysisoffleshingwascarriedoutandthevarious parameterslike temperature,pHandtimewere optimized.Thefleshing hydrolysatepreparedwere characterizeandusedformakingtheproductby mixingtogetherusingdifferent combination of emulsifierto improvethe stabilityofthe final product.

2.1.2 Sample Collection and Sample Pre-treatment

Enoughamountsofgoat, sheepandhidefleshing wastewerecollectedfromM/sBatu TanneryPLCandLIDI Modeltannery. Two types ofsampleswerecollected; green fleshing andlimedfleshing.Greenfleshing waswashedwithcopiousamountofwaterandtaken for hydrolysis.Thelimedfleshinghaslimeand sodiumsulphide.Hence,thelimedfleshing was washedwithwaterandde-limedwithammoniumchloride andtakenforfurtherprocessing. ThepHofthefleshing beforehydrolysiswas7.5-8andstoredat4ºCinrefrigerator.

2.2 Method

2.2.1 CharacterizationofFleshingWastes

Thefirststepinthesamplepreparationwasde-limedandwashingthentoreducethesize bycutting, the wet sampled.

a) pH:The samplespHwaschecked usingpH paper.

b) MoistureContent:-Moisturecontentinskinandhidefleshingwasteswerecarried outaccordingtoSLC3(IUC5),theamountofmoisturepresentinthefleshing was measuredusing agravimetricdifference.The entire samplesusedintheexperimentwere usedona wetweightbasis (SLC 7, 1996)

Calculatethemoisturecontentofthesampleiscalculatedusingthefollowing equation:

$$W\% = \frac{A-B \times 100}{B}$$

c) Nitrogencontent

Todetermine the totalnitrogencontentof the sample aKjeldhalmethodwasused(SLC 319 (ISO 2/14). It involvesthreestepsdigestion,distillationandtitration.

Using therecorded titratevalue and the relationbelowthe%ofnitrogenwasthencalculated.

%TotalNitrogen=14*(A-B)*N* 100

1000*1

d) CarbonHydrogenNitrogenRatio(CHNS)

Thecarbon tohydrogentonitrogenrationof the samplefleshingwasteswasdetermined by dividingthepercentage ofcarboncontenttothepercentageofhydrogentothe percentageofnitrogencontenttopercentageofsulphurcontentofthesamples.

2.2.2 Extractionof Fat

Soxhletmethodwasemployedfortheextractionoffatfromthefleshing.Thefleshing wasde-limed,washedanddriedinanoven.Measuredquantityofthedriedfleshing samplewasplacedinathimbleorbag filterpaperinsideSoxhletglasschamberofthe extractor. Shown fig 2.1

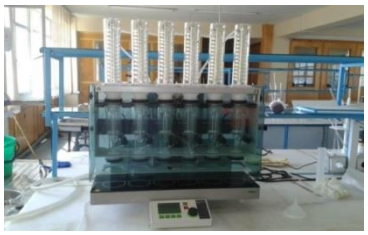

Figure 2.1: Fleshingwaste oil extraction manual electrical setup apparatus

2.2.2.1 Chemical CharacterizationofExtractedFleshing Fat/Oil

a. Determination offat extracted

Extractfat/oilcontentwasdeterminedfromgravimetric analysis.Thesampleswere weightedindigitalweightingbalanceapparatus.Themaximumyieldoffleshingwastesisdetermineddun derthisformula.Itshelpfor calculation offat amount present in each types offleshingwastes. (SLC 319 (ISO 2/14)

.

$$\text{Fat yeild \% by wt} = \frac{W_2 - W_1}{W} * 100$$

b. Acid value (Acid Number)

The acidvalue(*AV)is*thenumberthatexpresses,inmilligramsthequantityofpotassium hydroxiderequiredtoneutralizethefreeacidspresentin1g ofthesubstance.Theacidvalue ofthe extracted oil was obtained according(SLC 303 (SLO ¼, 1996) method.

$$AV = \frac{ml\ of\ KOH\ x\ Nx\ 56.1}{Weight\ of\ sample} = mg\ of\ KOH$$

N =NormalityofKOH

% FreeFattyAcid (FFA) =AV x0.503

Calculate theacid value(AV) and free fattyacid (%FFA)usingabovelaws.

c. Saponification Number accordingto (SLC 304(SLO 1/5, 1996) method: - Thesaponificationvalueisthenumberofmg ofpotassiumhydroxiderequiredto neutralizethefreeacidsandtosaponify theestersin1gofthesubstance.

Calculate thesaponification numberbyusingthefollowinglaw:

$$SP\# = \frac{56.1\ (B-S)x\ N\ of\ HCl}{gram\ of\ sample}$$

EsterValue(EV)=Saponification Value (SV)– Acid Value(AV)

d. IodineValue(I.V)accordingto (SLC 302 (SLO 1/3, 1996)method: - Theiodinevalue(*IV*)givesameasure oftheaveragedegree ofunsaturationofalipid: thehighertheiodinevalue,thegreaterthenumberofC=Cdoublebonds.

$$\text{Iodine Value} = \frac{(B-S)\ x\ N\ of \text{Na2S2O3 x 0.127 g/meq}}{Weight\ of\ sample\ (g)} \text{X } 100$$

e. Un-saponificationvalue:-Determinedtheamountofun-saponificationpresentin thefatliquordeterminedaccording tothe (SLC 305 (SLO 1/6, 1996) method.This method determinesthe materialsinoilwhichcannotbesaponifiedandwhicharenoteasily volatile.

$$\text{Un-saponification matter (\%)} = 100\ X\ \frac{w_1}{w}$$

2.2.3 Preparationof ProteinHydrolysate

AlkalineHydrolysis and Homogenizationof fleshing waste

Inthisresearchalkalinehydrolysismethodby sodium hydroxide intheautoclaveapparatus showninFigure 2.2 (a) wasemployed.Firstly,fleshingofsheep,goatandcow hide werecutin tosmallpiecesandweighted.100g offleshingwereputinbeakerand5% sodium hydroxidewasaddedtotheweighedsamples. Set the temperature at (75and85 ^{O}C),time(2and4hr),andpH(10and12)fordifferentsamples.

Thefleshing fromdifferentrawmaterialswerechopped,driedandgroundas powderform. Thedriedsampleswerethenputinmeasuredquantityof water and then homozenizedinthe homozenizer, shownin Figure2.2 (b).

a b

Figure2.2: Autoclave apparatusfor fleshedwastehydrolysis (a) and PowderedfleshingwasteHomogenizedmechanisms (b)

2.2.3.1 CharacterizationofFleshing Hydrolysate

Solid Content of thefleshingHydrolysate: - Solidcontentofthefleshinghydrolysatewasdetermined.Solid contentdeterminationwasusefultocalculate theactive matteranddegree of hydrolysis.

$$\text{Total solids} = \frac{(A-B)x\ 100}{Sample\ volume\ (ml)}$$

MeasurementofParticlesize distribution:-Particlesize distributionsof thesampleswere measured by using the integrated of dynamic Light Scattering (DLS) Instrument (Nanosizer,Malvernparticle sizeAnalyzer).

*Measurementofzetapotential:-*Zetapotential isascientifictermforelectrokinetic potential.Thezetapotentialisakey indicatorofthestability ofcolloidaldispersions.The magnitude of the zeta potentialindicatesthe degree of electrostatic repulsionbetween adjacent,similarly chargedparticlesindispersion.Thezetapotentialwasmeasuredusing Nanosizer, Malvern particlesizeAnalyzer. (*Ch.Gahwiller 1979*, Howard G.Barth 1979)

DeterminationofMolecularweight (Serway, Raymond A. 1996)*:-*The count rate and solventrefractive index calculatedfromatoluenereferencestandardaswellasthesampleconcentrationsand time averaged scattering intensities areentered into the MolecularWeightCalculator.

Viscosity:-Theviscosityismeasureofthefluidresistancetoshearorflowandisa measureoftheadhesive/cohesiveorfrictionalfluidproperty.Theresistanceiscausedby intermolecularfriction exerted when layers of fluidsattemptto slide byone another(P. Becher 1983).

*Determination ofdegreeof hydrolysis:*Thedegreeofhydrolysis wasestimatedbytaking10 grams offleshinghydrolysateand10 gramsof residueafterhydrolysisof fleshing.Weighed chinacrucibledishputthetwosamplesintwodifferentdisheskeptinovenfordryingat 102^{O}Cfor3 hr.anduntiltogetconstantweight. *%DH=AM%- RC%*

2.2.4 PreparationofFatliquor cumFillerAgent

Theoptimizedprocessparameterswereusedtoextractfatandtheproteinhydrolysate fromthefleshing.Thefatandthehydrolysatefromtheoptimizedprocesswereusedfor the preparation of fatliquor cum filing agent. There areso manyfactors, which needsto be considered for thepreparation of fatliquor, theyare

- Order of addition of theraw material
- Ratio of emulsifier: extracted fat:fleshinghydrolysate
- Selection of emulsifiers
- Temperature andreaction time

Two typesofproductbased onalkalihydrolysedfleshing andhomogenizedfleshing was prepared.

2.2.4.1 FatliquorfromAlkalihydrolysed and WaterBased HomogenizedFleshing waste

Synthesisof FH_{SDS}(A):- Oncethefatcompletelymeltsandtheflowcharacteristics improve,thestirringisstarted.Then,differentvolumes(15,30and40ml) of5%solution ofSDS(anionicemulsifier)wereaddedtothemoltenextractedfatslowly tilla homogeneousmassisobtained.Theresultantemulsionwasvery fine and homogeneous whendispersed in water.

Synthesisof FH_{M7}(B):-Once thefatcompletelymeltsandtheflowcharacteristics improve,thestirringisstarted.Then,differentvolumes(15, 30and40ml)of M7(anionic emulsifier)wereaddedtothemoltenextractedfatslowly tillahomogeneousmassis obtained.Thisproductaftercoolingwasusedasa

retanningagentduringleatherprocess.Theresultantemulsionwasvery fineand homogeneous when dispersed in water.

SynthesisofFH$_{SDS}$withM7(C):-Once thefatcompletelymeltsandtheflowcharacteristicsimprove, thestirring isstarted.Then,differentvolumesof5%solutionof SDSandM7(anionicemulsifier)wereaddedtothemoltenextractedfatslowly tilla homogeneousmassisobtained.Thisproductaftercooling wasusedasaretanningagentduringleatherprocess.Theresultantemulsionwasvery fine and homogeneous when dispersed in water.

Thesimilarprocedureasmentionedinabove wasfollowedforpreparing theproduct. Theonly differenceisinsteadofalkalinehydrolysedfleshing,waterbasedhomogenized fleshingwasemployed.

2.2.4.2 CharacterizationofFatliquor cumFiller

2.2.4.2.1 Stability ofFatliquor cumFiller

The stability of the prepared fatliquor emulsion has been studied by observing phase separation (as oil and hydrolysis liquor) if any takes place with respect to time.

2.2.4.2.2 DeterminationtheActiveIngredient and Total Alkalinity oftheFinal Product

TotalFatty Matter(TFM)isoneofthemostimportantcharacteristicsdescribingthe quality offatliquorcumfillerproductsanditisalwaysspecifiedincommercial transactions (1996, SLC 311 (SLO2/6)). The total alkalinities results can be calculated using the formula below: (ISO 2419:2006)

$$\text{Total alkalinity in ml 0.1N per grams of oil} = \frac{t \ x \ 5}{w} = A$$

2.4.5 ApplicationofFatliquor cumFillerinLeatherRetanning Process

Aftertheleathersareproduced,itisnecessarytotestthemtoassesswhethertheywillservethe ultimatepurpose.Astheproperties ofleatherareaffectedby atmospherictemperatureand varying humidityandasinthesameplaceindifferentseasonsoftheyearandthehourofthe day,itisessentialtoconditionstheleather,priortotesting,inaroomundercontrolled conditions.

Theconditions specified by the Indian Standard Specification are20±2^{O}C and 60% R.H.±2(R.H.= relativehumidity) overa periodof 48hrs.For leatherthisconditioning procedureisdefinedinISO2419testmethod(ISO3376:2002(IULTCS/UP6))

i. *TensileStrength:* -Itistheloadperunitareaofcross-sectionrequiredtopull apartorbreakastripofleather. Calculatingtensile strengthofthesample (ISO3377-2:2002(IULTCS/UP8)

$$\text{Tensile strength (N/ mm}^2\text{) or (Kg/cm}^2\text{)} = \frac{Breaking\ load\ in\ (kg)}{Thickness(cm)\ X\ width(cm)} \text{ or}$$

$$= \frac{Force(N)}{Area\ (\text{width in mm X Thickenss in mm})}$$

ii. *Elongation:* -Thepercentageelongationofleatherisalsoausefulindexofthestretchingquality inmany cases.Theelongationismeasuredsimultaneously withthemeasurementoftensilestrength.
Theextensioncanbeexpressedasthepercentageelongationatthat load (ISO5402:2002)

iii. *TearingStrength:* -Thisis theloadrequiredtocontinueatearinleather,oncestarted.Tearstrengthisalsoan importantbulkpropertytest.Thistestisthemostpreferabletestfor leather thantensile strength by many ofthecustomersincludingSafetyshoestandards (ISO3379/ 2005(IULTC/UP 9).Recordthemaximumforce.Continuethetestforremainingtestspecimen.

iv. *FlexingEndurance and Lastometer(BurstingBallTest):*-Test pieceswerecutfrom theleather45X70mm and placed onaflexometer(based onISO5402:2002).Twoendsoftheleatherspecimenwerefoldedandgrippedononeend,andth ensubjectedto25000flexes,afterwhichanysignofcracking orpeeling was observed (ISO3379/ 2005(IULTC/UP 9). Aimof thistestmethodisintendedtodeterminethegraincrackforceanddistensionof leatherwhenusedfor shoeupper.Thesecanbedefinedin(ISO11640:1993(E)). Shoeupperleatheroften showsslightcrackinthe toeareaatthetimeof lastingoperationinspiteoftheleatherhas goodtensile andtear strengthproperties

v. *Fat liquor cum Filler Effect on Organoleptic properties of leathers*: **-**Organoleptic feelings of colour-fixed leathers were determined by experienced technician/expertsontheleatherandthefixingcapacitiesweredeterminedthroughthe colourintensity. The softness, fullness, roundness, feels, colouruniformityand colourintensityoffatliquorcumfillerleathermightchange.
TheleatherhandleandFullnessismadeuse ofcontrast-scoring,scoresfrom1~10minutes bytouchedthecrust leatherineveryside. (ISO 2419:2006)

3. Results and Discussion

3.1 CharacteristicsofFleshingWaste

i. *pH, moisture and nitrogen content of fleshing wastes*

pHofthelimedfleshing usedfortheexperimentswasfoundtobe12.0. Theaverage moisturecontentof fleshingfromcow hide,goatand sheepwasfoundtobe64.88, 56.64and63.3%respectively.Fleshing obtainedfromsheepskinsshowedhighermoisturecontent.

Thenitrogencontent of hidefleshing hadthemaximumnitrogencontentof 12.59% whencomparedwithotherfleshingtypes.The %nitrogencontentwasusedtocalculate theproteincontentpresentinfleshing.From theresultsobtained,the nitrogencontentofthefleshingfromdifferentrawmaterialsource suchascowhide,goatandsheepskinwascalculatedtobearound64.96,54.90and 44.69%,respectively. Hence,itcouldbe observedthatthe fleshingfromcowhideshave moreproteincontent.

ii. CarbontoHydrogentoNitrogentoSulphurratio(CHNS)

Thecarbontohydrogentonitrogenratio(CHN)isvery importantfactortopreparevalue addedproductfromfleshingwasteby mixingwithothermodifiedchemicalsforleather industry itself.Theobtainedlaboratory resultwasshowninTable3.1,forallspeciesof fleshingtypes.

Table3.1:CHNScontent offleshingwastes

Samplec ode	Weight(mg)	N%	C%	H%	S%	C/N ratio	C/H ratio
SLF	4.75	2.4533	42.5405	6.309	0.0830	17.3398	7.0537
GLF	4.75	3.0512	30.8965	5.230	0.0792	10.1260	5.9076
HLF	4.75	4.1051	22.9567	4.589	0.0785	5.5922	5.0025

From the abovetableabasicunderstandingon the C:N couldbeobtained. HigherC: Nratio meansthe proteincontentishigh.Hence,fromtheTable itcouldbe observedthatthecow hide fleshinghadthehigherproteincontentandsheepskinfleshinghadthe lowestprotein content.Thuscowhidefleshingwouldbe themostsuitableproducttopreparethefatliquor cumretanningagent.

3.2 IdentifyingMaximumYieldofOilExtractionfromSpecificFleshing Wastes

3.2.1 Determinationof Fat contentandyield

Thefatcontentofvariousgreenandlimedfleshing fromdifferentrawmaterialsis determined. Itcouldbeobservedthatthegreenfleshing fromsheepskinhadthemaximum fatcontent of23.88%.Otherlimed fleshinghad lowerfatcontent.It is obvious that during liming process,thefatgetssaponifiedandhencethelowering offatcontentinthelimed fleshing.However,limedsheepfleshing hadthehigherfatcontentofaround12.29%.The goatandcowhidelimedfleshinghadfatcontentof5.09and4.83%, respectively.

The consolidatedresults obtainedfromthe%fatestimationaredepictedinFigure3.1.

Fat contentin fleshingwaste

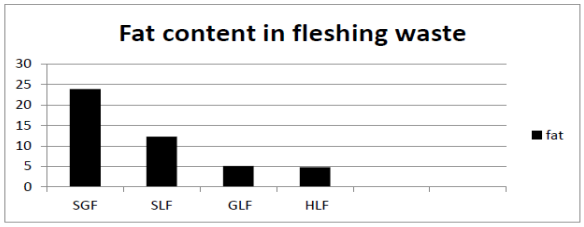

Figure3.1: The %fatyield present in different fleshingwaste.

3.2.2 ExtractionandCharacterizationofFleshing WastesOil

a. Saponification Value

Thesaponificationvalueofsheepgreenfleshing ($SGF_{average}$)was198.98, sheeplimedfleshing($SLF_{Average}$) was193.07, forgoatlime fleshing($GLF_{Average}$)214.185andforhidelimedfleshing($HLF_{average}$)228.890.Fromthe aboveresultshowstheHideOilfleshinghasshownhighermolecularweightthanthe othertypeoffatfleshing.Allresultswerefallsunderthestandardvaluethatis180-233(Gunstone, F D. 2004).

b. Acid Value

Acidvalueisameasureofrancidity.Ifthevaluesarehigh,thefatoroilwillbecome more rancidandvice versa. Fator oiltobeused for the preparationof fatliquor,itshould bebelow8.6mg/gofoil.Itisobservedtheaverageacidvalueforthe fatextractedfromgreenfleshing fromsheepskinis8.38mg andthatoflimedsheep fleshingis8.31mg/g ofoil.Theacidvalueofgoatlimedfleshing andthecowhidelimed fleshingis7.51and4.53mg/gofoil,respectively.Fromtheobtainedresult,itisvery clear thatacid valueof all the extracted fat/oilis lessthan 8.6 mg/gof oil. The%freefattyacidcanbecalculatedbasedonacidvalue.Theresultsareprovidedin Table 4.7, this can becalculated under the followingformulaAcid (FFA)=AVx0.503

c. Iodine value

Alowiodinenumber showsthatthefathasalowquantityofunsaturatedfatty acid(Serrato, A.G. 1981).Allthesamples showedloweriodinevalueindicating thatthefat/oilhadlowerlevelofunsaturationandis suitableformakingfatliquorandwouldgivebetterlubrication(International Standard ISO13321 , 1996). On this experiment determinediodinevalueoffleshingfat used for making fatliquor.

Alowiodinenumberalsoindicatesahighmelting pointandsoftlubricating valueofthe fleshingfat.Basedontheiodinevaluesofextractedfleshing fat,theycanbecallednon-drying oilsandalltypesoffatcanbeusedfor preparationoffatliquorcumfiller.Thechemical properties oftheextractedfleshing fataresummarized inTable 4.2.

Table 3.2:Physico-chemical properties of extracted fat from fleshing

S.No.	Characteristics	Source of Oil			
		Sheep		Goat	Hide
1	Colour	Light yellow	Light yellow	Light yellow	Light yellow
2	Acid value mg	8.35	8.01	7.51	4.53
3	Iodine value	61.995	59.94	57.35	56.91
4	Saponification	193.07	214.185	228.890	198.98
5	Free fatty acid	4.22	4.03	3.78	2.28

3.3 Particle SizeDistribution andZetaPotential oftheFleshingHydrolysates

Particlesizedistribution(PSD)ofthematerialisanimportantfactorinfluencing the efficiency ofvalue-addedprocessingandavaluableindicatorofquality andperformance [International Standard ISO13321]. The result had shown Figure3.2.Thetwo peaksof particle sizedistribution were found for hydrolysate obtained after hydrolysate of 4hr. Theparticle sizedistributionconcentratedwasshownintheregionsofhighpeak,forSLF962to 5.075,GLF766.5to2.488 andHLF5492to592.6. The4hrhydrolysate particlesizewaslowerthanthe2hr.hydrolysate.Inthecaseofsheep,goatandhide showndifferentparticle size atthe same hydrolysate times,and Sheepandgoathaslower particlesizethanthehidesample. It can suitable for making leather retanning material because easily penetrate skin pores size.

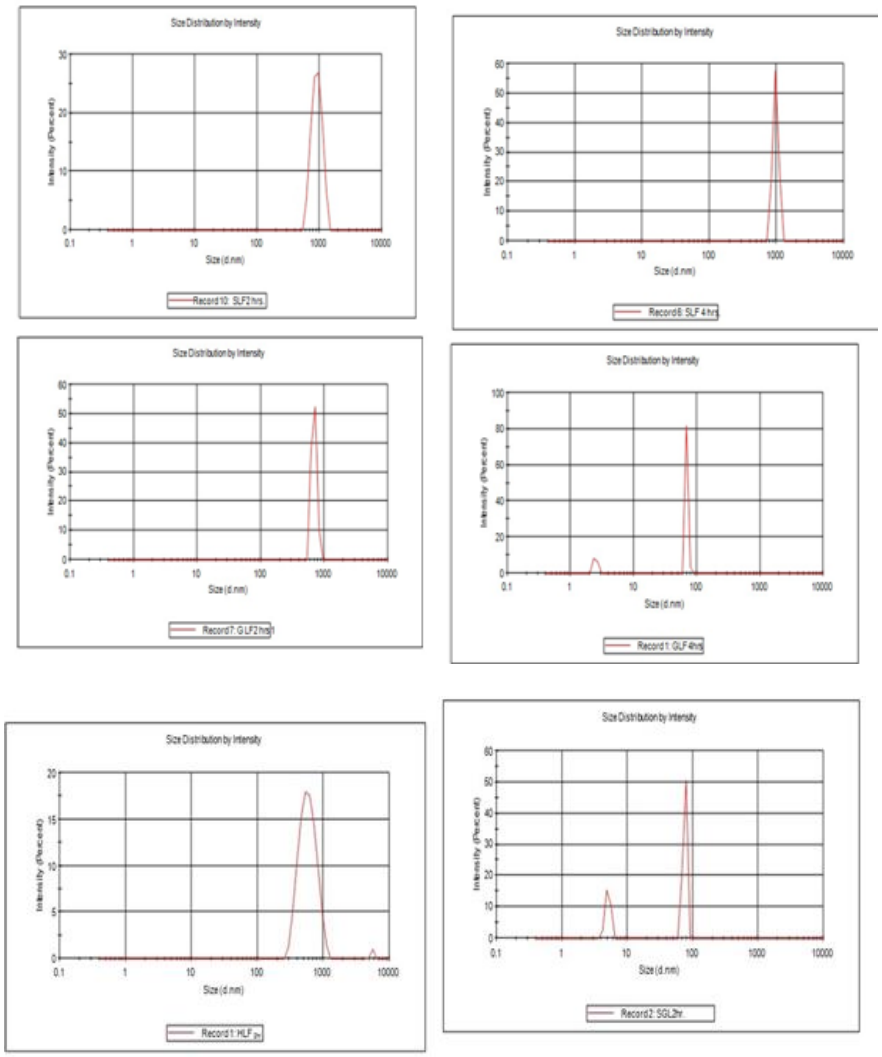

Figure 3.2: Graphical expression of each types of fleshinghydrolysates PSD

Zeta potentialistherefore afunctionof thesurfacecharge oftheparticleandthenature andcompositionofthesurrounding mediuminwhichtheparticleisdispersed.Thezetapotentialvaluewasobtained negativechargethatmeanstheanionicchargemoredominatedinthesystemofthe samples. Inall samplescase had been shows thezetapotentialwasdemonstrated below -25mV,it was indicated the higher degree of stability.Theconductivityvaluewereindicatedtheability ofa samplestoconductelectricalcurrentssampleGHL$_{2hr.}$haveahigherconductivitytocompared toother samples.Thisgave informationof higher saltconcentrationpresentinsample GHL$_{2hr.}$

3.4Synthesis,OptimizationandCharacterizationofFatliquor cumFiller Agents

Theproductwaspreparedby combinationofthehydrolysedprotein,fatandemulsifiers. SDSandM7are thetwoemulsifiersusedinthestudy. ThestabilityofsampleA (6% emulsifier)inacidmediawasfor3hrwithoutseparationofoil. InthecaseofsampleB (8% emulsifier) stability wasfor3:30hr.without separation ofoiland insamples C (10% emulsifier) thestabilitywas formore than 6

hoursandbetterthan products AandB.Hence, itcould be concludedthatthecombinationof2emulsifiersduring thepreparationoftheproductsis requiredtogetmaximumstability. The prepared fatliquor cum filler solution with combination emulsifier is stable without any phase separation as oil and hydrolysed protein liquor had given very good shelf life.

3.5 Physical TestingResults ofLeatherSamples

Thecrustleathers,bothupperandnappa leatherwereanalysedfor tensile strength,% elongationatbreak, teatstrengthandburstingstrength.Thedeterminedvaluesare providedinTable3.4.

Table 3.4:Physical characteristicsofcontrol andexperimentalleathers

Sample	Thickness	Tensile strength (N/mm^2)	% Elongation	Thickness (mm)	Tear strength (N/mm)	Lastometer test	
						Distension (mm)	Load (Kgf)
Upper							
Control (T_1)	1.142	15.6	66.55	1.0988	41.57	10.24	33.05
HT(T_2)	1.219	20.9	56.1	1.1129	47.55	11.7	51.56
HTC (T_3)	1.235	15	76.90	1.0206	50.22	13.9	45.47
Ho (T_4)	1.319	23.95	66.85	1.0813	48.72	13.9	34.46
Nappa leather							
Control (T_1)	0.892	15.330	64.535	1.085	44.38	13.4	27.09
HT (T_2)	1.133	15.706	57.83	0.9150	42.33	11.9	25.69

FromtheTable3.4,itcouldbeobserved

thattensilestrengthvaluesofcontrolupperandcontrolnappaleatherswere15.6and 15.330 N/mm^2, respectively. The leathers retanned with homogenized sample showed bettertensilestrengthof23.95N/mm^2.

Tensilestrengthofleathersmadeusingtheproductswashigher thanthestandardvalue of 15N/mm^2 (BureauofIndianstandards).Fatliquorcumfillerproductsformaking leather have beendevelopedanditgivessufficientstrengthandfullnesspropertiestothe leathers.

Theresultsaretabulatedin Table3.4.In thepresentstudy,leathersretanned with the alkaline hydrolysed product in combination with commercial syntan and fatliquorgavehighestvalueof76.9%.Whereas,theleatherobtainedfromexperiments T2andT3gaverelativelylesservalues.

The results aretabulated inTable3.4. Inthepresent study, leathersretannedwiththe alkalinehydrolysedproductin combinationwithcommercialsyntanandfatliquorgave highestvalueof50.22%.Whereas,theleatherobtainedfromexperimentsT2andT3 gaverelativelylesservalues.Thismightbeduetothefactthattheleathersarefuller dueto

moreproteinfractions.However,all thevaluesare on par withthestipulated minimumvalueof40N/mm (BureauofIndianstandards).

Flexing enduranceoftheupperleathersretannedwiththepreparedproductwas testedforflexingendurancefor250,000flexes.The leathersdidnotdevelopany damageafterthistest.Hence,itcouldbe inferredthattheproductsdoesnotaffect theflexingenduranceoftheleathers.

Itisessentialtostudy theinfluenceoffatliquorcumfilleragentontheorganoleptic properties ofleather. Thevarious organolepticproperties ofthe upperleather suchasuniformityofcolour,intensityof colour,roundness,fullness,feelandsoftnesswereevaluated bytannersandthevaluesareprovidedinTable3.5.

Table3.5: Organolepticproperties ofgoat upperchrome crust leathers

Parameter	Control (T_1)	HT (T_2)	HTC(T_3)	HO (T_4)
Uniformity of colour	7.5	9	9	9
Intensity of colour	7.5	8.5	9	8.5
Roundness	8	9	8.5	8
Fullness	8	8.5	8.5	8.5
Feel	8.5	8	8	8
Softness	8.5	8	8	8.5

4. Conclusion

Thisstudy focusesonthereutilizationoffleshingwastes(i.e.sheep,goatandhide)as beneficialproductinleather processing after somechemicalandthermalmodification. Fleshingwastesareone ofthe mostimportantby-productsfromleatherindustry.Fleshing have twopartof fractioni.e.proteinandfatcomponents.Thefleshinghydrolysatewas obtainedby alkalinehydrolysisorthehydrolysatewasobtainedby waterbasehomogenises of fleshingandthe fatwasextractedfromfleshingobtainedbydichloromethanesolvent.The hydrolysateand theextracted oilfromfleshingwasusedforpreparationoffatliquorcum filleragents andusedinretannageofupper andnappaleathers.

Theoilandtheproteinfractionswerecharacterizedandthenusedinthedevelopmentof theproduct. Various parameters, such as time,temperatureand pHofhydrolysishavebeen optimized.Theoptimizedproductwasusedinthepreparationoffatliquorcumfilling agent.Duringthepreparation,twotypesofsurfactantsSDSandM7wereusedandthe offer of these emulsifierswasoptimized.The optimizedproductwasusedinthe retanning ofupperand garmentleathers.

Thephysicalpropertiesofgoatshoeupperand nappaleatherwereon parwiththatofthecontrol leathers.Thecolourintensity ofthe experimentalleathers isbetter than thecontrol leathers.

5. Acknowledgements

Firstletmestartmythanksandglorytomyalmighty GODforprovidingmehope,strengthandcourage throughoutmy life.Iamdeeply indebtedtomysponsors,advisorsandfamily forthesupportand guidancethroughout thecourseof mystudies andresearch.

IgratefullyacknowledgeAto WonduLegesse, DirectorGeneral, ofLIDIforpermitting metocarryout myM.Sc.projectat CentralLeatherResearchInstitute,Chennai.Iwouldalsolikeexpressmy heartfelt thankstoDr.B Chandrasekaranand MrP.Saravanan,Coordinators,Twinning projectforsponsoring myvisit and stayin Chennai forcarryingout myM.Sc. project.

FirstandforemostIwishtoexpressmyheartfeltgratitudetomyadvisorsDr.GeethaBaskarandDr. R.Aravindhanfortheirvaluablesupport,coaching approach,encouragement,supervisionanduseful suggestions throughout myresearch work.

Secondly, Iwould like to acknowledgeDr.K.J. Sreeram. Inaddition,I wouldalsoliketoexpressmygratitudetotheorganizational all staffsofCentralLeather ResearchInstitute,especiallyDr.SwarnaV.Kanth,andlaboratoryassistantsfortheir technicalsupportandassistance.

My gratefulappreciationisalsoextendedtoallstaffmembers ofinLIDIespeciallyMr. TayeTibebu, leatherdirectoratedirector,Mis.SerkalemJogol,friendsandcolleagues.

Finally,Iwishtothanks my belovedfamily forsupport,loveandfriendshiphelped throughalltherough times.Theywerealwaysforme,mayGodblessthemall.

6. References

1. BureauofIndianstandards:LeatherSpecificationofCLRIGuideline.
2. Ch.Gahwiller, Powder Technology, 24, 91(1979)
3. Ethiopian Privatization Agency, 2002, “TheLeatherIndustry”
4. Gunstone, FD. 2004. The ChemistryofOilsandFatssources, Composition, Properties and Uses.Oxford:UK Blackwell.
5. Howard G.Barth”modern methods of particlesize analysisedited “volume73 in chemical analysis: A series of monographs on analytical chemistryand its application edited byP.J.Elvingand J.D. Wine fordner EditorEmeritus:I.M. Koithoff.
6. http://ethiopianleather.org/sector.asp

7. International Standard ISO13321 Methods for Determination of Particle Size Distribution Part 8: Photon Correlation Spectroscopy,International Organization for Standardization(ISO)1996.AndSouissi, N.,Bougatef, A.,Triki-Ellouz, Y.,and Nasri, M. 2007.
8. ISO 2419:2006; Leather -- Physical and mechanical tests -- Sample preparationandconditioning
9. ISO11640:1993(E)
10. ISO3376:2002(IULTCS/UP6)determinationoftensilestrengthandpercentage extension.
11. ISO3377-2:2002(IULTCS/UP8)determinationoftearload-part2:Doubleedgetears.
12. ISO3379/ 2005(IULTC/UP 9) Determination andstrength ofgrain--Ballburst test.
13. ISO3961:1996Animalandvegetablefatsandoils-Determinationofiodinevalue/ SLC 319 (ISO 2/14
14. ISO5402:2002)
15. Langmaier F., Kolozmik K., Sukop S., Mla Dek M. Products ofEnzymatic Decomposition of Chrome-TannedLeather Waste. JSLTC.83 (4), 187, 1999.
16. Leather IndustryDevelopment Institute(LIDI) and UnitedNation Development Program(UNID),July, 2010,Processing ofNationalworkshoponenhancing the EthiopiaLeatherIndustryand its Market Competitiveness ,Adama, Ethiopia.
17. MarvernInstruments formolecularweight measurements with the zetasizer nano systems.
18. P. Becher, Emulsions: Theoryand Practice, Reinhold PublishingCorp., New York (1957)
19. Serrato, A.G. "Extraction ofOil from Soybeans". Journal oftheAmerican Oil Chemists‟ Society, 58(3): 157– 159, 1981.
20. Serway, Raymond A. (1996).*Physics for Scientists&Engineers*(4th ed.). Saunders CollegePublishing.ISBN 0-03-005932-1.Or Tools and BasicInformationfor Engineeringand DesignofTechnical Application
21. Severin, S. andXia,W.S.2005.Enzymatichydrolysisofwheyproteinsbytwo differentproteasesandtheireffectonthe functionalproperties of resultingprotein hydrolysates. Journalof FoodBiochemistry30:77-97.
22. SocietyofLeather Technologists andChemists, Official Methods ofAnalysis 1996,SLC 304(SLO 1/5) orISO3657:2002Animal andvegetablefats and oils – Determinationofsaponificationvalue
23. SocietyofLeather Technologists andChemists, Official Methods ofAnalysis 1996, SLC 303 (SLO ¼)
24. SocietyofLeather Technologists andChemists, Official Methods ofAnalysis 1996,SLC 305 (SLO 1/6
25. SocietyofLeather Technologists andChemists, Official Methods ofAnalysis 1996,SLC 302 (SLO 1/3
26. SocietyofLeather Technologists andChemists, Official Methods ofAnalysis 1996,SLC 311 (SLO 2/6)
27. Tamper universityoftechnology, "Tannery Effluent Treatment in Advanced Integratedwaste waterpond system", Publications 425.

28. TaylorM.M.,CabezaL.F.,DimaioG.L.,BrownE.M.,MarmerW.N.,CarrioR., CelmaP.J.,Cot J.,ProcessingofLeatherWaste:PilotScaleStudiesonChrome Shavings.PartI.IsolationandCharacterizationofProteinProductsandSeparation ofChrome Cake. JALCA. 93 (3), 61, 1998.
29. Serrato, A.G. "Extraction ofOil from Soybeans". Journal oftheAmerican Oil Chemists' Society, 58(3): 157– 159, 1981.
30. International Standard ISO13321 Methods for Determination of Particle Size Distribution Part 8: Photon Correlation Spectroscopy,International Organization for Standardization(ISO)1996.AndSouissi, N.,Bougatef, A.,Triki-Ellouz, Y.,and Nasri, M. 2007.

IVL P-42

STUDY ON PREPARATION AND APPLICATION OF THE YELLOW POLYURETHANE DYE

Xiaoyan Pang*, Song Guo, Zhiwen Ding

China Leather and Footwear Industry Research Institute, No.18 Jiangtai West Road, Beijing, China, 100015, E-mail: pang_xiaoyan@163.com

National Engineering Laboratory for Clean Technology of Leather Manufacture, Sichuan University, Chengdu China, 610065, E-mail: pang_xiaoyan@163.com

The polymer dyes are safe and with low toxicity because they have big molecular size, better chemical and thermal stability, which is not easy to be absorbed by skin. They have not only the characters of polymers with high strength, easy film formation, good heat, and solvent migration resistance but also the colorful features of organic dyes. At present, it becomes the hot spots that the study on polymeric dyes as a substitute for the forbidden dyes or the environmental dyes. The yellow polyurethane dye was synthesized by self-emulsification method with tolylene-2, 4-diisocyanate, polyethylene glycol, dimethylolpropionic acid, glyceryl monostearate and acid yellow G. The structure was confirmed by Fourier transform infrared spectroscopy. Compared with acid yellow G, it is found that the yellow polyurethane dye has the same color absorption peak in the UV-vis spectra. Experiments show that the color polyurethane film has good heat resistance which shows the starting decomposition temperature is 315.0℃. The yellow polyurethane dye was used in synthetic leather which shows the dye absorption is more than 99% and the resistance to dry and wet rubbing are more than 4 grades.

Key words：Yellow polyurethane dye, Synthesis leather; Dyeing; color fastness

1 Introduction

Polyurethane dye is a new colorful polymer of high molecular which is obtained by grafting reaction that the dye will be grafted to the molecular chain of waterborne polyurethane. This combination gives dual function for the polymer dyes that the properties of polymer which are high strength, film formation, solvent resistance, migration resistance, heat resistance and workability as well as the properties of organic dye which are strong absorption for light and colorfulness.

When polymeric dyes are applied to dyeing process, the high dyeing absorption rate and a bright color and high color fastness will be got. In addition, due to the large molecular size of polymeric dye, it has good chemical and thermal stability, poor absorption for the skin so that the safe and low toxic features are got. These advantages make the study on the polymeric dye becomes a hot research field. Using polymer dye to dyeing is a new coloring process, which not only can obtain the color and transparency but also bring in the new reactive functional groups. Because of its special staining performance and environmental protection property, it has a huge value of research and development [1-4].

In recent years, polymeric dyes have obtained a certain development on the field of plastic and textile. But it is just begin in the application of synthetic leather materials. In this paper, based on the preliminary experiment and the orthogonal design [5, 6], the yellow polyurethane dye was prepared and the performances are studied.

The synthesis of emulsion was showed in scheme 1.

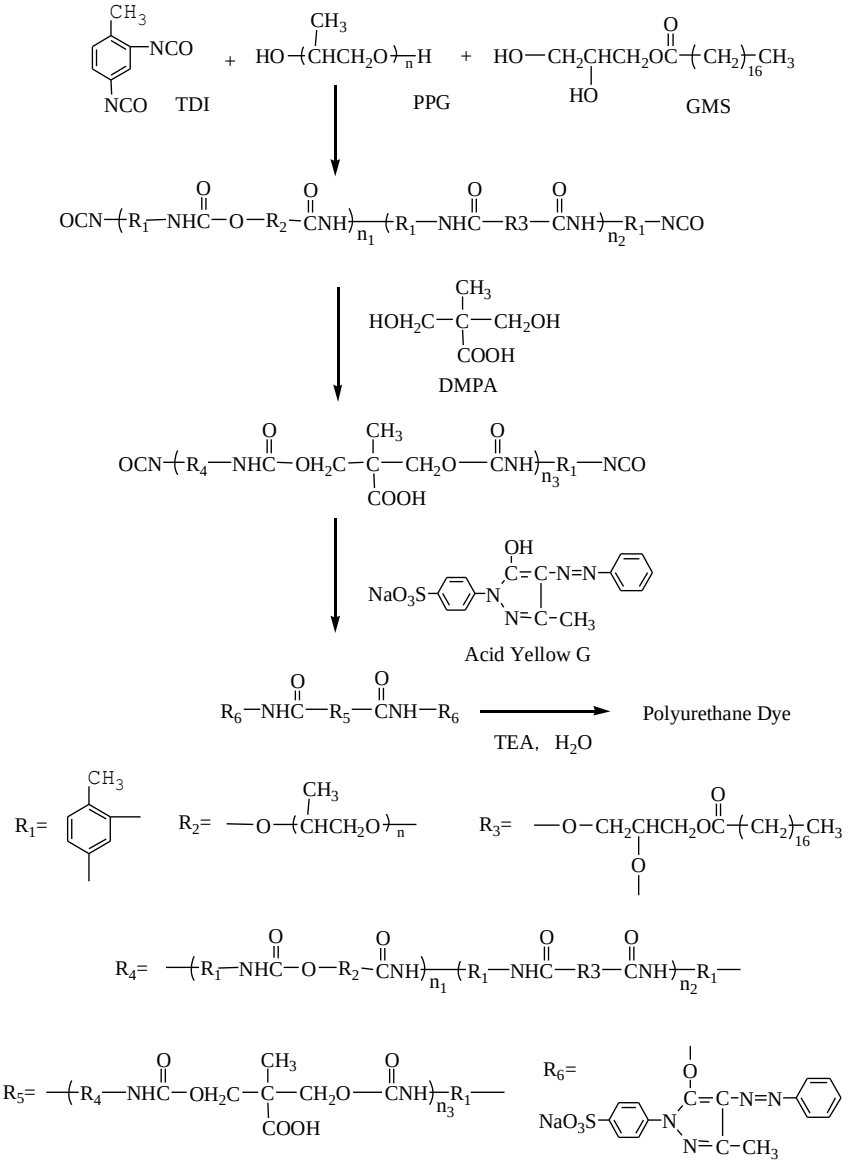

Fig.1 Synthesis scheme of the yellow polyurethane dye

2 Material and methods

2.1 Materials

Acid Yellow G (C.I. Acid Yellow 11), industrial grade, Jinan Longteng chemical plant; Toluene diisocyanate (TDI), industrial grade, Cangzhou Dahua Co., Ltd (TDI with n-hexane at 1:1 volume by heating reflux 2h, filtrating after distilling off the hexane); Polypropylene glycol (PPG, Mn = 1,000), industrial grade, Jiangsu Haian petrochemical plants (dehydration 2h at 110 ℃ vacuum); 2,2-dimethylol propionic acid (DMPA), industrial grade, Jiangxi Nancheng Hongdu Chemical Technology Development Co., Ltd; Glycerol monostearate (GMS), AR, Tianjin Guangfu Fine Chemical Research Institute; Triacetate amine (TEA), AR, Tianjin Hengxing chemical reagent Co., Ltd.; Acetone, AR, Beijing chemical Plant (driedwith 0.3nm molecular sieve which is activated at 500 ℃ before use).

Fourier infrared spectrometer, Tensor27, Bruker Inc. Germany ; Electric constant temperature drying oven, DHG-9140A, Yashilin laboratory equipment Ltd. Co.; Thermogravimetry Analyzer, TGA Q500, TA Instruments of America; Ultraviolet and visible spectrophotometer, TU-1810, Puxitongyong instruments Ltd. Co.

2.2 Experimental methods

2.2.1 Synthesis of the polyurethane emulsion dye

In a three-necked round-bottomed flask of 250ml equipped with a stirrer, thermometer and a condenser pipe, metric TDI, PPG, GMS and suitable amount of acetone were added. The temperature was heated to 75℃ and kept for 2h under N_2 atmosphere protection. When the NCO value was up to the expected, the temperature was cooled to 50 ℃. Then the DMPA was added and heated to 80 ℃ till the NCO value reaches the expected. Cooling to 50℃, the dye Acid Yellow G was added and the dosage was according to the NCO measured value. Then the temperature was heated to 80℃ until the NCO value could not be detected. Neutralizing agent TEA was added in 50℃ and stirred for 30min, then the product was poured into the emulsion barrel, the suitable amount of deionized water was added in high-speed stirring and shearing then the emulsion was got. The NCO group value was measured by di-n-butylamine titration method [7].

2.2.2 Preparation of cured film

The prepared polyurethane dye emulsion was placed horizontally at the teflon plate after 48h at room temperature and placed in a vacuum drying oven. The sample was dried to a constant weight at 60℃ and the film with the thickness of about 100μm was got.

2.2.3 Dyeing process of synthetic leather

Polyurethane dyes were used in the dyeing process of sea-island super-fine fiber synthetic leather. The dyeing process was as follow: firstly, the synthetic leather was put into the dyeing cup after weighing with the water ratio of 1500%, dye dosage of 5.0% (dry basis weight) and pH value of 5.0. Secondly, the dye solution temperature will be heated to 60 ℃ with heating rate of 1 ℃ / min, keeping 30min. then the dye solution was heated to 110℃ with heating rate of 0.5℃/min, keeping 60min. 1% formic acid was added to fix the color and keeping 30min. At last, the temperature was cooled to 70℃ and washing.

2.2.4 Characteristic method

(1) Fourier transforms infrared spectroscopy

The cured film was tested by the Fourier transforms infrared spectroscopy, the scanning range in the spectrum of 600~4000cm^{-1}.

(2) UV-visible absorption spectrum

The polyurethane dye and acid dye yellow G were prepared the concentration of 0.05g/L water solution which tested by TP-1810 ultraviolet-visible spectrophotometer. The test range of wave length is 200 ~780nm and the thickness of the sample pool is 10mm.

(3)The test of dye-uptake

The dyeing bath in the dyeing process of synthetic leather was diluted 50 times and tested in the wave length of 400 nm. The test method shows in the reference [8].

(4) The test of TGA

Shimadzu TGA-50H thermogravimetric analyzer was used to test TGA with a heating rate of 10℃ /minute in nitrogen atmosphere. The sample weight is between 6~10mg and the temperature range is from25℃ to 700℃.

(5) Test of color fastness

Dry rubbing fastness test: the rubbing cotton was adjusted 24h in the temperature of (23 + 2) ℃ and humidity of 55% ~ 55%. Wet rubbing fastness test: the white cotton was immersed in distilled water for 10min and then squeezing for the water content of 70% ~ 75%.

The sample of 25mm×220 mm was adjusted under the condition of constant temperature and humidity for more than 16h. The samples were tested in reciprocating at a speed of 30 times/min and one-way trip is 100 mm. Dry rubbing runs the 25 reciprocating and wet rubbing runs 20

reciprocating. The cotton cloth was removed and will be dry in the backlight, natural air condition at room temperature, and then judge the results.

3 Results and discussion

3.1 FTIR analysis.

Fig. 2 is the infrared spectrums of yellow polyurethane dye and the Acid Yellow G. The yellow polyurethane film spectrum shows three characteristic vibration peaks of carbamate in polyurethane including that 1713cm^{-1} which is stretching vibration peak of C=O; 3300 cm^{-1}, 1596 cm^{-1} and 1539 cm^{-1} which are the stretching, bending and deformation vibration peaks of N-H. It indicates the carbamate is got in the product. The stretching vibration peak of C-O-C is appeared in around 1101 cm^{-1} which shows the polyether polyol was brought into the product. In addition, the spectrum of acid yellow G shows that the stretching vibration of -OH is located at 3444 cm^{-1}, but the corresponding absorption peak disappeared in the spectrogram of yellow polyurethane dye which shows -OH groups in acid yellow G has reacted with -NCO completely[9, 10].

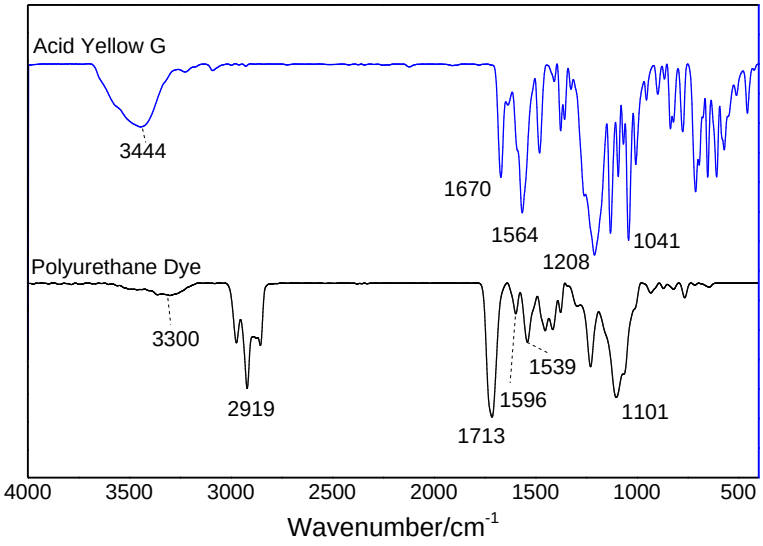

Fig.2 FTIR spectrum of the yellow polyurethane dye

3.2 UV-visible spectrum Analysis

Ultraviolet-visible spectra of the yellow polyurethane dye solution and the solution of acid yellow G are shown in Fig. 3 which shows that in the visible range absorption peak associated with polyurethane dye and acid yellow G can be seen. Both the absorption peaks are clear and obvious at 400nm, so they give the same yellow color. In addition, the absorption peak at 226nm has a red shift

of 18nm because the auxochrome -OH is disappeared and chromophores -N=N- and the benzene ring affected the the n→n* transition in the uitraviolet region and the peaks and absorption peak at 254nm have the overlap after the transition [11].

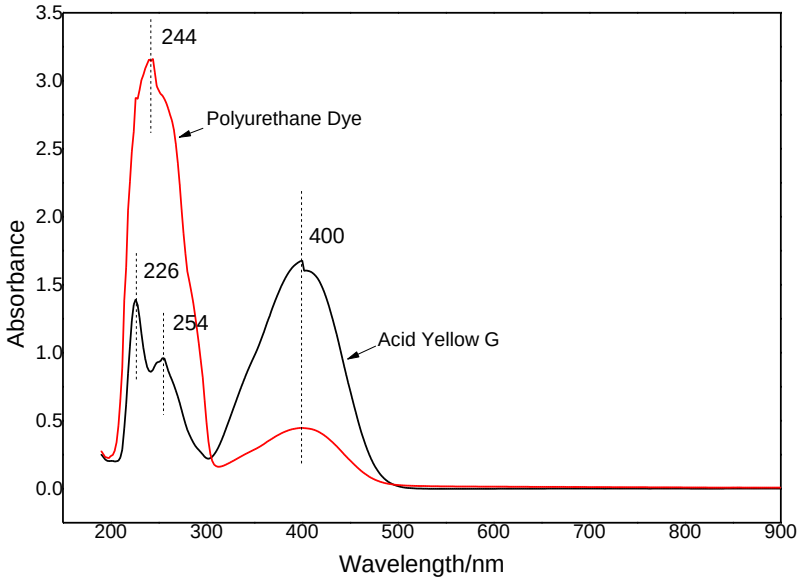

Fig.3 UV spectrum of the yellow polyurethane dye

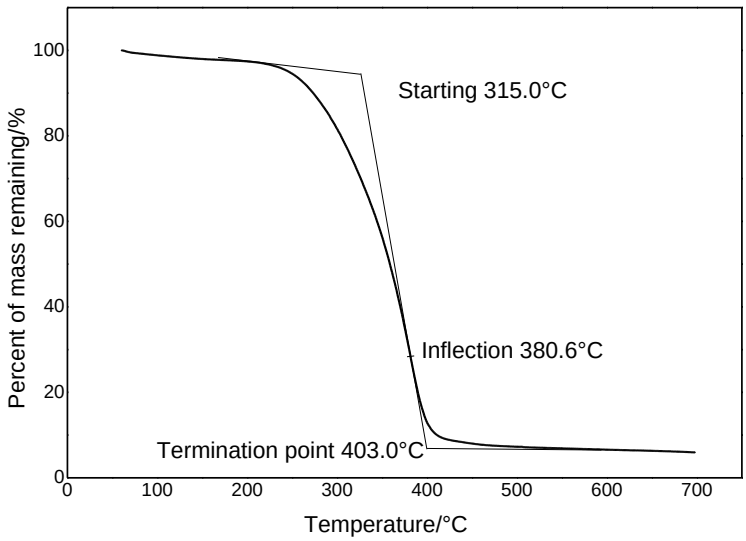

Fig.3 TGA curves of yellow polyurethane dye

3.3 Polyurethane dye film heat resistance

Fig. 3 is the TGA curve of the yellow polyurethane dye. As it can be seen there are two stages in the degradation of yellow polyurethane dye. The hard segment degradation starts at about 315.0℃, while the soft segment begins to degrade at 380.6℃. The thermal weight loss of product is up to 90% at 403.0℃. It is shown the polyurethane dye film has good heat resistance for the higher decomposition temperature of the initial material.

3.4 Application of yellow Polyurethane Dye

The yellow polyurethane dye was used in dyeing process of synthetic leather. The dyeing bath of 50-fold dilution was taken and tested by ultraviolet-visible spectrophotometer and the surface and incision of the samples after dyeing were tested. The results are shown in Tab. 1.

From Tab.1 we can see the color of synthesis leather from light to bright folling the increasing of the amount of polyurethane dye and the color is even in the synthetic leather. The bright color with dry fastness of 5grade and wet fastness of 4grade was got when the amount of dye is 6% and at this time the dye-uptake can reach 99.0%.

Tab. 1 Results of polyurethane dye in synthesis leather

The amount of dye /%	Absorbance /Abs	Rubbing fastness		Dye-uptake (%)	Appearance and the permeation
		Dry fastness	Wet fastness		
2.0	0.0829	5	4	99.5	Light color, full impregnated
4.0	0.0657	5	4	99.2	Light color, full impregnated
6.0	0.0495	5	4	99.0	Bright color, full impregnated
8.0	0.1011	5	4	98.1	Bright color, full impregnated

4 Conclusions

A new style of yellow polyurethane dye was synthesized and the structure was characterized by FTIR which shows the characteristic functional group has appeared in the dye. The UV-visible spectrum

shows the peak of yellow polyurethane dye in the visible range is the same with acid yellow G which means the color and hue didn't change after the modification. In addition the yellow polyurethane film has good heat resistance and its decomposition starting temperature is 315.0℃. The application test shows the yellow polyurethane dye can give the synthesis leather even permeation, good fastness and high color uptake when the dosage is 6%.

5 Acknowledgments

The authors are grateful to the National Natural Science Foundation of China (21376259) and National High Technology Research and Development Program (TS863) of China （2013AA065701） for financial support.

6 References

[1]TANG Ren-cheng, CHENG Wan-li. The synthesis methods of polymeric colorants and their application to fiber coloring[J]. Journal of Soochow University (Engineering Science Edition), 2002, 22 (02): 18-23.

[2] Zhang Shufen, Yang Jinzong. Research of Polymeric dyes by Chemical Modification of a Polymer by a Dye [J]. Dye Industry, 1998, 35 (06): 12-15.

[3] Angelina Altomare, Francesco Ciardelli, Giada Faralli. Synthesis of Reactive Polymeric Dyes as Textile Auxiliaries[J]. Macromolecular Materials and Engineering, 2003, 288: 679-692.

[4] Bingtao Tang, Shufen Zhang, Jinzong Yang, Feng Liu. Synthesis of a novel water-soluble crosslinking polymeric dye with good dyeing properties[J]. Dyes and Pigments, 2006, 68(1): 69-73.

[5]Zhang Yue, Qiang xihuai, Niu Ze, et al. Polyurethane Dyestuff with High Color Fastness[J]. Chinese Leather, 2015, 44(03): 22-25.

[6]Guo Song, Pang Xiaoyan, Ding Zhiwen, et al. Application of polyurethane dye in leather dyeing process[J]. China Leather, 2016, 45 (01): 15-18.

[7] Chen Jianfu, Huang Huizhen, Lin Xun. Improvement of the Test Method of Isocyanate Group Content in Polyurethane Prepolymer[J]. West Leather, 2012, 34(8):19-21.

[8] Lan Yunjun.Study on the synthesis Maleic acid derivatives - acrylic monomers copolymerization and the application in leather chemicals［D］. Dalian：Dalian University of Technology，1998：48

[9]Wang Chengzhong, Huang Li, Xu Desheng, et al. Synthesis and properties of colored polyurethane[J]. Journal of Beijing University of Chemical Technology (Natural Science), 2010, 37 (04): 44-47.

[10]Wang Ke, Peng ya, Wang Yan. Effects of hard segment content on the properties of aliphatic anionic waterborne polyurethanes[J]. Chemical Industry and Engineering Progress, 2010, 29(1): 119-123.

[11] Hu Xianhai, Zhang Xingyuan, Dai Jiabing. Synthesis and cured film property of waterborne polyurethane dye based on eriochrome black T[J]. Journal of Functional Materials, 2011, 42(2): 351-354.

STUDY ON THE TREATMENT OF DYES SOLUTION BY IMMOBILIZED *Trametes versicolor*

Xudong Xu, Yanchun Li, Deyi Zhu

Qilu University of Technology, No.3501, Daxue Rd, Changqing District, Jinan, Shandong Province,250353, China. E-mail: 15508633788@163.com

Qilu University of Technology, No.3501, Daxue Rd, Changqing District, Jinan, Shandong Province,250353, China. E-mail: qlulyc@126.com

Qilu University of Technology, No.3501, Daxue Rd, Changqing District, Jinan, Shandong Province,250353, China. E-mail: zhdy@qlu.edu.cn

Thebiological method was used to treat leather dye solution, immobilized *Trametes versicolor* gel particles and immobilized *Phanerochaete chrysosporium* gel particles were prepared by entraping the hypha into calcium immobilized. Acid gold yellow G dye solution was treated by some immobilized gel particles. The change of decolorization rate and the laccase activity were determined. When the existence of chrome tanning agent and NaCl, the decolorization rate of immobilized *Trametes versicolor* to the acid dyes, direct dyes, basic dyes solution were researched. Results indicate that immobilization *Trametes versicolor* gel particles to the acid gold yellow G dye (50mg/L) had a high decolorization rate, the 8 days decolorization rate was 96.86%. The existence of NaCl (1%) did not influence immobilized *Trametes versicolor* to dye decolorization rate. Under the gradient changes of dye concentration, immobilized *Trametes versicolor* gel particles to dyes showed good decolorization rate. The uv-visible spectrum research found that the maximum absorption peak of dye disappeared or decreased. The immobilized *Trametes versicolor* gel particles showed a broad spectrum of dye decolorization which had better decolorization effect for different types of dyes. At same time, the laccase was proved to have an important action on dye decolorization.

Key words：white rot fungus, immobilization,*Trametes versicolor,*dye decolorization, laccase

1. Introduction

A wide variety of dyes are used in leather industry, it can be divided into acid dyes, direct dyes, reactive dyes, basic dyes and metal complex dyes, acid and direct dyes were used a lot. At present,

more than half of dyes used in leather industry were azo dyes. Azo dye intermediates are carcinogens, they have toxicity to human and ecological environment, so treatment of dye waste water is important. Dye waste water usually were treated by physical method and chemical method, but the chromaticity color of waste water removing effect was not obvious, on the other hands the treatment process cost was very high. In recent years the researches of treatment of dyes waste water focus on microbial treatment. Large numbers of microorganisms degradation or adsorption of dyes have been reported, mainly microbes of fungi, especially white-rot fungus.

White-rot fungus used in treatment of dye waste water started with Jeffrey K (1983); The phanerochaete chrysosporium fungus to Poly real B - 411, Poly real R - 481, Poly real Y - 606 three dye degradation effect was very good, these had proved that the white-rot fungus can decolorize polymeric dye. Huang Yahe (2007) used the phanerochaete chrysosporium fungus to decolorize direct scarlet dye; the study found that suitable vibration and stirring was helpful to improve the effect of decolorization. Under the experimental conditions, the best time for inoculation bacteria was fourth day, the optimal concentration of dealt dye was 60~80 mg/L, the best pH is from 4 to 5, a theoretical basis for treatment of actual dye waste water had been acquired. White-rot fungus decolorization and degradation of dye was mainly relied on the secretion of enzyme system, it can reduce the chromophore of dyes and make dye decolorization, degradation and eventually mineralization (Hou Hongman et al. 2004) . Relative to the free cells, immobilized cells can grow stable and with strong degradation ability. Immobilized cells can use aromatic compounds in the waste water to grow and become fully biodegradable material, like phenol, naphthalene and phenanthrene all can be completely degraded (Bi Shenglei et al. 2015) .

Dede Heri Yuli Yanto (2014) studied the immobilized enzyme produced by *Trametes versicolor* in bioreactor to treat the textile dyes, the study found that it can improve the efficiency of the dye decolorization, immobilized enzyme applied in the bioreactor for the treatment of dye waste water had potential application value. Maria Jonstrup (2013) used the mix of *Trametes versicolor*, phanerochaete chrysosporium fungus and Bjerkandere adusta to decolorize azo dyes and the waste straw was used as co-substrate, then they were applied in bioreactor to decolorize dye, in 12 days decolorization rate maintained within 65 ~ 90%. Brandt Bertrand (2014) used the softwood and hardwood timber as co-substrates culture of *Trametes versicolor*, then used the *Trametes versicolor* to decolorize of Orange II, and the laccase enzyme activity 1.92±0.15 U mL^{-1} was measured. Dalel Daassi (2013) utilized sodium alginate and calcium chloride to immobilize *Trametes versicolor*, then used the immobilized calcium alginate beads to decolorize metal textile Grey Lanaset G dye, decolorization effect and repeat use performance were good. Sun Hongfei (2015) and the others used chitosan to graft polyacrylamide hydrogel, then used them to immobilize laccase produced by *Trametes versicolor*, immobilized laccase had more chemical stability than free laccase and dye decolorization effect was better. Laccase production by pre-growth pellets of Trametes versicolor

using two types of textile dyes as inducers was studied by N. Casasa (2013). Experimental results indicated that Grey Lanaset G can be used as an inducer and as an N source.

In this paper, the embedding method was used to immobilize white-rot fungus, decolorization ability of the immobilized *Trametes versicolor* gel particles and immobilized *Phanerochaete chrysosporium* gel particles to dyes was explored. The researched results will provide a theory basis for biological method to treat dye waste water.

2. Materials and methods

2.1 Materials

Trametes versicolor CICC 50001 was obtained from the China Center of Industrial Culture Collection, Phanerochaete chrysosporium BKM-F-1767 was obtained from the Guang dong Microbiological Culture Center; Acid golden yellow G, Basic Fuchsine, Reactive red K-2G, Reactive blue K-2BP, Acid mordant dark PV, Direct green BG, Directly lake blue 5B dye, domestic industrial grade dye obtained from Tianjin Yadong Chemical Dyestuff Factory of China were used in the study.

2.2 Liquid medium

Glucose 20 g/L, KH_2PO_4 2 g/L, $MgSO_4$ 0.25 g/L, $CaCl_2$ 0.1 g/L, $MnSO_4$ 5 mg/L, VB_1 15 mg/L, Ammonium tartrate 0.2 g/L, The concentration of trace elements was 150 mL/L.

2.3 Trace elements

NaCl 1.0 g/L, $MgSO_4 \cdot 7H_2O$ 3.0 g/L, $FeSO_4 \cdot H_2O$ 100 mg/L, $CoSO_4 \cdot 7H_2O$ 100 mg/L, $CaCl_2$ 100 mg/L, $ZnSO_4 \cdot 7H_2O$ 100 mg/L, $CuSO_4 \cdot 5H_2O$ 10mg/L, $KAl(SO_4)_2$ 100 mg/L, H_3BO_3 10 mg/L, Na_2MoO_4 10 mg/L.

2.4 Experimental method

2.4.1 Immobilization methods

Trametes versicolor and *Phanerochaete chrysosporium* were cultured in liquid medium, 1.5 g *Trametes versicolor* and1.5 g *Phanerochaete chrysosporium*, 3 g *Phanerochaete chrysosporium*,3 g *Trametes versicolor* hypha was mixed with 40mL distilled water respectively, 60 mL sodium alginate solution (2 g sodium alginate was dissolved in 60 mL water) was added into the system. Then 5 mL mixture was extracted and dripped into 2% calcium chloride solution. The immobilization *Trametes versicolor* sodium alginate-calcium chloride gel particles, immobilization *Phanerochaete chrysosporium* sodium alginate-calcium chloride gel particles, immobilization *Phanerochaete chrysosporium and Trametes versicolor* sodium alginate-calcium chloride gel particles were obtained after two hours reaction. The gel particles were obtained as a fixed amount.

2.4.2Influence of time to the decolorization rate of dye by the immobilization gel particles

The dye solution (using the liquid medium compound with 50 mg/L) was treated by fixed amount of immobilization gel particles. Then they were cultured in the constant temperature oscillation incubator (27 ℃, 100 r/min), decolorization rate determination was observed in eight days (d).

2.4.3 Influence of time to the enzyme activity of laccase

The dye solution (using the liquid medium compound with 50 mg/L) was treated by fixed amount of immobilization gel particles and bioequivalence of hypha, separately. Then they were cultured in the constant temperature oscillation incubator (27 ℃, 100 r/min), enzyme activity of laccase was observed in eight days (d). The absorbance changes before and after eight days was measured.

2.4.4 Influence of 1% NaCl to the decolorization rate of dye by the immobilized *Trametes versicolor* gel particles

The dye solution containing 1% NaCl (using the liquid medium compound with 50 mg/L) was treated by fixed amount of immobilization gel particles. Then they were cultured in the constant temperature oscillation incubator (27 ℃, 100 r/min) for six days, the change of decolorization spectrogram was measured.

2.4.5 Influence of 1% chrome tanning agent to the decolorization rate of dye by the immobilized *Trametes versicolor* gel particles

The dye solution containing 1% chrome tanning agent (using the liquid medium compound with 50 mg/L) was treated by fixed amount of immobilization gel particles. Then they were cultured in the constant temperature oscillation incubator (27 ℃, 100 r/min) for six days, the change of decolorization spectrogram was measured.

2.4.6 Influence of the dye concentration to the degradation rate of dye by the immobilized *Trametes versicolor* gel particles

The liquid medium was used to compound with 25 mg/L ~ 150 mg/L acid gold yellow G dye solution, 25 mg/L was taken as a concentration gradient. Then they were treated by fixed amount of immobilization gel particles under the condition of constant temperature oscillation incubator (27 ℃, 100 r/min) for six days, the change of decolorization spectrogram was measured.

2.4.7 Influence of different types of dye to the degradation rate of dye by the immobilized *Trametes versicolor* gel particles

The dye solution (using the liquid medium compound with 50 mg/L) of Acid gold yellow G, Basic Fuchsine, Reactive red K-2G, Reactive blue K-2BP, Acid mordant dark PV, Direct green BG, Directly lake blue 5B dye was treated by fixed amount of immobilization gel particles respectively. Then they were cultured in the constant temperature oscillation incubator (27 ℃, 100 r/min) for six days, the change of decolorization spectrogram was measured.

2.5 The determination of dye decolorization rate

The UV-vis spectrophotometer was employed to determine the absorbance of dye solution before and after the decolorization. The dye decolorization rate by white-rot fungu was calculated by formula (1).

$E=(A_0-A_t)\ /A_0\times100\%$ (1)

Where, A_t was the absorbance of dye solution at t time, A_0 was the absorbance of original dye solution, E is decolorization rate.

2.6The determination of enzyme activity of the laccase

Guaiacol colorimetric method: 0.15 mol/L sodium acetate was used to prepare 3 mmol/L guaiacol mixture solution. Then take 1 mL mixture solution to react with 2 mL enzyme solution for 5min under 30℃. The absorbance changes in the 465 nm before and after reaction were determined by uv-vis spectrophotometer. An enzyme activity unit was defined as per minute causing absorbance a 0.01 unit changes required amount of enzyme liquid (Dhawan Shikha et al.2005) .

3. Results and Discussion

3.1 Influence of the time to the decolorization rate of dye and enzyme activity of the laccase by the immobilized gel particles

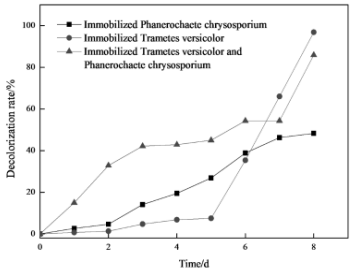

Fig.1 Influence of the time to the decolorization rate of dye by the immobilized gel particles

According to the obtained results, we could see that the immobilization *Trametes versicolor* had the highest decolorization rate to the acid gold yellow G in three kinds of immobilized gel particles, the decolorization rate was 96.86% in eight days. *Trametes versicolor* and *Phanerochaete chrysosporium* belong to white-rot fungus, there are more difference of the dye decolorization rate of these two kinds of bacteria, the reason may be that the two bacteria would produce different extracellular

enzymes, *Trametes versicolor* have produced a kind of laccase more than *Phanerochaete chrysosporium*, the laccase have large effects to the immobilized gel particles decolorization of dye.

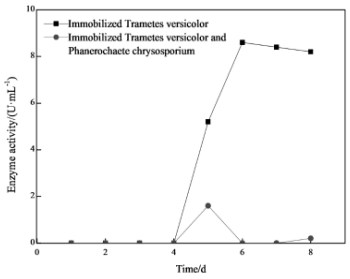

Fig.2 Influence of the time to the laccase enzyme activity

Through the comparison for Fig. 1 and Fig. 2 we make out that the two kinds of embedding *Trametes versicolor* immobilization gel particle were undetectable laccase in the first four days, but the immobilization gel particles had a certain effect to dye decolorization. The embedding of two kinds of bacteria immobilization gel particles to dye decolorization rate was higher at the beginning, visible initial decolorization of dye depended on other extracellular enzymes or adsorption by the hypha. The largest enzyme activity was 8.2 U/mL, at the late immobilized *Trametes versicolor* gel particles for dye decolorization rate increased rapidly that was the effects of laccase.

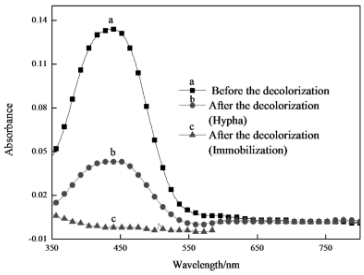

Fig.3 Dye solution absorbance changes before and after treatment by the immobilization *Trametes versicolor* gel particles and the free hypha

From Fig.3 can be seen that immobilized *Trametes versicolor* gel particles to decolorization rate of acid gold yellow G was obviously higher than free hyphae decolorization of dye. Free hypha to decolorization of dye main depended on adsorption, for dye absorption maximum peak did not disappear; Immobilized *Trametes versicolor* gel particles to decolorization of dye main depended on degradation of dye, for dye absorption peak is disappear.

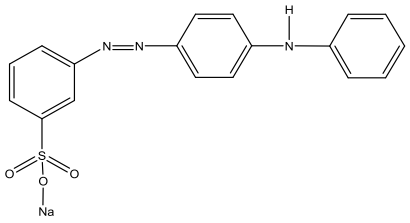

Fig.4 The formula of acid gold yellow G

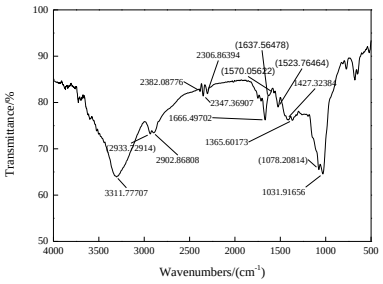

Fig.5 The infrared spectra of dye solution （Before the decolorization)

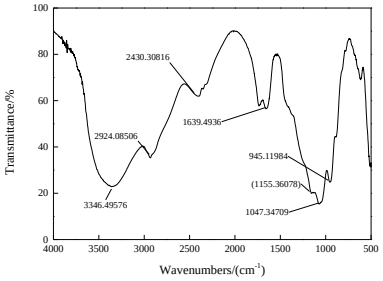

Fig.6 The infrared spectra of dye solution （After the decolorization)

Acid gold yellow G molecular formula is shown in Fig.4. Fig.5 is the infrared spectra of dye solution (using liquid medium compound with 50 mg/L acid gold dye yellow G) before the decolorization, there are several characteristic 1523 cm^{-1}, 1570 cm^{-1} for benzene ring frame vibration absorption peak of C=C; 1427 cm^{-1} for N=N vibration absorption peak; 1365 cm^{-1} for the aromatic carbon to nitrogen atom connection of C-N characteristic absorption peak; 1078 cm^{-1} for sulfonic acid root characteristic absorption peak; 3311 cm^{-1} for N-H characteristic absorption peak. The infrared spectra of dye solution after treatment by the immobilization *Trametes versicolor* gel particles are shown in Fig. 6, it shows that 1523 cm^{-1}, 1570 cm^{-1} in benzene ring skeleton C=C vibration absorption peak disappeared, it illustrates that the benzene ring was cracked. 1427 cm^{-1} N=N vibration absorption peak disappeared, meaning that the azo bond was cracked and disappeared. 1365 cm^{-1} nitrogen atoms connected to the characteristics of C-N aromatic carbon absorption peak disappeared, illustrating that the C-N was cracked.

3.2 Influence of 1% NaCl to the decolorization rate of dye by the immobilized *Trametes versicolor* gel particles

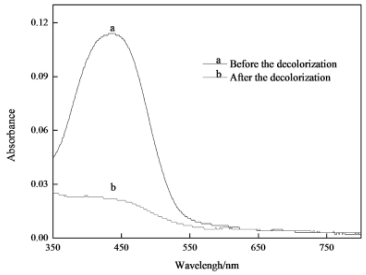

Fig.7 Dye solution absorbance changes before and after treatment by the immobilization *Trametes versicolor* gel particles under the concentration of 1% NaCl

In the presence of 1% NaCl immobilized *Trametes versicolor* gel particles decolorization rate to acid gold yellow G dye remained very high and the dye maximum absorption peak disappeared. It illustrates that the dye was degraded. Its significance lies in the fact that in the wastewater of retanning and dyeing there is a certain concentration of NaCl (general concentration below 1%), its existence does not affect the immobilized *Trametes versicolor* gel particles to decolorize to dye.

3.3 Influence of 1% chrome tanning agent to the decolorization rate of dye by the immobilized *Trametes versicolor* gel particles

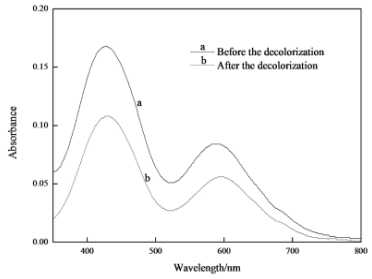

Fig.8 Dye solution absorbance changes before and after treatment by the immobilization *Trametes versicolor* gel particles under the concentration of 1% chrome tanning agent

In the presence of 1% of chrome tanning agent immobilized *Trametes versicolor* gel particles decolorization rate of acid gold yellow G was not high, the absorption peak of dye and chrome tanning agent are still remain, fully biodegradation was failed, it illustrates that the chrome tanning agent has some side effect to immobilized *Trametes versicolor* gel particles decolorization to dye. The main reason is that chrome tanning agent has certain toxicity and had affected the biological activity of *Trametes versicolor*, so dye decolorization rate reduced.

3.4 Influence of the dye concentration to the degradation rate of dye by the immobilized *Trametes versicolor* gel particles

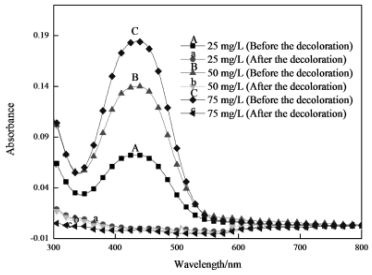

Fig.9 Dye solution absorbance changes before and after treatment by the immobilization *Trametes versicolor* gel particles (25~75mg/L)

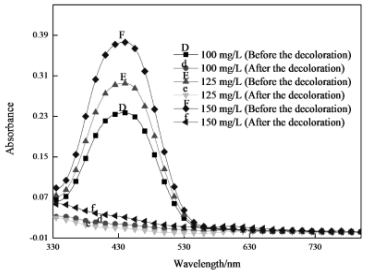

Fig.10 Dye solution absorbance changes before and after treatment by the immobilization *Trametes versicolor* gel particles (100~150mg/L)

The immobilized *Trametes versicolor* gel particles to different concentration of acid gold yellow G (25 mg/L to 150 mg/L) all have good decolorization effects, the maximum absorption peak of dye all disappeared. The results illustrate that the immobilized *Trametes versicolor* gel particles to decolorization of dyes were kept high ability within the scope of a certain concentration of dye. So these have provided theoretical basis for application immobilized *Trametes versicolor* gel particles in treatment of different qualities dyestuff wastewater in the bioreactor.

3.5 Influence of different types of dye to their decolorization rate by the immobilized *Trametes versicolor* gel particles

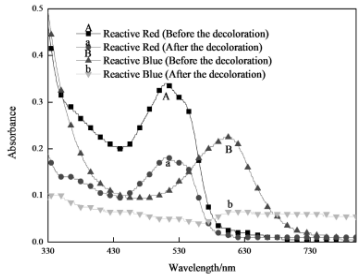

Fig.11 Reactive dye solution absorbance changes before and after treatment by the immobilization *Trametes versicolor* gel particles

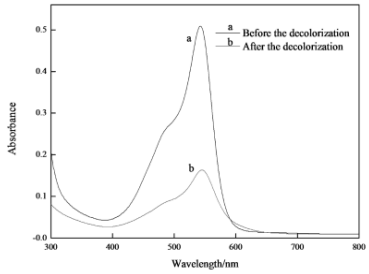

Fig.12 Basic Fuchsine dye solution absorbance changes before and after treatment by the immobilization *Trametes versicolor* gel particles

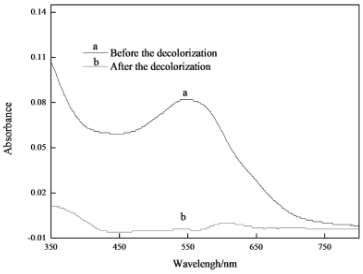

Fig.13 Acid Complex Black dye solution absorbance changes before and after treatment by the immobilization *Trametes versicolor* gel particles

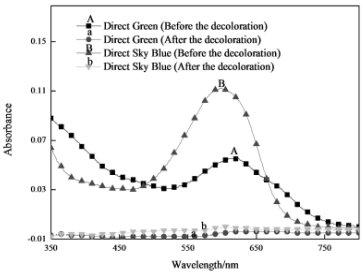

Fig.14 Direct dye solution absorbance changes before and after treatment by the immobilization *Trametes versicolor* gel particles

The Fig.11 ~ Fig.14 showed that dye decolorization by immobilized *Trametes versicolor* gel particles, in addition to active red dye and fuchsine dye, the rest of the dyes were decolorized completely, the dye maximum absorption peaks disappeared. The result indicated that immobilized *Trametes versicolor* gel particles have a good decolorization efficiency.

4. Conclusion

(1) Comparing with free hyphae, dye decolorization rate of the immobilized *Trametes versicolor* had a bigger enhancement. The results indicated that immobilization can improve the decoloriziation ability of *Trametes versicolor*.

(2) In the process of dye decolorization, laccase enzyme activity reached a relatively high value 8.2 U/mL, two kinds of *Phanerochaete chrysosporium and Trametes versicolor* hyphaes immobilized together would affect the enzyme activity of laccase. The presence of 1% NaCl had little influence to the immobilized *Trametes versicolor* decolorization to dye, the presence of 1% chrome tanning agent had some influence to the immobilized *Trametes versicolor* decolorization to dye.

(3) The decolorization ability of immobilized *Trametes versicolor* to dyes are universality, the maximum absorption peak of several dyes disappeared after decoloriziation. The results indicate that immobilized *Trametes versicolor* can realize the degradation of dye.

5.Acknowledgements

The authors would like to gratefully thank the support of National Natural Science Foundation (No. 21276150), China; and Shandong Province key research and development project (No.2015GGX108004).

6.References

[1] Jeffrey K, Glenn and Michael H. Gold. Decolorization of several Polymeric Dyes by the lignin-Degrading Basidiomycete

Phanerochate chrysosporium. Appiled and Environmental Microbiology, 1983, 45 (6): 1741-1747.

[2] Huang Yahe, Chang Tianjun, Yang Zhongdong. Study on Decoloration of Dye Waste water by White-Rot-Fungi.

Industrial Heating, 2007, 36 (6): 43-44.

[3] Hou Hongman, Zhou Jiti, Wang Jing,et al. Characteristics of laccase from white-rot fungus pleurotous ostreatus Strain

3.42 and its decolorization effect on anthraquinone dye. Chemistry and Industry of Forest Products, 2004, 24 (1): 48-52.

[4] Bi Shenglei, Zhang Chengming, Li Shizhong, et al. Research and Application Progress of Immobilization

Technology in Bio-energy and Environmental Engineering. Liquor-making Science and Technology, 2015, (1): 102-105.

[5] Dede Heri Yuli Yanto, Sanro Tachibana, Kazutaka Itoh. Biodecolorization of textile dyes by immobilized

Enzyme in a vertical bioreactor system. Procedia Environmental Sciences, 2014, (20): 235-244.

[6] Maria Jonstrup, Naresh Kumar, Benoit Guieysse, et al. Decolorization of textile dyes by Bjerkandera sp. BOL13 using

waste biomass as carbon source. Journal of Chemical Technology and Biotechnology, 2013, 88 (3): 388-394.

[7] Brandt Bertrand, Fernando Martínez-Morales, Raunel Tinoco, et al. Induction of laccases in Trametes versicolor by

aqueous wood extracts. World Journal of Microbiology and Biotechnology, 2014, 30 (1): 135-142.

[8] Dalel Daâssi, Tahar Mechichi, Moncef Nasri, et al. Decolorization of the metal textile dye Lanaset Grey G by

immobilized white-rot fungi. Journal of Environmental Management, 2013, 129: 324-332.

[9] Sun Hongfei, Yang Hua, Huang Wenguang, et al. Immobilization of laccase in a sponge-like hydrogel for enhanced

durability in enzymatic degradation of dye pollutants. Journal of Colloid and Interface Science, 2015, 450: 353-360.

[10] N. Casasa, P. Blánqueza, T. Vicenta, et al. Laccase production by *Trametes versicolor* under limited-growth conditions

using dyes as inducers. Environmental Technology, 2013, 34 (1): 113-119.

[11] Dhawan Shikha, Lal Rup, Hanspal Manjit, et al. Effect of antibiotics on growth and laccase production from Cyathus

bulleri and Pycnoporus cinnabarinus. Bioresource Technology, 2005, 96 (12): 1415-1418.

RESEARCH ON FORMALDEHYDE EMISSION CHARACTERISTICS OF FORMALDEHYDE TANNED LEATHER BY SEALED JAR METHOD

Yuan Xuzheng, Wang Xuechuan, Lu Weina,and Jiang Sujie

College of Bioresources Chemical and Materials Engineering, Shaanxi University of Science & Technology, Xi'an710021, P.R.China, wxc-mail@163.com

Jiaxing Fur and Footwear Research Institute,Tongxiang314500, P.R.China, yuanxuzheng@163.com

This study presented a first effort to focus on the formaldehyde emission characteristics of formaldehyde tanned leather. Formaldehyde release tests were carried out according to ISO 17226-3 standard-sealed jar method. Effects of temperature on the release behavior were investigated. The formaldehyde emission model of formaldehyde tanned leather in sealed system was established according to the law of mass transfer under several reasonable assumptions and verified by the fitting of actual release data.Application and prospect of release theory were discussed.

The results showed that formaldehyde emission could be divided into three stages: the linear free release, barrier release and chemical release stage. The linear release time inversely correlated with mass transfer coefficient which positively correlated with temperature. The release temperature had significant promotion impact to release during linear release time. The higher the temperature was, the faster the formaldehyde release. Because of the difference of porosity, different types of leather showed different release characteristic. The average release speed of sheepskin was faster than that of cowhide at the same temperature. The release of formaldehyde in cowhide was more sensitive to the temperature. The temperature increased from 30℃ to 60℃, the formaldehyde release speed of sheepskin increased 19.39% for every increase of 1 degree Celsius by average, and that of cowhide increased 29.92%.

Keywords: formaldehyde, emission model, leather

1. Introduction

Around the globe, people spend approximately 90% of their time indoors, thus making the indoor air quality have a significant impact on the modern life (Wei et al.2015). Formaldehyde is a member of a large group of compounds known as volatile organic compounds (VOCs) which will off-gas into the air. Exposures to VOCs have recently become a public concern. Many studies indicated that short- and long-term exposure to mixtures of VOCs may cause mucosal irritation, non-specific symptoms

(Araki et al.2010; Mendell et al.2002). Therefore, VOCs like the formaldehyde emitted from a wide range of building materials and consumer products often pose a threat to the environment safety and human health. To understand and control this issue, the research on product formaldehyde emissions has become a hot interdisciplinary topic in the fields of material and environmental sciences. However， almost all of the studies are focused on wood building materials (Cui et al.2015; Ding et al.2013; Xiong et al.2011; Salem et al.2013), scarcely mentioned about leather products.

Leather industry, an age old enterprise provide a wide range of consumer goods such as garments, home furnishings leather, automotive upholstery leather etc (Sumita et al.2015). The formaldehyde emission of these leather products may cause poor indoor air quality (Bin et al.2016; Tao et al.2015).However, most of our researches concerning formaldehyde content of leathers are analyzed according to the standard ISO 17226-1 and ISO 17226-2, after aqueous micellar extraction of the shredded leather sample (Blanc et al.2009; Font et al.2008; Mentes et al.2014). The free formaldehyde and formaldehyde which was hydrolysed during extraction to yield free formaldehyde are detected by these two methods. Actually， in the process of using leather products, the chance of exposure to water is relatively small, and most of the time, leather products are exposed in the air with certain temperature and relative humidity. Obviously, the eluted condition was not consistent with actual use environment condition of leather products. The standard ISO 17226-3 called sealed jar method specifies a method for determining the emission of formaldehyde from leathers, which can be more realistic to simulate the release of formaldehyde to the gas phase in using the leather and its products.

To deepen the insight into the emission characteristic, reduction measures and the risk assessment for leather products formaldehyde emissions, especially formaldehyde tanned leather, a series of attempts have been recently made by the present work, and this work would present a first effort to focus on the formaldehyde emission characteristics of leather materials. Formaldehyde release tests were carried out according to ISO 17226-3 standard. Effects of temperature on the release behavior were investigated. The release equation was derived based on the release model and verified by the actual release data. The applications of release equation were introduced at the end.

2. Material and methods

2.1 Materials

Formaldehyde tanned sheepskin and cowhide were prepared by local leather factory (using the same process). Formaldehyde (approximately 37% (w/w) stabilized with 10methanol), HPLC grade acetonitrile, o-phosphoric acid, iodine,sodium hydroxide, sulphuric acid, sodium thiosulphate, carbon tetrachloride and starchwere obtained from Sinopharm Chemical Reagent Co., Ltd.(Shanghai, China). 2,4-dinitrophenyl hydrazinewas purchased from Richjoint Chemical Reagent Co., Ltd.(Shanghai, China). Otherwise stated, all reagents used wereanalytical grade.

2.2 Pretreatment of Leather Samples

After formaldehyde tannage, shrinkage temperature of the leather was measured. The leather was hanged to dry in the natural air for 12 hours, and put into vacuum drying oven with temperature at 50℃ for 3 hours during the second days. Finally, the leather was cut into (100×40) mm specimens by the knife mold, sealed in inert gastight plastic bags, and put into the refrigerator for cold storage until used.

2.3 Procedure for the Determination of Formaldehyde Emission by the HPLC Method

The emission apparatus and procedure were described as ISO 17226-3.The sealed 1L bottles were stored in a heated oven (DHG-9070A, China). In order to collect the data of formaldehyde emission, pipette 1mL absorption solution into a 10 mL volumetric flask as far as possible with specified time intervals. Fill the volumetric flask with demineralized water up to the mark and shake it briefly by hand. The formaldehyde absorbed in the water were identified according to ISO 17226-3 standard with HPLC (Agilent 1200, America).

2.4 Determination of Porosity of Leather by Carbon Tetrachloride Permeation Method

Formaldehyde tanned leather was cut into small narrow strips with 20mm length and (2~3) mm width. Leather scraps attached on the strips were clean up carefully. Weigh 5g strips to 0.01g, put into 50mL (denoted by V_0) volumetric flask, fill the volumetric flask with carbon tetrachloride up to the mark by the burette; the volume of carbon tetrachloride used was denoted by V_1. After standing for 24 hours, to ensure that the volume of carbon tetrachloride in the bottle was constant. Fill the volumetric flask with carbon tetrachloride up to the mark by the burette again, the volume of carbon tetrachloride used was denoted by V_2. Carbon tetrachloride and strips were poured out the volumetric flask, carbon tetrachloride on the strips surface was absorbed with the filter paper. The strips were put back into volumetric flask, carbon tetrachloride was added to the scale and the volume was denoted by V_3. Porosity of leather (denoted by P) was calculated by the formula 1.

$$P\,(\%) = \frac{V_1 + V_2 - V_3}{V_0 - V_3} \times 100 \qquad (1)$$

2.5 SEM Observation

Formaldehyde tanned leather was cut into a small narrow strip with (3~5) mm width. The strip was put into desiccator with 65% relative humidity to a constant weight. Then the strip was broken off

when it was put in liquid nitrogen. The cross section was coated with gold; the scanning electron microscope (SU-1500, Japan) was used to observe the surface topography of its cross section.

2.6 Effect of Temperature on Release Behavior

The sealed 1L bottles were stored in a heated oven at 30℃, 40℃, 50℃ and 60℃ separately. Pipette 1mL absorption solution into a 10 mL volumetric flask quickly every 1 hour within 7 hours. Fill the volumetric flask with demineralized water up to the mark and shake it briefly by hand. The formaldehyde absorbed in the water were identified according to ISO 17226-3 standard with HPLC.

2.7 Release Kinetics of Formaldehyde Tanned Leather

The sealed 1L bottles were stored in a heated oven at 60℃. Pipette 1mL absorption solution into a 10 mL volumetric flask quickly every 1 hour. Fill the volumetric flask with demineralized water up to the mark and shake it briefly by hand. The formaldehyde absorbed in the water were identified according to ISO 17226-3 standard with HPLC. The difference of the formaldehyde concentration absorbed in the water between the two adjacent sampling points was less than 5% (EUR13216EN, 1990); it can be considered that the release was balanced and experiment could be over. The trials were repeated 3 times and then to get the average value.

3. Results and Discussion

3.1 Results of the Porosity of Leather

From a mesoscopic point of view, leather could be considered as a porous material, in which the macro- and meso- holes distributed were connected to each other, so as to form the main channel for the release of formaldehyde and the main place for the absorption and storage of water. Porosity of leather mainly depends on the tightness of organizational structure of the raw skin, the combination and filling effect of tanning agents in the tanning process. The greater the porosity was, the looser the structure of leather was. As a result, the formaldehyde was easier to release through the pore diffusion, the sum of pore volume for water absorption was larger and the water absorption of the sample was likely to be the largest. The porosity of the leather sample was measured by carbon tetrachloride penetration method, and the specific results were shown in Table I. According to Table I, the porosity of the formaldehyde tanned sheepskin was larger than that of the formaldehyde tanned cowhide, which was mainly caused by the structure of the raw skin, the collagen fibers of cowhide was tighter than that of the sheepskin. Obviously, the porosity of the leather sample may affect formaldehyde release.

TABLE I

Results of the porosity of leather

Sample	V_0 (mL)	V_1 (mL)	V_2 (mL)	V_3 (mL)	P (%)
sheepskin	50.00	45.57	0.62	43.80	38.55
cowhide	50.00	45.87	0.35	44.60	30.00

3.2 SEM Images of Leather Cross Section

The surface topography of formaldehyde tanned leather cross section was investigated by SEM technique, and the results were illustrated in Figure 1. Compared with the formaldehyde tanned sheepskin（see Figure 1 a）, the structure of the formaldehyde tanned cowhide（see Figure 1 b）was more compact and tighter. These observations were consistent with the experimental results of the porosity of the samples.

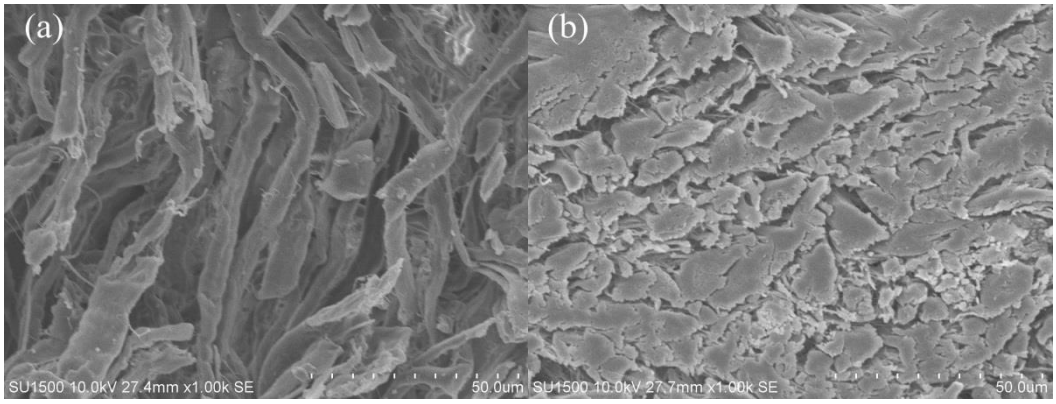

Figure 1. SEM images of (a) sheepskin; (b) cowhide

3.3 Effect of Temperature on Formaldehyde Emission

The quantity of emitted formaldehyde (denoted by Q) from sheepskin and cowhide at 30℃, 40℃, 50℃ and 60℃ within 7 hours were displayed in Figure 2 and Figure 3. According to the ASTM standard (D5157-97, 2003),the correlation coefficient (denoted by R) was higher than 0.9 (i.e. R^2 was higher than 0.81), it can be believed that the fitting result was credible. According to figures, all of the R^2 of fitting curves were higher than 0.98, which was to say, formaldehyde release showed rapid linear characteristics during the early stage (within 7 hours) and there were a stable average release speed.

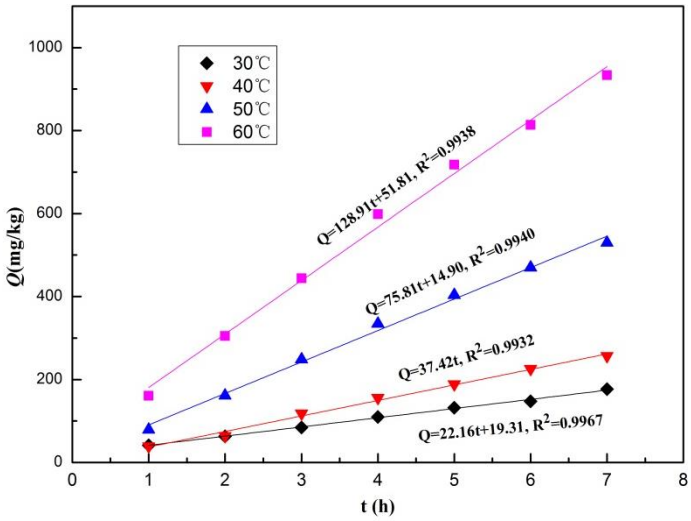

Figure 2. Release fitting curves of sheepskin under different temperature within 7 hours

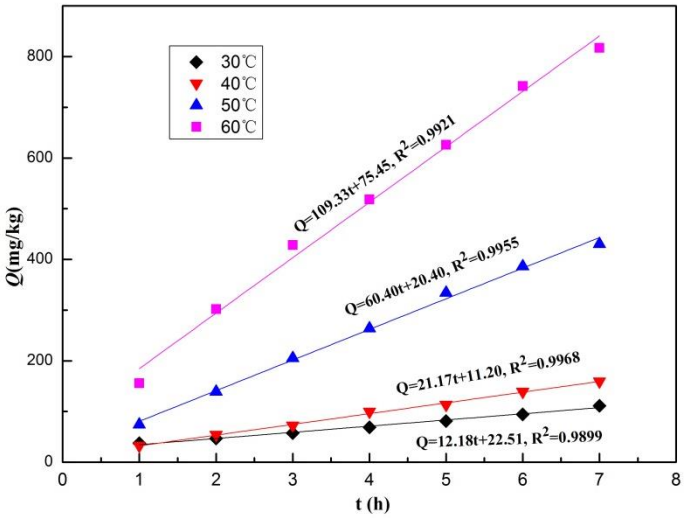

Figure 3. Release fitting curves of cowhide under different temperature within 7 hours

Temperature had significant effects on formaldehyde release. The higher the temperature was, the faster the formaldehyde release. For sheepskin, the average release speed at 40℃ was 1.69 times of that at 30℃, 50℃ was 3.42 times and 60℃was 5.82 times. For cowhide, the average release speed at 40℃ was 1.74 times of that at 30℃, 50℃ was 4.96 times and 60℃ was 8.98 times. According to the results of the porosity, leather was a porous material with strong adsorption capacity. With temperature increase, the molecule thermal motion of free formaldehyde or formaldehyde adsorbed in the capillary of leather was promoted; the formaldehyde diffusion coefficient and capacity was enhanced; a large amount of formaldehyde was desorbed from leather and released to the air. Besides, temperature could promote the water absorption of leather. The higher the temperature was, the more the water was absorbed. Water had different saturated vapor pressure under

different temperatures, which were 4.25kPa, 7.38kPa, 12.34kPa and 19.93kPa at 30℃, 40℃, 50℃and 60℃ respectively. The higher the saturated vapor pressure was, the faster the water volatilized. Therefore, the increase of temperature leaded to the increase of the water adsorption, which could promote the hydrolysis of reversible binding formaldehyde with collagen fibers; a large amount of formaldehyde was desorbed from leather and released to the air.

According to figures, different types of leather showed different release characteristic. The average release speed of sheepskin was faster than that of cowhide at the same temperature. The average release speed of formaldehyde tanned sheepskin was 22.16 mg/(kg·h), 37.42mg/(kg·h), 75.81mg/(kg·h), 128.91 mg/(kg·h); and that of formaldehyde tanned cowhide was 12.18mg/(kg·h), 21.17mg/(kg·h), 60.40mg/(kg·h), 109.33 mg/(kg·h) at 30℃, 40℃, 50℃, 60℃, respectively. The release of formaldehyde in cowhide was more sensitive to the temperature. The temperature increased from 30℃ to 60℃, the formaldehyde release speed of sheepskin increased 19.39% for every increase of 1 degree Celsius by average, and that of cowhide increased 29.92%. The reasons were because the porosity of sheepskin was greater than that of cowhide. The collagen fiber structure of sheepskin specimen was looser, the formaldehyde release channel was more unimpeded, and so the formaldehyde release speed was faster at the same temperature. When the temperature increased, the thermal motion of formaldehyde molecule had been strengthened and a large amount of formaldehyde molecules obtained potential energy for desorption. Because of differences in porosity, it was relatively easy to release for sheepskin, formaldehyde molecule with low potential energy could be released at low temperatures, so the temperature did not have obvious promoting effect on release. The release was very difficult for cowhide, by raising the temperature so as to more and more formaldehyde molecules with low potential energy gained more energy to release, which demonstrated that the release of formaldehyde in cowhide was more sensitive to temperature.

3.4 Theoretical Assumptions of the Release Model and Derivation of Release Equations

Due to time constraints, the release law of above factor investigation test was summed up by the relevant analysis of release data within 7 hours which can not be generalized and applied. Therefore, it was very necessary and meaningful to establish the general release model and deduce the release equation.

Drawing on the formaldehyde emission model of the artificial board in the closed system designed by Berge.A (1980), the process of leather formaldehyde release in the seal system was designed as Figure 4. In order to simplify the mathematical treatment, make the following assumptions:

⑴The leather interior was considered to be a continuous multilayer, in which formaldehyde diffusion only related to temperature was uniform and continuous. The formaldehyde concentration between each layer kept the same and release occurred in the surface of leather only. There was no difference between the two sides of the leather.

⑵There was a very thin layer beside leather surface, from where the formaldehyde released to close air. When the climate factors (temperature, relative humidity, gas exchange rate) kept a stable state, the formaldehyde concentration of air and the leather surface would achieve dynamic balance. The ratio of formaldehyde transferred to the air from the leather surface can be described by the mass transfer coefficient (denoted by ***K***, m/h).

⑶The formaldehyde gas in the closed system can be mixed completely immediately. It had very good solubility in absorption water and can be absorbed completely.

Based on the above assumptions, in the unit time, the amount of formaldehyde transferred to the air should be equal to the quantity of emitted formaldehyde from leather surface. It could be described by the equation 2.

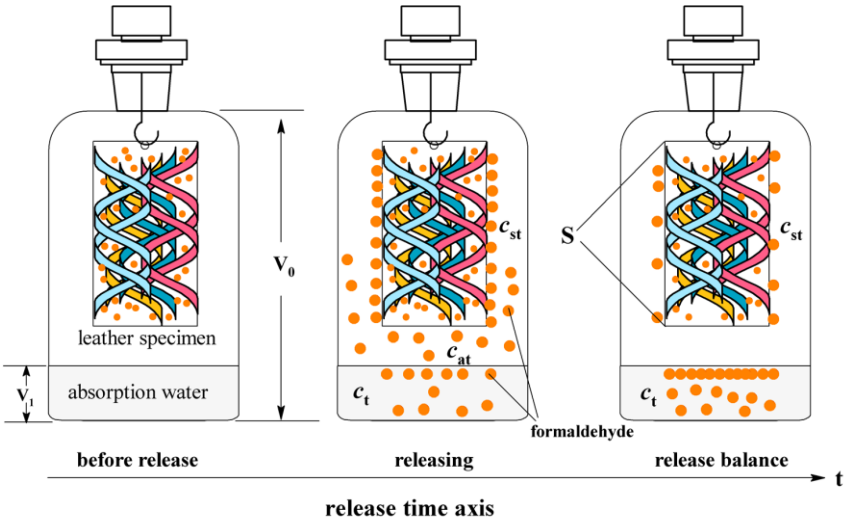

Figure 4. Schematic diagram of the process of formaldehyde release in the seal system

*(**V_0**-the volume of sealed bottle, mL; **V_1**-the volume of absorption water, mL; **c_t**-the formaldehyde concentration of absorption water, mg/mL; **c_{at}**-the formaldehyde concentration of air, mg/mL; **c_{st}**- the formaldehyde concentration of leather surface, mg/mL; **S**-the surface area of leather specimen, m^2)*

$$(V_0 - V_1) \times \frac{\partial c_{at}}{\partial t} = K \times S \times (c_{st} - c_{at}) \quad (2)$$

Initial condition equation 3 was

$$t = 0, c_{\text{at}} = 0 \quad (3)$$

The differential equation was solved through the MATLAB, the formula of the formaldehyde concentration of air was

$$c_{at} = c_{\text{st}} \times (1 - e^{\frac{-K \times S \times t}{V_0 - V_1}}) \quad (4)$$

Because of the formaldehyde was absorbed completely by water. On the base of the mass balance of formaldehyde was

$$(V_0 - V_1) \times c_{at} = V_1 \times c_t \quad (5)$$

The formula of the formaldehyde concentration of absorption water was

$$c_t = \frac{V_0 - V_1}{V_1} \times c_{\text{st}} \times (1 - e^{\frac{-K \times S \times t}{V_0 - V_1}}) \quad (6)$$

The initial mass of specimen was denoted by W_0. Representation by quantity of emitted formaldehyde from leather, the formula was

$$Q = \frac{V_0 - V_1}{W_0} \times c_{\text{st}} \times (1 - e^{\frac{-K \times S \times t}{V_0 - V_1}}) \quad (7)$$

3.5 Collection and Fitting of Actual Release Data

The sealed 1L bottles were stored in a heated oven at 60℃. The release data of formaldehyde tanned sheepskin and cowhide were collected with an hour interval until balance. The fitting curves and their first derivatives (i.e. instantaneous release speed, denoted by ***V***) were showed in Figure 5 and Figure 6. The fitting correlation coefficient R^2 is higher than 0.98, so the fitting curves were in line with exponential growth function (ExpGro1) of Origin 8.5. The general formula was described as equation 8.

$$Q = A_1 \times e^{t/t_1} + y_0 \quad (8)$$

According to the fitting results, the parameters t_1 and A_1 were negative and the absolute value of A_1 was equal to y_0. For ease of use, the equation 8 can be translated into equation 9 in which parameters were positive.

$$Q = y_0 \times (1 - e^{-t/t_1}) \quad (9)$$

Compared to formula 7 and equation 9, it was obvious that they were consistent.

So, the correctness of theoretical derivation was well verified by the fitting of actual release data. The assumptions reasonability of the release theory were fully proved meanwhile and the formula 10 and 11 should be satisfied.

$$y_0 = \frac{V_0 - V_1}{W_0} \times c_{st} \quad (10)$$

$$t_1 = \frac{V_0 - V_1}{K \times S} \quad (11)$$

According to figures, the formaldehyde emission obviously could be divided into three stages. The first stage is the initial stage of formaldehyde release and the formaldehyde concentration of the leather surface was higher. Formaldehyde gas with higher release speed can be freely volatile. There was usually a good linear relationship between the quantity of emitted formaldehyde and the time (factor investigation test had proved). The second stage was the formaldehyde slow release stage, compared with the first stage, the formaldehyde concentration of leather surface decreased gradually with release time extended. Formaldehyde physical deposition in leather or intermolecular binding with collagen fiber overcome the resistance gradually and spread outward. Due to the impact of resistance force, the diffusion speed and volatilization quantity decreased gradually, in this stage, formaldehyde emission quantity was likely to reach the maximum. The third stage was the balanced stage of formaldehyde release. There was a limited release of formaldehyde tanning agent which was cross linked with the collagen fiber and fixed in leather because of reversible reaction in certain humidity until equilibrium. Based on the above theory, the three stages can be called linear free release, barrier release and chemical release respectively. The relevant parameters in equation 9 were given reasonable meaning as Table II and marked as Figure 7.

TABLE II

Meaning of the parameters in the release equation

Parameter	**Unit**	**Meaning**
y_0	mg/kg	Equilibrium release quantity
t_1	h	Linear initial release time

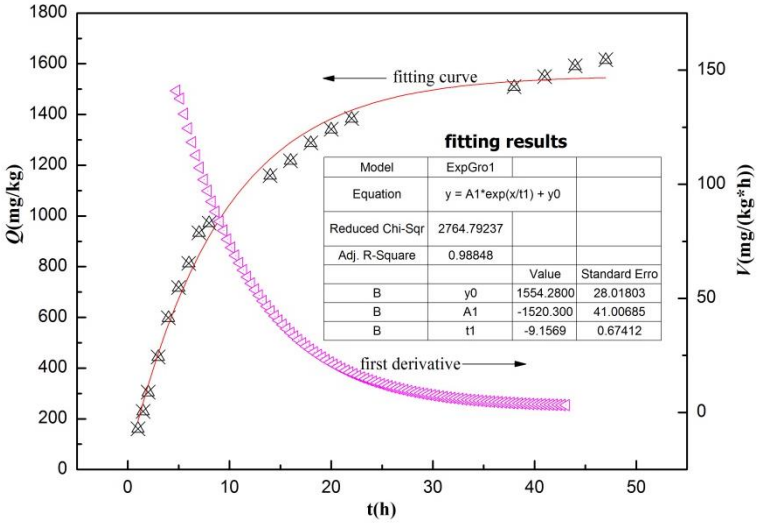

Figure 5. Release fitting curve of formaldehyde tanned sheepskin and its first derivative

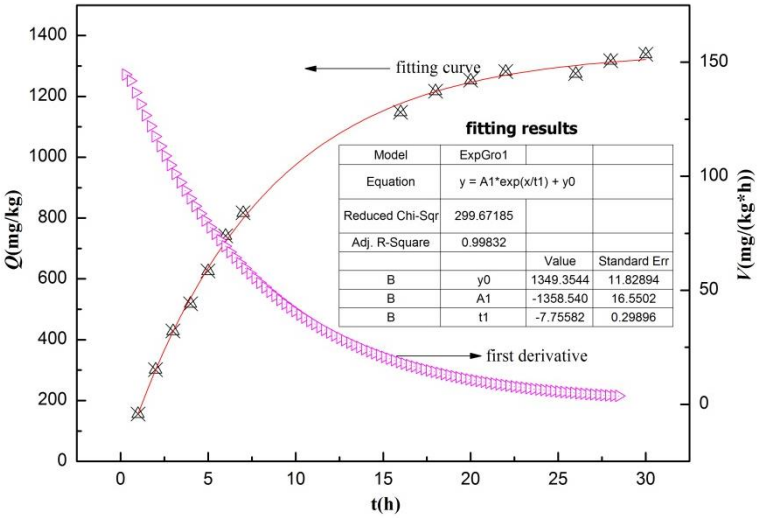

Figure 6. Release fitting curve of formaldehyde tanned cowhide and its first derivative

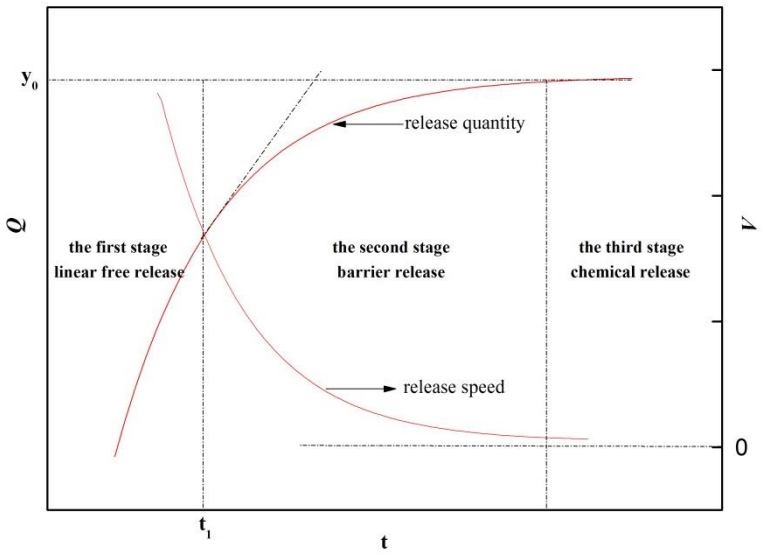

Figure 7. Sketch of stages of formaldehyde release

TABLE III

Known value of the parameters and calculation of *K*

Sample	V_0(mL)	V_1(mL)	W_0(g)	S(m^2)	t_1(h)	y_0(mg/kg)	K(m/h)
SHEEPSKI	**1000**	**50**	**2.6089**	**0.08**	**9.1569**	**1554.28**	1.2968×10^{-3}
COWHIDE			**5.4730**		**7.7558**	**1349.35**	1.5311×10^{-3}

3.6 Application and Prospect of Release Theory

According to the above discussion, formaldehyde emission model can be divided into two categories: mass transfer model and empirical model. Mass transfer model was established according to the law of mass transfer and its parameters had clear physical meaning. Empirical model was summed up and fitted based on a large number of experimental data to predict leather formaldehyde emission, most of parameters in which had no definitude physical meaning. There were several uses if combined with those two. According to the formula 10 and 11, the equilibrium release quantity (y_0) and linear release time (t_1) of formaldehyde tanned leather were affected by the volume of storage space (V_0), mass transfer coefficient (K) which positively correlated with temperature except the conditions of leather itself (W_0, S). The stages of formaldehyde emission could be changed during the use or storage of the leather products because of these conditions changing. Therefore the formaldehyde emission was continuous and periodic. For the sake of environmental protection and the health of consumers, the formaldehyde of leather especially formaldehyde tanned leather should

be fully released after the completion of the production. Based on economic reasons, the leather should be placed in a spacious, ventilated environment with appropriate high temperature to speed up the release in order to shorten time. Based on the ISO 17226-3 conditions and the fitting results of actual release data, the value of other parameters were shown as Table III, the value of ***K*** could be calculated which could be used to predict the formaldehyde emission or design the leather products with specific release requirements for the further study.

4. Conclusion

The formaldehyde emission model of formaldehyde tanned leather in sealed system was established according to the law of mass transfer under several reasonable assumptions and verified by the fitting of actual release data.Application and prospect of release theory were discussed.The results showed that formaldehyde emission could be divided into three stages: the linear free release, barrier release and chemical release stage. The linear release time inversely correlated with mass transfer coefficient which positively correlated with temperature. The release temperature had significant promotion impact to release during linear release time. The higher the temperature was, the faster the formaldehyde release. Because of the difference of porosity, different types of leather showed different release characteristic. The average release speed of sheepskin was faster than that of cowhide at the same temperature. The release of formaldehyde in cowhide was more sensitive to the temperature. The temperature increased from 30℃ to 60℃, the formaldehyde release speed of sheepskin increased 19.39% for every increase of 1 degree Celsius by average, and that of cowhide increased 29.92%.

5. Acknowledgements

The authors wish to acknowledge financial support from National Natural Science Foundation of China (21476134), Key Scientific Research Group of Shaanxi Province (2013KCT-08), Scientific Research Group of Shaanxi University of Science and Technology (TD12-04).

6. References

1. Wei W, Ramalho O, Mandin C, Indoor air quality requirements in green building certifications. *Building and Environment,* 2015, **92**, 10-19.

2. Araki A, Kawai T, Eitaki Y, et al, Relationship between selected indoor volatile organic compounds, so-called microbial VOC, and the prevalence of mucous membrane symptoms in single family homes. *Sci. Total Environ.* , 2010, **408**, 2208-2215.

3. Mendell M J, Fisk W J, Kreiss K, et al, Improving the health of workers in indoor environments: priority research needs for a national occupational research agenda. *Am. J. Public Health*, 2002,**92**, 1430-1440.

4. Cui Y, Chang J M, Wang W L, et al, Preparation of activated carbon using bio-oil phenol-formaldehyde resin. *BioResources*, 2015, **10**, 3865-3873.

5. Ding W, Li W, Gao Q, et al, The effects of sealing treatment and wood species on formaldehyde emission of plywood. *BioResources*, 2013, **8**, 2568-2582.

6. Xiong J, Zhang Y, Huang S, Characterisation of VOC and formaldehyde emission from building materials in a static environmental chamber: Model development and application. *Indoor and Built Environment*, 2011,**20**, 217-225.

7. Salem MZM, Böhm M, Understanding of formaldehyde emissions from solid wood: An overview. *BioResources*, 2013, **8**, 4775-4790.

8. Sumita D, Ashish Y, Premendra D D, et al, Toxic hazards of leather industry and technologies to combat threat: a review. *Journal of Cleaner Production*, 2015, **87**, 39-49.

9. Bin X, Ya W, Yu G, et al, Investigation of volatile organic compounds exposure inside vehicle cabins in China. *Atmospheric Pollution Research*, 2016, **7**, 215-220.

10. Tao H T, Fan Y S, Li X Q, et al, Investigation of formaldehyde and TVOC in underground malls in Xi'an, China: Concentrations, sources, and affecting factors. *Building and Environment*, 2015, **85**, 85-93.

11. Blanc N, Humbert N, Cannot J, et al, HPLC versus Spectrophotometry for the Quantitation of Trace Amounts of Formaldehyde in Leathers. *JALCA*, 2009, **104**, 1-8.

12. Font J, Viera S, Rius T, et al, Inter-laboratory study on formaldehyde determination by HPLC. *JALCA*, 2008, **103**, 53-61.

13. Mentes C S, Dandar U, Kilic E, Antioxidant effect of tannic acid on formation of formaldehyde and hexavalent chromium compounds in leather. *TEKSTIL VE KONFEKSIYON*, 2014,**24**, 105-110.

14. Joint Research Centre-Environment Institute. Indoor air pollution by formaldehyde in European countries. *Buildingecology Com*, 1990, **EUR13216EN**.

15. ASTM. D5157-97.Standard guide for statistical evaluation of indoor air quality models. West Conshohocken, PA: American Society for Testing and materials, 2003.

16. Berge A, Mellegaard B, Hanetho P, et al, Formaldehyde release from particleboard evaluation of a mathematical model. *Holz als Roh-und Werkstoff*, 1980, **38**, 251-255.

ACSIL P-29

THE ANTIBACTERIAL PROPERTY AND ABRASION RESISTENCE OF POLYACRYLATE/GRAPHENE COMPOSITES IN FINISHED LEATHER

Zhang Wenbo*, Wei Linfeng，Ma Jianzhong

College of Bioresources Chemical and Materials Engineering, Shaanxi University of Science and Technology, Xi'an 710021, China; E-mail: 466566133@qq.com
Shaanxi Collaborative Innovation Center of Industrial Auxiliary Chemistry and Technology, Shaanxi University of Science and Technology, Xi'an 710021, China; E-mail: zhangwenbo@sust.edu.cn
College of Bioresources Chemical and Materials Engineering, Shaanxi University of Science and Technology, Xi'an 710021, China; E-mail: majz@sust.edu.cn
Corresponding author: E-mail: majz@sust.edu.cn

Graphene has high specific surface area, good mechanical properties and electrontransfer ability and has been widely used in polymer in order to improve the relevant performances. Reduced graphene oxide (rGO) was prepared by graphene oxide (GO). GO and rGO were introduced into polyacrylate emulsion (PBA-MMA-GMA) respectively to prepare PBA-MMA-GMA/GO and PBA-MMA-GMA/rGO composites. The composites were applied in leather finishing. The influences of GO and rGO on antibacterial property of composites and abrasion resistance of finished leather were investigated. The result of XRD showed that the interlayer spacing of GO was increased compared with graphite. The result of FT-IR showed that GO was reduced. The particle sizes of GO and rGO were 225 nm and 155.7 nm, respectively. The results of antibacterial test showed that PBA-MMA-GMA/GO composite had no antibacterial property. The antibacterial rates of PBA-MMA-GMA/rGO composite and the leather finished by PBA-MMA-GMA/rGO to *Escherichia coli* were 77.5% and 68.0%, respectively. PBA-MMA-GMA/GO and PBA-MMA-GMA/rGO composites could improve the abrasion resistance of finished leather，and rGO had a better performance than GO.
Keywords: Polyacrylate, Graphene oxide, Composite, Antibacterial, Abrasion resistence.

Intrduction

Graphene is an atomically thin layer of sp^2-bonded carbon atoms, stacked in a two-dimensional (2D) honeycomb lattice, forming the basic building block for carbon allotropes of any dimensionality. This special structure make graphene has many excellent performances, such as high specific surface area, good mechanical properties and electrontransfer ability. Graphene has been widely used in polymer in order to improve the relevant performances.

Graphene is a potential additive to fabricate composites with good abrasion resistance due to its large specific surface areas, self-lubrication and extremely thin laminated structure. Shen and his

coworkers [1] have studied the tribological properties of GO/epoxy resin, the wear rate is reduced by 90.0-94.1% when GO content was 0.50%; compared with other nano fillers(SiO_2、TiO_2、Al_2O_3、Si_3N_4 and carbon nanotubes), GO is a better material to promote the abrasion resistance of epoxy resin with a low content. Lahiri [2] has investigated the lubricating of graphene nano sheets in PS. When graphene content added from 0.1.wt% to 1.0wt%, the lubricating of graphene nano sheets was gradually promoted, and the wear rate wss reduced by 4 times caused by the good mechanical properties and shearing action of graphene.

Graphene is also a new type of antibacterial material. In 2010, Huang Qing [3] first reported the antimicrobial properties of graphene to the *E.coli*. He found that the inhibitory rate of graphene oxide suspension reached more than 90% after 2 h's incubation with *E.coli*, and its antibacterial mechanism to *E.coli* is mechanical cutting destruction of GO to the cell membrane.

Liu [4] studied the effect of GO and graphene on cell viability of *E.coli*, and found that the antibacterial ability of GO is higher than rGO. The "large" GO has a higher antibacterial ability compared with the "small"GO. At the same time, it was found that GO and graphene can oxidize the reduced glutathione in bacteria. On one hand, GO and graphene could damage the cell membrane by mechanical cutting. On the other hand, GO and graphene could produce oxygen free radicals which induce oxidative damage of cell.

Tian [5] thought the antibacterial properties of graphene-derived materials may be caused by: firstly, after adhering on bacteria, the sharp edges of graphene can cut cell membrane. Sencodly, superoxide mediated oxidative stress leads to the death of bacteria. Krishnamoorthy [6] demonstrated that graphene can be antibacterial by lipid peroxidation, indicating that the antibacterial properties of graphene may be related to its oxidative damage.

In this work, we introduced GO and rGO into polyacrylate emulsion (PBA-MMA-GMA) respectively to prepare PBA-MMA-GMA/GO and PBA-MMA-GMA/rGO composites. The composites were applied in leather finishing. The influences of GO and rGO on antibacterial property of composites and abrasion resistance of finished leather were investigated.

Experimental section

Materials

Graphite was purchased from Shanghai Macklin biochemical science and Technology Co., Ltd. Sulfuric acid(98%), potassium permanganate($KMnO_4$) were purchased from Sinopharm Chemical Reagent Co(China). Linear alkylbenzene sulfonate(LAS) was purchased from Guangzhou City Li Sheng Chemical Co. Ltd. Hydrazine hydrate($N_2H_4{\cdot}H_2O$)， butyl acrylate(BA), Methyl methacrylate(MMA), beef extract，peptone, potassium bromide and powdered agar were purchased from Tianjin Kermel Chemical Reagent Co., Ltd. Sodium hydrate(NaOH), Potassium persulfate($K_2S_2O_8$), phosphorus pentoxide(P_2O_5),sodium dimetallic phosphate(Na_2HPO_4), monopotassium phosphate(KH_2PO_4), hydrogen peroxide(H_2O_2)(30%) and ammonium persulfate(APS) were purchased from Hedong District of Tianjin City Hongyan Reagent Factory. Glycidyl methacrylate(GMA) was purchased from Shanghai Yuan Ji chemical Co., Ltd. Sodium dodecyl sulfate(SDS) was purchased from Tianjin BASF Chemical Co., Ltd. Branched Secondary Alcohol Ethoxylates was purchased fromGutian Nanjing Chemical Industry Co., Ltd. Ammonia(25%) was purchased from Tianjin City Fu Yu Chemical Co., Ltd. All of the reagents were used as received.

The synthesis of PBA-MMA-GMA/GO and PBA-MMA-GMA/rGO composites

PBA-MMA-GMA latex was fabricated by the methods in our previous work[7], GO was synthesized by modified Hummers methods, rGO was reduced by $N_2H_4 \cdot H_2O$ with the stabilization of LAS. Briefly, 0.5 g of GO、1 g of LAS and 0.5 mL of $N_2H_4 \cdot H_2O$ was dispersed in 50 mL distilled water with magnetic stirring, then pH of the mixture was adjusted to 7 with NaOH aqueous solution, the mixture was heated to 98 ℃ for 90 min with refux to get the suspension. A stable rGO aqueous suspension was obtained by ultrasonic treatment with adding another 1 g LAS into the suspension. Different amounts of GO and rGO were added into PBA-MMA-GMA latex with magnetic stirring to obtain PBA-MMA-GMA/GO and PBA-MMA-GMA/rGO composites.

Abrasion resistance testing

The composites were applied in leather finishing, and the finished leather was cut into standard specimen. The abrasion resistance of specimen was tested by GB/T1768-2006 method with a Taber machine. First, the quality of standard specimen was weighed. Then, the sample was placed in the Taber machine and wear and tear for 50 times. The quality of worn leather sample was weighed. The wear rate was calculated according to the formula 1:

wear index = wear loss mass / test rotation number（50） × 1000 (1)

Antibacterial property testing

The antibacterial property of the composites and the leather finished by the composites were tested by a spread plate method. Briefly, a quantity of latex was shocked 4 h with the bacterial at 25 ℃. Then, it was spread into agar medium and cultured for 24 h. The antibacterial rate was calculated by recording the number of colonies. The antibacterial property of coating leather was tested by the same method.

Characterization

A D/max2200pc type X-ray diffraction meter(Rigaku Corporation, Japan) with Cu Ka radiation (k = 0.154 nm) was used for the X-ray diffraction (XRD) analysis. The FT-IR spectra were acquired on a Vecture-22 transform infrared spectrometer (Bruker, Germany). The specimens for FT-IR measurement were prepared by grinding the dried powder of GO or rGO with KBr.

Results and Discussion

GO was prepared in the previous work by our group. XRD was used to detect its spacing to prove that the GO is exfoliated. Figure 1 is XRD spectrum of GO. It could be seen that the peak at 10.54°which belongs to GO indicated the layer spacing was 0.838 nm according to the Prague formula. While the original graphite layer spacing is 0.34 nm. Those proved that the GO had been exfoliated [8].

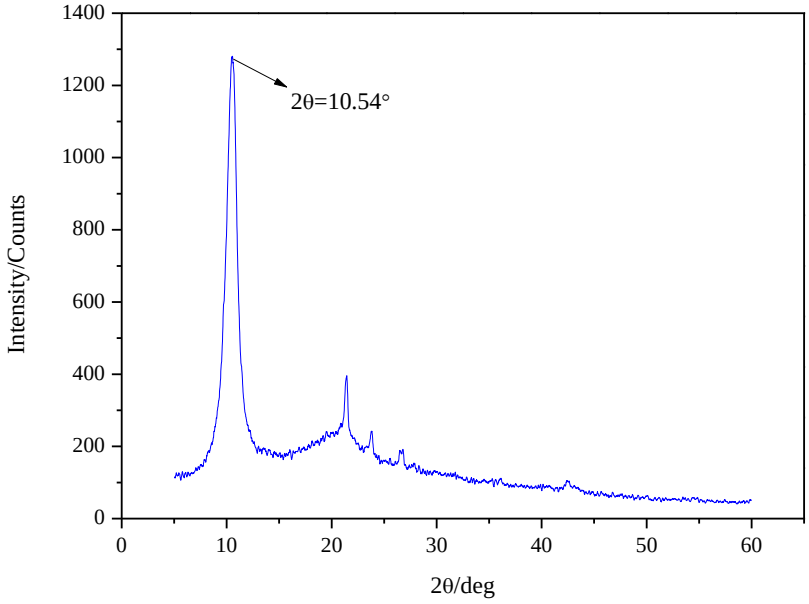

Figure 1 XRD spectrum of GO

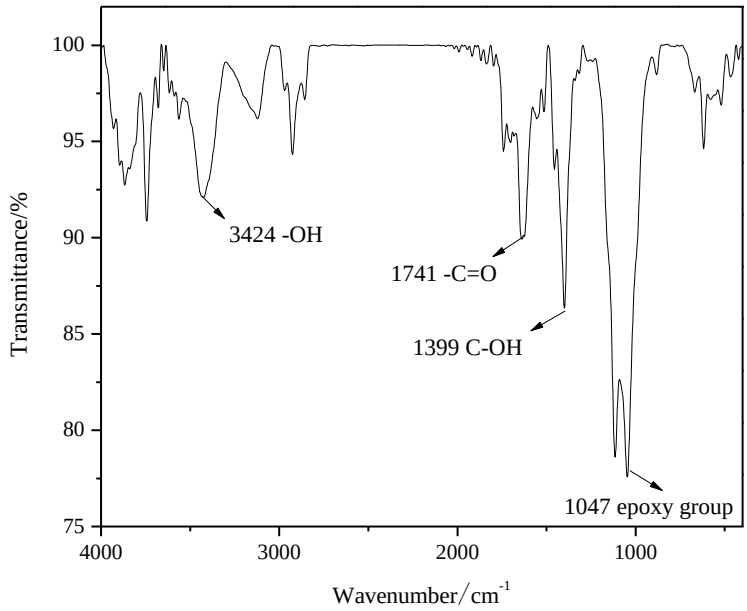

Figure 2 FT-IR spectrum of GO

Figure 2 showed the FT-IR spectrum of GO. GO showed a broad peak at 3424 cm^{-1} which corresponded to the stretching vibrations of hydroxyl. The peak of the 1741 cm^{-1} belonged to the stretching vibration peak of carbonyl group C=O, the peak of 1399 cm^{-1} corresponded to C-OH stretching vibration peak, and the peak at 1047 cm^{-1} corresponded to the stretching vibration peak of epoxy group. These results showed that GO had oxygen functional groups such as hydroxyl, carboxyl and epoxy.

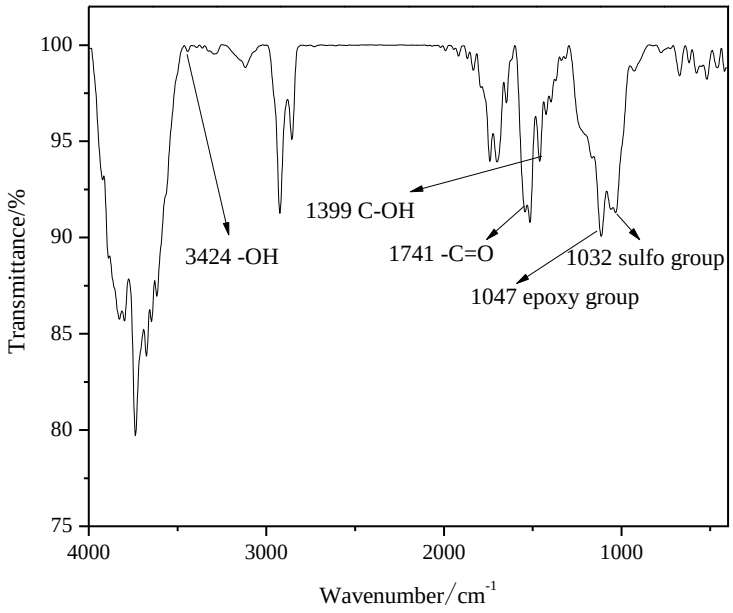

Figure 3 FT-IR spectrum of rGO

Figure 2 showed the infrared spectrum of rGO prepared with hydrazine hydrate as the reducing agent. It can be seen that the peak at 1741 cm^{-1} corresponded to the stretching vibration peak of carboxyl carbonyl C=O, the peak of 1047 cm^{-1} corresponded to the stretching vibration peak of epoxy group, the peak of 1399 cm^{-1} peak corresponded to the stretching vibration peak of C-OH. Compared with the peak in Figure 2, all peaks of rGO were decreased. The peak of -OH was almost completely disappeared. This shows that the GO is reduced. In addition, the peak of 1032 cm^{-1} corresponded to the sulfonic acid groups which caused by adding LAS.

The abrasion resistance property

Figure 4 is the result of the wear index of finished leather. The bigger the wear index was, the worse the wear resistance was. Compared with the pure PBA-MMA-GMA coating leather sample, the wear index of leather finished by PBA-MMA-GMA/GO and PBA-MMA-GMA/rGO decreases, showed that two kinds of composites both have played important roles in wear resistance. The results showed PBA-MMA-GMA/rGO composite had better performance on wear resistance than PBA-MMA-GMA/GO while compared coating leather samples finished by PBA-MMA-GMA/GO and PBA-MMA-GMA/rGO which had the same amount of nanofiller. In this paper, PBA-MMA-GMA/rGO composite had better performance on wear resistance.

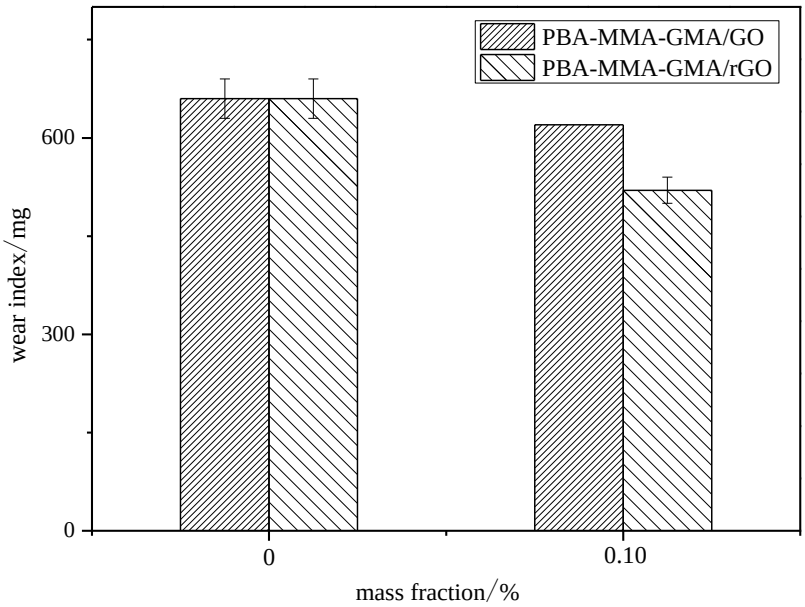

Figure 4 The wear index of coating leather samples finished by PBA-MMA-GMA/GO and PBA-MMA-GMA/rGO

The antibacterial Properties

Figure 5 is an optical image of antibacterial effect of PBA-MMA-GMA/GO. Table 1 is the cfu of PBA-MMA-GMA/GO after culturing. It can be seen that PBA-MMA-GMA/GO does not interact with *E.coli*, which may be due to the edge of GO sheets is not sharp enough to cut the cell membrane.

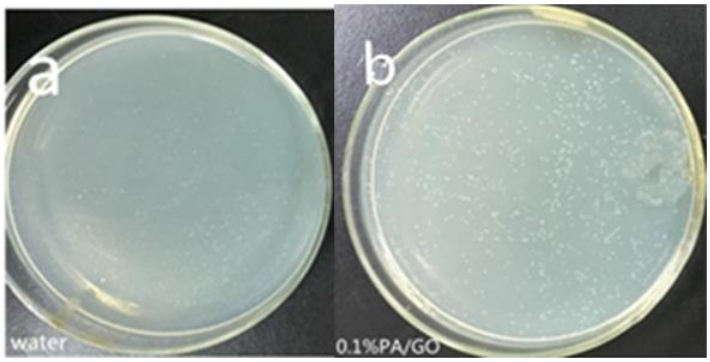

Figure 5 Optical image of antibacterial effect of PBA-MMA-GMA/GO：

a）control group；b）PBA-MMA-GMA/GO（0.10%）

Table 1 The cfu of PBA-MMA-GMA/GO after culturing

materials	cfu
water	400
PBA-MMA-GMA/GO	400

Figure 6 is an optical image of antibacterial effect of PBA-MMA-GMA/rGO. Figure 7 is the antibacterial rate of PBA-MMA-GMA/rGO. When the mass fraction of RGO was 0.10%, antibacterial rate

of PBA-MMA-GMA/rGO composite material for E.coli was more than 77.5%, which can be considered to have antibacterial ability.

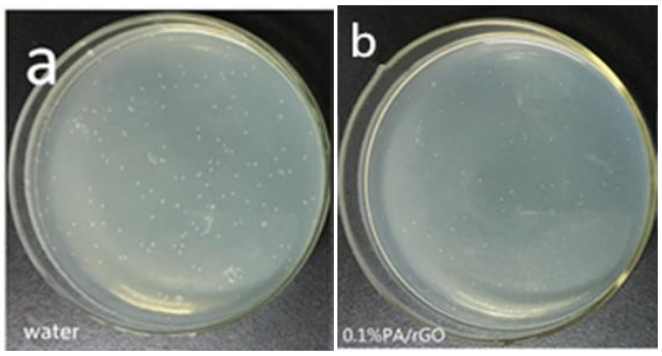

Figure 6 Optical image of antibacterial effect of PBA-MMA-GMA/rGO

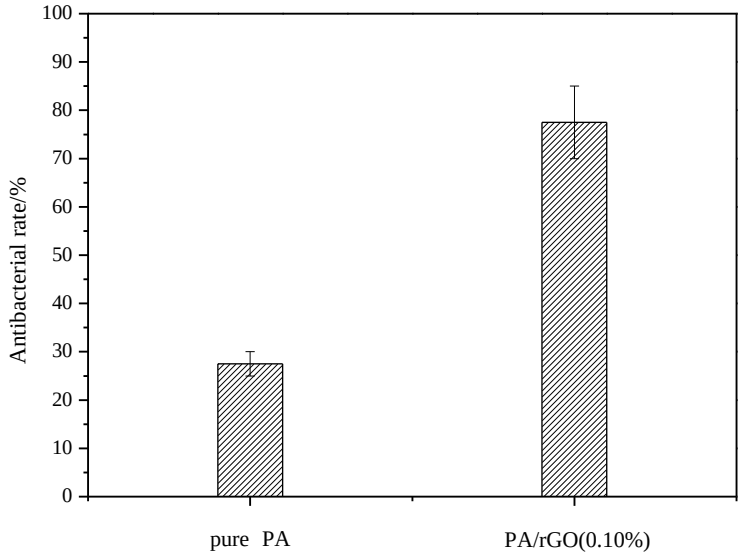

Figure 7 The antibacterial rate of PBA-MMA-GMA/rGO

Through the comparison of antibacterial properties between PBA-MMA-GMA/GO and PBA-MMA-GMA/rGO composite materials, it can be demonstrated that the PBA-MMA-GMA/rGO composite showed more excellent antibacterial ability to *E.coli*, which coinside with the related reports, the antibacterial ability of graphene and its derivatives had a great relationship with their morphology and structure.

Conclusion

In this work we have prepared two types of composites which added with GO and rGO respectively and the composites were applied in leather finishing. The influences of GO and rGO on antibacterial property of composites and abrasion resistance of finished leather were investigated. The results of antibacterial test showed that PBA-MMA-GMA/GO composite had no antibacterial property. The antibacterial rates of PBA-MMA-GMA/rGO composite and the leather finished by PBA-MMA-GMA/rGO

to *E.coli* were 77.5% and 68.0%, respectively. PBA-MMA-GMA/GO and PBA-MMA-GMA/rGO composites could improve the abrasion resistance of finished leather， and rGO had a better performance than GO.

References

[1] Shen X. J., Pei X. Q., Fu S. Y, et al. Significantly modified tribological performance of epoxy nanocomposites at very low graphene oxide content [J]. Polymer, 2013, 54(3): 1234-1242.

[2] Lahiri D., Hec F., Thiesse M, et al. Nanotribological behavior of graphene nanoplatelet reinforced ultra high molecular weight polyethylene composites [J]. Tribology International, 2014, 70(2): 165-169.

[3] Hu W., Peng C., Luo W, et al. Graphene-based antibacterial paper [J]. ACS Nano, 2010, 4(7): 4317-4323.

[4] Liu S., Zeng T. H., Hofmann M, et al. Antibacterial activity of graphite, graphite oxide, graphene oxide and reduced graphene oxide: membrane and oxidative stress [J]. ACS Nano, 2011, 5(9): 6971-6980.

[5] Tian Tian, Lv Min, Tian Yang, et al. Study on biological safety of graphene[J]. Science Bulletin, 2014, 59 (20):1927-1936.

[6] Krishnamoorthy K., VeeraPndian M., Zhang L. H, et al. Antibacterial efficiency of graphene nanosheets against pathogenic bacteria vialipid peroxidation [J]. Journal of Physical Chemistry, 2012, 116(32): 17280-17287.

[7] Zhang W. B., Ma J. Z., Gao D. G, et al. Preparation of amino-functionalized graphene oxide by hoffman rearrangement and its performances on polyacrylate coating latex [J]. Progress in Organic Coatings, 2016(94): 9-17.

[8] Zhang sensitive, Guo Xinli, Hao Wei, et al. Hydrothermal synthesis and adsorption properties of three-dimensional graphene[J]. Functional Materials, 2014(45):73-80.